In vivo consequences of AML1-ETO fusion protein expression for hematopoiesis

A THESIS
for the award of the Degree of

DOCTOR OF NATURAL SCIENCES

submitted at

FACULTY OF CHEMISTRY, PHARMACY AND GEOSCIENCE
JOHANNES GUTENBERG-UNIVERSITÄT
MAINZ, GERMANY

by

NINA CABEZAS WALLSCHEID

born in Roses (Spain) on 09.03.1982

JANUARY 2010

ABSTRACT

The t(8;21) (q22;q22) translocation fusing the ETO (also known as MTG8) gene on human chromosome 8 with the AML1 (also called Runx1 or CBFα) gene on chromosome 21 is one of the most common genetic aberrations found in acute myeloid leukemia (AML). This chromosomal translocation occurs in 12 % of *de novo* AML cases and in up to 40 % of the AML-M2 subtype of the French-American-British classification. To date, the *in vivo* function of aberrant AML1-ETO fusion protein expression has been investigated by several groups. However, in these studies, controversial results were reported and some key issues remain unknown. Importantly, the consequences of aberrant AML1-ETO expression for self-renewing hematopoietic stem cells (HSCs), multipotent hematopoietic progenitors (MPPs) and lineage-restricted precursors are not known.

The aim of this thesis was to develop a novel experimental AML1-ETO *in vivo* model that (i) overcomes the current lack of insight into the pre-leukemic condition of t(8;21)-associated AML, (ii) clarifies the *in vivo* consequences of AML1-ETO for HSCs, MPPs, progenitors and more mature blood cells and (iii) generates an improved mouse model suitable for mirroring the human condition. For this purpose, a conditional tet on/off mouse model expressing the AML1-ETO fusion protein from the ROSA26 (R26) locus was generated.

Aberrant AML1-ETO activation in compound ROSA26/tetOAML1-ETO (R26/AE) mice caused high rates of mortality, an overall disruption of hematopoietic organs and a profound alteration of hematopoiesis. However, since the generalized activity of the R26 locus did not recapitulate the leukemic condition found in human patients, it was important to restrict AML1-ETO expression to blood cell lineages. Therefore, bone marrow cells from non-induced R26/AE mice were adoptively transplanted into sublethal irradiated $RAG2^{-/-}$ recipient mice. First signs of phenotypical differences between AML1-ETO-expressing and control mice were observed after eight to nine months of transgene induction. AML1-ETO-expressing mice showed profound changes in hematopoietic organs accompanied by manifest extramedullary hematopoiesis. In addition, a block in early erythropoiesis, B- and T-cell maturation was observed and granulopoiesis was significantly enhanced. Most interestingly, conditional activation of AML1-ETO in chimeric mice did not increase HSCs, MPPs, common lymphoid precursors (CLPs), common myeloid progenitors (CMPs) and megakaryocyte-erythrocyte progenitors (MEPs) but promoted the selective amplification of granulocyte-macrophage

progenitors (GMPs).

The results of this thesis provide clear experimental evidence how aberrant AML1-ETO modulates the developmental properties of normal hematopoiesis and establishes for the first time that AML1-ETO does not increase HSCs, MPPs and common lineage-restricted progenitor pools but specifically amplifies GMPs. The here presented mouse model not only clarifies the role of aberrant AML1-ETO for shaping hematopoietic development but in addition has strong implications for future therapeutic strategies and will be an excellent pre-clinical tool for developing and testing new approaches to treat and eventually cure AML.

ZUSAMMENFASSUNG

Die t(8;21) (q22;q22) chromosomale Translokation führt zu einer Fusion zwischen dem ETO-Gen (auch bekannt als MTG8) auf dem humanen Chromosom 8 und dem AML1-Gen (Runx1 oder CBFα) auf Chromosom 21 und ist eine der häufigsten genetischen Abberationen, welche bei akuten myeloischen Leukämien (AML) gefunden wird. Das AML1-ETO Fusionsprotein tritt etwa bei 12% aller AML Patienten auf und ist gemäß des französisch-amerikanisch-englischen Klassifizierungsschemas (FAB) bei etwa 40% von AML Patienten der AML-M2 Untergruppe nachweisbar. Trotz intensiver Forschung auf diesem Gebiet, ist die genaue *in vivo* Funktion dieses Fusionsproteins weiterhin größtenteils unbekannt. Vor allem der Einfluss von AML1-ETO auf hämatopoetische Stammzellen (HSZ), multipotente hämatopoetische Vorläuferzellen (MHV) und linienrestringierte Progenitoren ist unbekannt.

Das Ziel der vorliegenden Arbeit war die Etablierung eines neuen AML1-ETO Mausmodells, welches (a) ein besseres Verständnis für die frühe Pathogenesse von AML mit t(8;21) liefert, (b) eine Untersuchung der Funktion von AML1-ETO in HSZ, MHV, unreifen und reifen Blutzellen ermöglicht und (c) die Situation im Patienten möglichst genau widerspiegelt. Hierfür wurde ein *tet on/off* Mausmodell entwickelt, in dem die Expression des AML1-ETO Fusionproteins unter dem Einfluss des ROSA26 (R26)-Lokus steht.

Aberrante Expression von AML1-ETO in ROSA26/tetOAML1-ETO (R26/AE) Mäusen führte zu einer hohen Mortalität, einer Atrophie hämatopoetischer Organe und einer gestörten Blutzellbildung. Aufgrund der ubiquitären Aktivität des R26-Lokus im Organismus, war es wichtig, die Induktion von AML1-ETO auf Blutzellen zu beschränken, um so die im Patienten gefundene Situation zu rekapitulieren. Um diese Voraussetzung experimentell umzusetzen, wurden Knochenmarkzellen aus nicht induzierten R26/AE Mäusen in subletal bestrahlte $RAG2^{-/-}$ Mäuse adoptiv transferiert. Nach acht bis neun Monaten zeigten sich in den AML1-ETO induzierten Mäusen erste phänotypische Veränderungen. Diese äußerten sich in einer Atrophie hämatopoetischer Organe sowie der Induktion von extramedullärer Hämatopoese. Des Weiteren wurde durch AML1-ETO Expression die initiale Ausreifung von roten Blutzellen, B- und T-Zellen blockiert, die Granulopoese jedoch verstärkt. Interessanterweise führt die konditionelle Aktivierung von AML1-ETO in chimären Mäusen nicht zu einer

Vermehrung von HSZ, MHV, gemeinsamen lymphopoietischen, myeloischen und Megakaryo-/Erythrozytären-Vorläufer, aber zu einer spezifischen Expansion der Granulozyten-/Makrophagen-Vorläuferzellen (GMV).

Die vorliegende Arbeit beschreibt den Einfluss von AML1-ETO Expression auf die normale Hämatopoese und zeigt erstmals, dass AML1-ETO keine Auswirkung auf HSZ, MHV und gemeinsame linienrestringierte Vorläuferpopulationen hat, sondern zu einer spezifischen Expansion von GMV führt. Im Rahmen dieser Arbeit ist es mit Hilfe des hier etablierten Mausmodells gelungen, die funktionelle Auswirkung aberranter AML1-ETO Aktivierung für die Entwicklung von Blutzellen aufzuklären und gleichzeitig neue Therapiestrategien für die zukünftige Behandlung von AML aufzuzeigen.

DECLARATION

"I hereby declare that I wrote the dissertation submitted without any unauthorized external assistance and used only sources acknowledged in the work. All textual passages which are appropriated verbatim or paraphrased from published and unpublished texts as well as all information obtained from oral sources are duly indicated and listed in accordance with bibliographical rules. In carrying out this research, I complied with the rules of standard scientific practice as formulated in the statutes of Johannes Gutenberg-University Mainz to insure standard scientific practice."

Nina Cabezas Wallscheid

January 2010

LIST OF FIGURES

LIST OF ABBREVIATIONS

α	alfa
β	beta
Δ	delta
γ	gamma
*	p value smaller than 0.05
**	p value smaller than 0.01
***	p value smaller than 0.001
<	smaller than
±	plus minus
x	amplified
%	percentage
°C	Celsius degrees
°	degree
bp	base pair
dl	deciliter
cm	centimeter
kb	kilobase
µl	microliter
µg	microgram
µM	micromolar
µm	micrometer
M	molar
mg	milligram
ml	milliliter
nm	nanometer
pM	picomolar
rad	radiation
sec	second
u	unit
UV	ultra violet light
V	volt
7AAD	7-amino-actinomycin D
AML	acute myeloid leukemia
AML1	acute myeloid leukemia one gene
AML1-ETO	fusion protein product of the translocation between chromosome 8 and 21
BFU-E	burst-forming unit erythroid
BM	bone marrow
CBF	core binding factor complex
CBFβ	core binding factor β
cDNA	complementary DNA
CFU	colony-forming unit
CFU-GEMM	colony-forming unit granulocyte/erythroid/macrophage/megakaryocyte
CFU-GM	colony-forming unit granulocyte/macrophage
CLPs	common lymphoid progenitors
CML	chronic myeloid leukemia
CMPs	common myeloid progenitors
Cre	causes recombination; Cre recombinase enzyme
Ct	cycle number at which the fluorescence exceeds the background signal
DN	double negative for CD4 and CD8 markers
DNA	deoxyribonucleic acid
DOX	doxycycline
DP	double positive for CD4 and CD8 markers
EO	eosinophil
ERY	erythrocyte
ES	embryonic stem cell
ETO	eight-twenty one gene

FACS	fluorescence-activated cell sorting
GEM	genetically engineered mice
GMPs	granulocyte-monocyte progenitors
HDACs	histone deacetylases
hGFP	humanized green fluorescence protein
HSCs	hematopoietic stem cells
loxP	locus of recombination P1
lin-	lineage negative
LKS	$lineage^-/c\text{-}Kit^+/Sca\text{-}1^+$
LN	lymph node
LSC	leukemic stem cell
MAC	macrophage
MEPs	megakaryocyte-erythroid progenitors
min	minute
modPBS	modified phosphate buffered saline
MPPs	multipotent progenitors
mRNA	messenger ribonucleic acid
n	number
NHR	Drosophila Nervy protein
NE	neutrophil
NOD/SCID	non-obese diabetic/severe combined immunodeficient
n.s	non significant
PLT	platelet
QPCR	real time PCR
R26	ROSA26-iM2
RAG2-/-	recombination-activating gene 2 knock-out
RHD	runt homology domain
rpm	revolutions per minute
rtTA	reverse tetracycline transactivator
Spl	spleen
t(8;21)	translocation between chromosome 8 and 21
tet	tetracycline
Thy	thymus
TUNEL	TdT-mediated dUTP nick end labeling

TABLE OF CONTENTS

1 INTRODUCTION

1.1 The impact of leukemia in our society

Although the diagnosis and therapy of leukemia has improved over the last decades, this disease still represents a major health care problem for our society and for the diagnosed patients (Ten Cate et al., 2010). For the year 2009, the North American Association of Central Cancer Registries (NAACCR) estimated a total of 44790 new cases of leukemia to be diagnosed in the United States of America (USA). Among those patients 20540 will present with chronic myeloid leukemia (CML) and 18570 will be diagnosed with acute myeloid leukemia (AML). Furthermore, of the 21870 leukemic patients to be expected to die in 2009, about 9000 will succumb to AML (Figure 1). These numbers illustrate that there is a strong need for improving our general understanding of the disease and for developing better and possibly curative therapies.

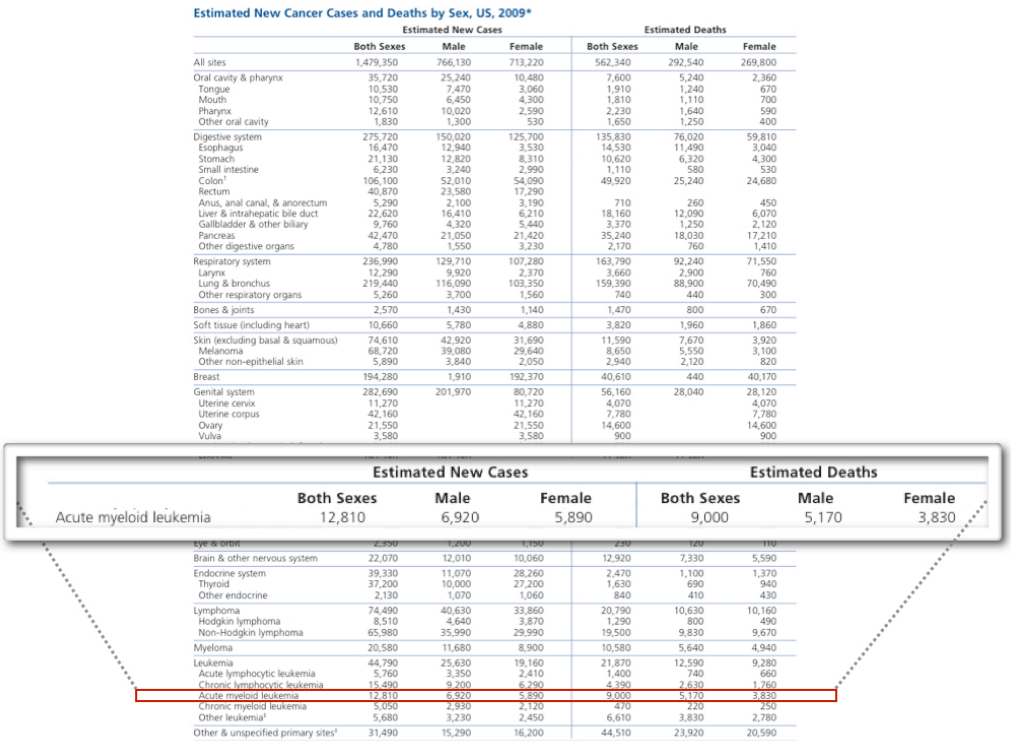

<u>Figure 1:</u> Representation of estimated new cancer cases and deaths by sex in the US in 2009
Estimated new cases are based on 1995-2005 incidence rates from 41 states and the District of Columbia as reported by the NAACCR, representing about 85% of the USA population. Estimated deaths are based on data from USA Mortality Data, 1969-2006, National Center for Health Statistics, Centers for Disease Control and Prevention, 2009. Figure provided by the American Cancer Society in Cancer Facts and Figures 2009 (Society 2009).

One important strategy for improving our general knowledge about leukemia and for providing *in vivo* systems for preclinical trial testing is the use of genetically modified mouse models (Bockamp et al., 2002; Bockamp et al., 2008; Frese and Tuveson, 2007; Koentgen et al., 2010). In this respect it is central that these models can recapitulate the human condition and thus closely mirror the disease or parts of the disease in an *in vivo* setting.

1.2 Hematopoiesis

Leukemia is a malignancy of the hematopoietic system. Hematopoiesis is considered to have a pyramidal shape with one or a few initiating stem cells generating large populations of committed progenitor cells with restricted lineage potential, which finally give rise to all differentiated mature blood cells (Figure 2).

1.2.1 Hematopoietic stem cells (HSCs)

Hematopoietic stem cells (HSCs) are located at the top of the pyramid of blood cell development and possess the capacity to self-renew and the ability to give rise to all differentiated blood cell types (Fleischman et al., 1982; Krause et al., 2001; Lemischka et al., 1986; Spangrude et al., 1988). The first experimental evidence to indicate the existence of HSCs was the discovery in 1961 by Till and McCulloch of a population of clonogenic bone marrow cells that were able to generate myelo-erythroid colonies in the spleen of lethally irradiated hosts (Till and McCulloch, 1961). Nowadays, the current functional test for HSC is the ability to engraft lethality irradiated recipients (the radiation destroys the host bone marrow) and to establish long-term multi-lineage hematopoiesis (Morrison et al., 1995). The vast majority of HSCs reside in the bone marrow, which is referred to as the bone marrow and the vascular niche (Kopp et al., 2009; Zhang et al., 2003). In addition, a minor percentage of HSCs are located in the spleen (Metcalf, 2007). Under normal conditions, self-renewal occurs spontaneously in HSCs and is strongly affected by the microenvironment of the niche. At present, HSC behavior is assumed to be activated both by external microenvironment stimuli and by intrinsic factors that coordinately control HSCs fate decisions (Wilson and Trumpp, 2006). Currently, the

development of clonal assays for all major hematopoietic lineages together with the availability of multiparameter fluorescence-activated cell sorting (FACS) has enabled the prospective purification of HSCs from mice and also to highly enrich for HSCs from humans according to the cell-surface expression of specific markers and their functional read-out *in vivo* and *in vitro* (Domen and Weissman, 1999). After the identification and isolation of murine HSCs, considerable progress has been made regarding the characterization of mechanisms controlling HSCs fates. The decision to self-renew or to give rise to more differentiated progenitors, is a delicate balance between maintaining the level of functional HSCs in the bone marrow and the constant provision of progenitors for the different hematopoietic lineages (Passegué et al., 2003). Figure 2 depicts a schematic representation of normal hematopoiesis.

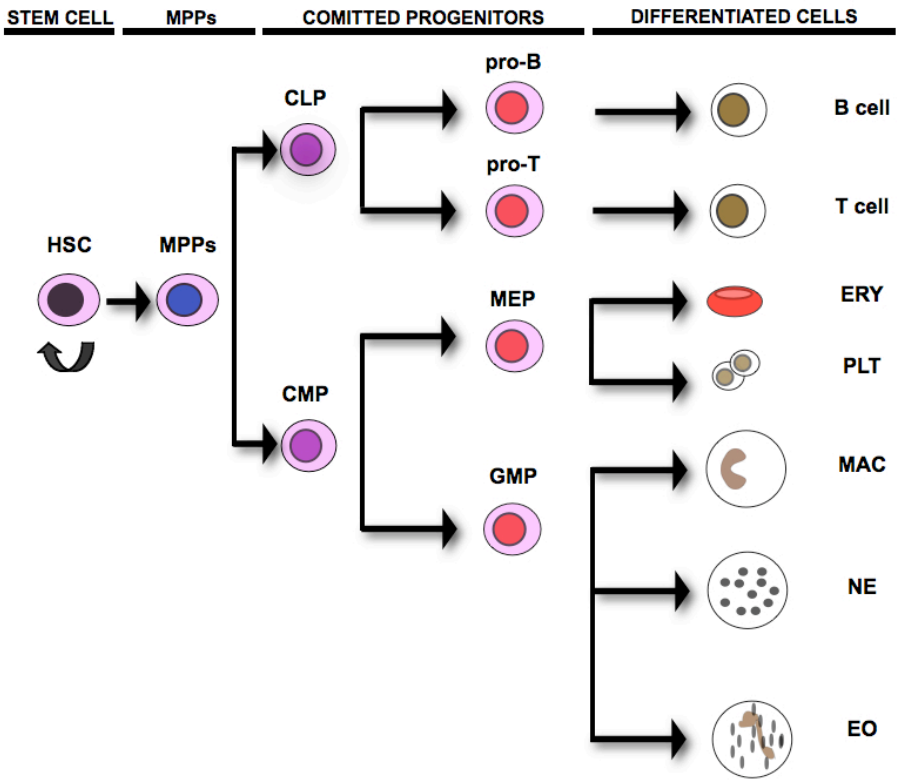

Figure 2: Schematic representation of normal hematopoiesis
HSC, hematopoietic stem cell; MPPs, multi potent progenitors; CLP, common lymphoid progenitor; pro-B, pro-B cell; pro-T, pro-T cell; CMP, common myeloid progenitor; MEP, megakaryocyte-erythroid progenitor; ERY, erythrocyte; PLT, platelet; GMP, granulocyte-macrophage progenitor; MAC, macrophage; NE, neutrophils; EO, eosinophils.

1.2.2 More committed progenitors and differentiated blood cells

Following the hierarchical organization of hematopoiesis, multipotent progenitors (MPPs) are downstream of HSCs and retain the ability to give rise to all differentiated blood lineages but do not have the capacity to self-renew (Akashi et al., 2000a; Chao et al., 2008; Morrison et al., 1997). Downstream of MPPs, two developmental choices can be identified: common lymphoid progenitors (CLPs), able to give rise to all lymphoid cells, and common myeloid progenitors (CMPs), capable of differentiating into all myeloid cells (Akashi et al., 2000b; Kondo et al., 1997). As shown in Figure 2, CMPs can further develop into granulocyte-monocyte progenitors (GMPs), which subsequently generate macrophages (MAC), neutrophils (NE) and eosinophils (EO) or differentiate into megakaryocyte-erythroid progenitors (MEPs), capable of producing platelets (PLT) and erythrocytes (ERY). Equally, CLPs can develop into mature B- and T-lymphocytes. All of these progenitors can be purified as single populations by using cell surface markers and have been shown to lack self-renewal activity after transplantation (Na Nakorn et al., 2002).

1.3 Leukemia

Leukemias are characterized by the uncontrolled overproduction of hematopoietic cells, which can be immature or differentiated. Acute leukemias consist of either immature progenitor cells without lineage differentiation or immature but already lineage-determined cells. Mature cells characterize chronic leukemias. In addition, leukemia can be further classified on the basis of the origin of malignant cells. For instance, leukemic granulocyte, monocyte, erythroid or megakaryocyte cells are considered of myeloid origin, and are grouped together as myeloid leukemias; whereas leukemias involving B-cells, T-cells and natural killer cells are considered as lymphoid leukemias (Krause and Van Etten, 2007).

1.3.1 Leukemic stem cells (LSCs)

The leukemic stem cell (LSC) concept emerged in 1970 and is based on several

studies showing that only a small subset of leukemic cells retained the ability of extensive proliferation *in vitro* and *in vivo*. Using ascites-derived mouse myeloma cells, Park and colleagues showed that only 1 in 10000 to 1 in 100 leukemic cells were able to form colonies *in vitro* in clonal colony-forming assays (Park et al., 1971). In addition, only 1 to 4% of total leukemic cells transplanted *in vivo* could form spleen colonies, even using different types of leukemic cells (Wodinsky et al., 1968). Interestingly, not until 1997, it was demonstrated that most leukemic cells were unable to proliferate extensively and only a small subpopulation of cells expressing stem-cell markers were clonogenic and could initiate and maintain leukemia upon transplantation (Blair et al., 1997; Bonnet and Dick, 1997). In these experiments, Blair and colleagues and Bonnet and Dick identified and purified LSCs from human AML as $Thy1^-/CD34^+/CD38^-$ cells from various patient samples. They demonstrated that although these cells represented a small percentage of all leukemic patients cells (0.2 to 1%), they were the only cells able to transfer AML to non-obese diabetic/severe combined immunodeficient (NOD/SCID) mice. Currently, the general concept of LSCs is well established and serves as a reference for the identification of other cancer stem cells in solid tumors (Brendel and Neubauer, 2000; Reya et al., 2001). For most leukemias, as for most cancers, the target cell of transforming mutations remains in most cases unknown (Pardal et al., 2003; Passegué et al., 2003).

1.3.2 Leukemic therapies: conventional versus new therapeutic therapies

Conventional chemotherapeutic drugs have been shown to mostly target highly proliferating leukemic cells thus being by and large ineffective in completely eradicating LSCs. Although stem cells have the potential for self-renewal, they spend the majority of their time in the G_0 phase of the cell cycle. This means that chemotherapeutic drugs, which act on cycling cell populations, are less effective on LSCs than on regular leukemic cells (Ravandi and Estrov, 2006). The quiescent, non-cycling state of LSCs may thus contribute to their resistance to conventional chemotherapeutics (Misaghian et al., 2009). Regardless of knowing the precise cell type where the original genetic mutation occurred, stem cells most likely constitute both the key and barrier to discovering

effective leukemia therapies.

Currently, promising approaches showing potential in recognizing LSCs include the targeting of key signal transduction pathways like Wnt, RAC and constitutively activated tyrosine kinases with small-molecule inhibitors; and specific cell surface molecules like CD44, CD33 or CD123 with effective cytotoxic antibodies (Misaghian et al., 2009).

1.4 The AML1-ETO/t(8;21)(q22,q22) chromosomal translocation

Transcriptional regulation is a key mechanism controlling HSC homeostasis, development, and lineage commitment and transcription factors are frequently deregulated in leukemia (Gery and Koeffler, 2007; Shivdasani and Orkin, 1996). AML is often associated with recurring genetic abnormalities that affect cellular pathways of myeloid maturation and proliferation (Vardiman, 2009). A common translocation in AML involves the AML1 (also called RUNX1, core binding factor protein alfa (CBFα), and PEBP2αB) gene encoded on human chromosome 21, and the ETO (also called MTG8) gene located on human chromosome 8 (Erickson et al., 1992; Erickson et al., 1994; Gao et al., 1991; Miyoshi et al., 1991; Nisson et al., 1992; Shimizu et al., 1992) (Figure 3). In 1973 the t(8;21)(q22;q22) translocation was for the first time reported by Prof. Janet Rowley in AML-M2 patient samples (Rowley, 1973). This chromosomal aberration occurs in 12 % of *de novo* AML cases and in up to 40 % of AML subtype M2 of the French-American-British classification (Langabeer et al., 1997; Nucifora and Rowley, 1995; Rege et al., 2000; Rowe et al., 2000). Figure 3 shows a schematic representation of the different functional domains in AML1, ETO and AML1-ETO polypeptides.

Being AML1 a member of the RUNX family of transcription factors, AML1 is characterized by a Runt homology domain (RHD) at the amino terminus (De Braekeleer et al., 2009; Ito, 2004; Levanon and Groner, 2004). The RHD is required for DNA-binding and for heterodimerization with core binding factor β (CBFβ) to form the core binding factor (CBF) complex. The CBF complex binds to a specific DNA sequences and activates or represses the expression of a number of hematopoietic genes, relevant to myeloid and lymphoid development (Link et al., 2010; Meyers et al., 1993; Peterson and Zhang, 2004; Yoshida and Kitabayashi, 2008). AML1 is also one of the key

transcription factors required for the establishment of definitive hematopoiesis as shown by knock-out studies where AML1$^{-/-}$ mice displayed a complete lack of definitive hematopoiesis (Okuda et al., 1996; Wang et al., 1996). After organogenesis high expression of AML1 is primarily restricted to cells of the hematopoietic lineage (Corsetti and Calabi, 1997). Moreover, disruption of AML1 function is found in familial platelet disorders, myelodysplastic syndrome and AML (De Braekeleer et al., 2009; Harada and Harada, 2009).

The ETO gene possesses four phylogenetically conserved segments homologous to the *Drosophila* Nervy protein (NHR) and under normal conditions appears to function as a scaffolding factor for the assembly of protein complexes (Feinstein et al., 1995; Peterson and Zhang, 2004). Although ETO is a nuclear zinc-finger-containing protein there is no experimental evidence demonstrating that it can directly bind to DNA. Nevertheless, the structure of ETO suggests that it is likely to function as a transcriptional regulator. This theory is supported by experiments from several groups demonstrating that ETO can directly interact with the nuclear co-repressors N-CoR and Sin3A, and through these interactions can recruit and activate histone deacetylases (HDACs) (Hug and Lazar, 2004; Lutterbach et al., 1998; Wang et al., 1998). In addition, the ETO protein is involved in early gastrointestinal development as shown by ETO knock-out experiments in mice (Calabi et al., 2001). However, the function of ETO in normal physiology has not yet been fully clarified.

The AML1-ETO fusion protein found in leukemic patients, retains the ability to specifically interact with AML1 DNA binding sites and the ETO moiety of the fusion has the capacity to recruit additional cofactors, mostly corepressors like the N-CoR-mSin3-HDAC1 complex that normally execute histone deacetylases activity. This interaction results in lower levels of histone acetylation making DNA-regulating elements less accessible, and thus results in transactivational repression of AML1 wild-type target genes. In addition, AML1-ETO interferes with the normal functions of ETO and other ETO/MTG family members expressed in hematopoietic cells (Elagib and Goldfarb, 2007; Gelmetti et al., 1998; Lutterbach et al., 1998; Wang et al., 1998). Interestingly, several reports were published also demonstrating that the AML1-ETO fusion protein can activate transcription of the BCL-2 promoter through an AML1-binding site that resides within a negative regulatory region of the promoter (Klampfer et al., 1996). Similarly, AML1-ETO can synergize with AML1 to activate the CSF-1R promoter (Rhoades et al.,

1996). The mechanism through which AML1-ETO activates transcription remains to be determined; however, these data, although controversial (Banker et al., 1998), raise the possibility that the activity of AML1-ETO is both promoter and cell context dependent.

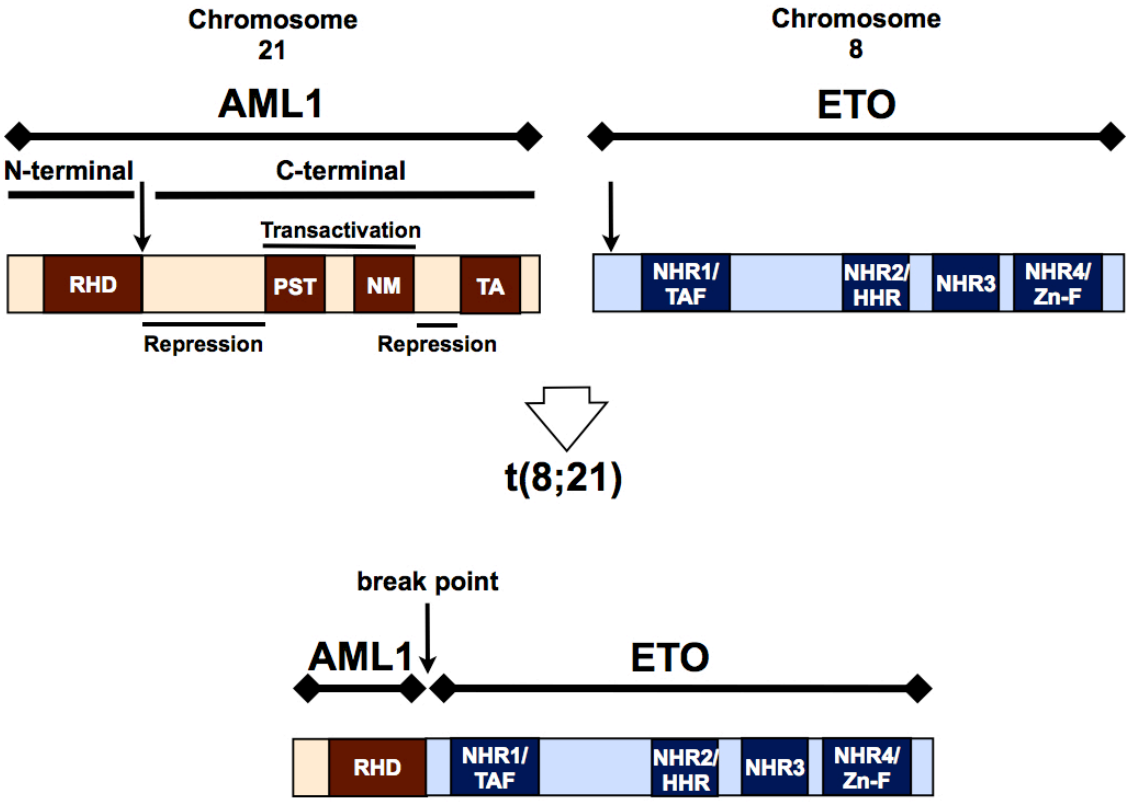

Figure 3: Schematic representation of the AML1-ETO translocation showing functional domains of AML1, ETO and AML1-ETO fusion proteins

The AML1 protein is organized into a N-Terminal Runt homology DNA-binding domain (RHD), a proline/serine/threonine-rich region (PST), a nuclear matrix attachment sequence (NM), and a C-terminal transcriptional activation domain (TA). A second transcription activation domain has also been localized to a region that encompasses both the PST and NM motifs. In addition, the region of AML1 C-terminal to the RHD also contains two repression domains. The ETO protein contains four regions that have high homology to the Drosophila protein Nervy and to ETO family members. These regions include an N-terminal domain with homology to transcription-activating factors (NHR1/TAF), a hydrophobic heptad repeat (NHR2/HHR), a small region with homology to the ETO group of proteins referred to as the Nervy homology region 3 (NHR3), and a C-terminal domain that contains two Zinc-finger motifs (NHR4/Zn-F). The t(8;21) translocation occurs between the AML1 and the ETO gene encoded on chromosome 21 and 8 respectively (break points are indicated by black arrows). The fusion AML1-ETO protein consists of the N-terminal region of AML1, containing the DNA binding site (RHD), fused in frame to almost the complete ETO protein.

T(8;21), translocation between chromosome 8 and 21; RHD, runt homology domain; AML1, acute myeloid leukemia 1; PST, proline/serine/threonine-rich region; NM, nuclear matrix attachment sequence; TA, terminal transcriptional activation domain; ETO, eight-twenty one; NHR1/TAF Drosophila Nervy protein homology region 1/ to transcription-activating factors; NHR2/HHR Drosophila Nervy protein homology region 2/ hydrophobic heptad repeat; NHR3, Drosophila Nervy protein homology regions 3; NHR4/Zn-F, Drosophila Nervy protein homology region 4/ Zinc-finger motifs. Vertical black arrows point to the fusion junction between AML1 and ETO.

1.5 AML1-ETO and leukemia

Current knowledge suggests that the t(8;21) translocation is only the initiating event of the disease and that secondary lesions are required for the onset of leukemia (Kelly and Gilliland, 2002). This view is strongly supported by experiments demonstrating the presence of clonotypic t(8;21) rearrangements at birth from children with later suffered from AML (Wiemels et al., 2002). The argument that AML1-ETO expression alone is not sufficient for promoting AML is also supported by the presence of AML1-ETO-specific transcripts in individuals with no clinical manifestation of acute leukemia (Miyamoto et al., 2000; Nucifora et al., 1993). Therefore, the pathogenesis of t(8;21)-associated AML can be seen as a multi-step process during which aberrant AML1-ETO activation by itself only predisposes for AML and secondary lesions are required for the development of overt leukemia (Kelly and Gilliland, 2002). Moreover, the observation of the AML1-ETO translocation still being detected after remission in a patient that contained both t(8;21) and an activating mutant c-Kit also supports the notion that the chromosomal aberration is the first event initiating the disease (Wang et al., 2005). Since human patients carrying the t(8;21) translocation show no immediate clinical symptoms and since only a small subset of cells express the AML1-ETO fusion gene, it is inherently difficult to study how aberrant AML1-ETO expression shapes the properties of HSCs, blood progenitors and more differentiated hematopoietic cells using patient samples.

One possible avenue for studying the effects of aberrant AML1-ETO expression for hematopoiesis and leukemia is the use of genetically modified animals and in particular the analysis of murine models.

1.6 *In vivo* mouse models

Nowadays, the use of animal models has become an important approach to address the *in vivo* function of genes, regulatory elements and micro RNAs. The laboratory mouse (*Mus musculus*) is one of the best model systems for investigating cancer for various reasons including its extensive physiological and molecular similarities to humans, its entirely sequenced genome, its small size and propensity to breed in captivity and its relatively short lifespan of about three years. Murine cancer models have

progressed through several phases of increasing complexity starting from xenograft tumors derived from tumor cell lines or explants, chemically and virally induced carcinogenesis and increasingly more complex and better variations of genetically engineered mice (GEM) (Bockamp et al., 2002; Bockamp et al., 2008; Frese and Tuveson, 2007).

1.6.1 Xenograft tumor models

At present, the vast majority of preclinical efficacy studies have been carried out using xenograft models. Xenograft tumor models are generated in immunodeficient mice following the implantation of tumor cells or tumor tissue into ectopic or orthotropic sites of the recipient animals. The use of tumor xenografts has several advantages including the little effort of model generation and the fact that therapeutic assessment occurs in human cancer tissues and not in cells derived from other species. Moreover, patient-specific xenograft models have recently been described as a means to develop personalized therapies for some malignancies (Rubio-Viqueira et al., 2006; Shu et al., 2008). However, the results obtained from a number of xenograft studies (Boehm et al., 1997; Sarraf et al., 1998) have not substantially helped to translate theoretical knowledge into the clinic (Kulke et al.; Twombly, 2002). Therefore, GEM are considered to be better models for predicting the response to anti-cancer drug therapies and for modeling cancer in the context of living organisms.

1.6.2 Genetically engineered mouse models

GEM models are generated through the introduction of genetic mutations associated with particular human malignancies. Such mutant genes could be gain-of-function oncogenes or loss-of-function tumor suppressor alleles that are either constitutively or conditionally expressed in mice. Currently, GEM models have been developed for many tumor types including colon, lung, prostate, breast cancers, and have been previously reviewed (Frese and Tuveson, 2007). One important advantage of GEM models is the so called “tumor niche”. The genetic lesion in a GEM, through the use of conditional systems, can be induced in the tissue that is relevant to the type of tumor

being modeled. As a result, tumor initiation and progression occur in the correct cell type and in the specific environment. Moreover, the tumor is surrounded by normal cells, and therefore being comparable to the situation found in human malignancies. Another advantage of GEM when compared to xenograft tumor models is the presence of an intact immune system (de Visser et al., 2006; Dunn et al., 2004; Gopinathan and Tuveson). Therefore, GEM are probably more suitable to recapitulate the human condition than xenograft tumor models.

1.6.2.1 Conventional transgenic strategies

The injection of DNA into the pronucleus of one-cell mouse embryos and the generation of the first transgenic mice created a starting point for studying human disease *in vivo* (Gordon et al., 1980). Theoretically, the injected DNA can be functional once integrated into the murine genome. However, there are several aspects to be considered because the insertion of the DNA occurs randomly and the number of copies inserted often varies between different transgenic lines. It has also to be taken into account that endogenous genes could be affected by the insertion of a transgene (Wilson et al., 1990) or that transgene expression could be influenced by surrounding elements (Rijkers et al., 1994). One possible solution to avoid these issues is the single-copy integration of the transgene into a selected site or the use of insulator elements (Bronson et al., 1996; Cvetkovic et al., 2000; Evans et al., 2000; Fukumura et al., 1998; Misra et al., 2001). The use of so called transient transgenic mice can be alternatively used for studying transcriptional elements in mice (Rodríguez et al., 2000). However, only the generation and analysis of sufficient founder lines provides enough evidence to clarify if the observed phenotype is due to the transgene itself or to position effects.

1.6.2.2 Conventional germ line-targeting

Mouse genetic engineering technology suffered a profound change in 1981 when murine embryonic stem (ES) cells were first established and the enzymatic machinery that specifically recombines homologous DNA sequences exactly with its counterparts on the chromosome were discovered (Evans and Kaufman, 1981; Martin, 1981; Smithies et

al.). Only few years later, the first knock-out mice were generated by homologous recombination in ES cells (Doetschman et al.; Thomas and Capecchi, 1987). Using this technique, it is possible to delete gene function (knockout), to insert selected genes or DNA fragments into a given locus (knock-in), to introduce point mutations, and to produce chromosomal rearrangements in the germ line of the mouse. One of the most important advantages of gene targeting is that homologous recombination in ES cells defines the site of integration and thus facilitates a more accurate interpretation of the phenotype.

However, the conventional systems either transgenic or germ line-targeting do not allow to bypass a possible embryonic lethality or to conditionally activate or deactivate the gene of interest in adult mice.

1.6.2.3 Conditional gene targeting and expression using site-specific recombinases

To avoid embryonic lethality or to be capable to activate and study the function of a specific gene in a given tissue, several systems have been generated. The Cre-lox system was the first site-specific recombination system ever used for introducing conditionally inducible genetic changes in mice (Lakso et al., 1992; Orban et al., 1992). This system uses the activity of the enzyme Cre (for “causes recombination”) originally isolated from the bacteriophage P1. Cre is capable to induce site-specific genetic recombination to sequences flanked by loxP (locus of recombination P1) sites (Hamilton and Abremski, 1984; Hoess et al., 1982). In a similar way the *S. cerevisae* recombinase Flp causes recombination (Kilby et al., 1993).

Recombinase mediated targeting solves the problem of spatio-temporal deletion/activation but is an irreversible system. However, in some research settings it will be of importance to use a conditional system capable of reversibly switching the activity of a selected gene or genetic element.

1.6.2.4 Conditional transgene expression

In order to spatio-temporally control and reversibly switch transgene expression, several model systems have been successfully generated using ligand-mediated activation

of a transcriptional transactivator, conditional DNA binding of the transactivator or transactivator-induced transcriptional activation. This system requires in one hand, an effector mouse expressing the ligand-inducible transcriptional transactivator and on the other hand, a responder mouse line that expresses a chosen transgene due to stimulation by the transactivator. These two mouse lines are intercrossed and the resulting bitransgenic offspring can be used to conditionally express the transgene of interest (Bockamp et al., 2002; Bockamp et al., 2008).

1.6.2.4.1 The tet on/off system

Over the last decade the tetracycline- (tet-) regulatory system has been extremely useful for generating conditional transgenic mouse models (for reviews see (Bockamp et al., 2002; Bockamp et al., 2008; Sprengel and Hasan, 2007)). This system shows several advantages. For example, the tet on/off system allows to bypass embryonic lethality facilitating the proper analysis of adult phenotypes. Moreover, the tet on/off system contains the unique potential of reversible gene regulation. This is achieved by adding the inducer molecule doxycycline (DOX). Additionally, the level of transgene expression can be adjusted by predetermined amounts of DOX (Bornkamm et al., 2005; Katsantoni et al., 2007; Roth et al., 2009). This graded responsiveness of transgene expression with the tet-regulatory system thus provides the unique opportunity to analyze the effect of gene dosage in living animals.

1.7 AML1-ETO *in vivo* mouse models

In the past, numerous AML1-ETO-specific mouse models have been generated (reviewed in (McCormack et al., 2008; Muller et al., 2008; Peterson et al., 2007)). In these experiments, several approaches were used to study the *in vivo* consequences of AML1-ETO protein expression including non-conditional knock-in mouse models, which showed lethal hemorrhage between embryonic days 11.5-13.5 and did not allow further analysis of AML1-ETO function in adult animals (Okuda et al., 1998; Yergeau et al., 1997). In order to bypass embryonic lethality and to determine the function of AML1-ETO for adult leukemogenesis, AML1-ETO-inducible models were generated.

Interestingly, all genetically modified AML1-ETO mouse models remained healthy during their life-time (Buchholz et al., 2000; Higuchi et al., 2002; Rhoades et al., 2000) except for a knock-in strategy, which used Sca-1 regulatory elements for expressing AML1-ETO. In this Sca-1 knock-in model, AML1-ETO-expressing animals showed a myeloproliferative-like disorder (Fenske et al., 2004). Additional information has been provided by other approaches using reconstitution of lethally irradiated mice with bone marrow (BM) or hematopoietic stem/progenitor cells that were retrovirally transduced to express AML1-ETO. In these experiments, constitutive AML1-ETO activation led to perturbed erythro- and lymphopoiesis and induced the selective amplification of LKS (lineage$^-$/c-Kit$^+$/Sca-1$^+$) cells, containing immature blood progenitors and HSCs (de Guzman et al., 2002; Schwieger et al., 2002). A major conclusion of this work was that AML1-ETO-expressing HSCs or blood cell progenitors no longer seemed to be restricted by the normal genetic controls regulating HSC pool size. Complementary experiments with AML1-ETO transduced CD34$^+$ human bone marrow cells also confirmed the increase of immature progenitors seen with murine cells (Bäsecke et al., 2005; Mulloy et al., 2003). Although the above studies showed for the first time that aberrant AML1-ETO expression specifically increased LKS and CD34$^+$ populations, the effect of AML1-ETO on HSCs or progenitors is not known, and in particular the ability of AML1-ETO to cause expansion of premalignant stem cell populations, thereby possibly increasing the probability of acquiring a second hit, remain elusive. Taken together, the in the past reported genetically modified AML1-ETO mouse models and the adoptive transfer experiments with retrovirally transduced stem cells produced conflicting results and interpretations. Therefore, there is a need to clarify these controversies and to elucidate the function of aberrant AML1-ETO for hematopoietic development in a mouse model that appropriately modulates the human condition. Also very important for foreclosing our general understanding of AML disease is the fact that it remains unknown if HSCs and/or more committed progenitors are the target of AML1-ETO-mediated expansion.

1.8 Focus of the presented study

To overcome the current lack of insight into the pre-leukemic condition of t(8;21) associated to AML, to clarify the *in vivo* effect of AML1-ETO for HSCs, MPPs, progenitors and more mature blood cells and to generate a mouse model suitable to

mirror the human condition, it was important to develop a novel experimental AML1-ETO model system. The aim of this PhD thesis was therefore to create such a novel model and to experimentally address the above important and still controversial issues.

2 MATERIAL AND METHODS

2.1 Material

2.1.1 Reagents

Reagent	Company
7-amino-actinomycin D (7AAD)	BD Biosciences (Heidelberg,G)
Agarose	Invitrogen (Karlsruhe, G)
Annexin V	BD Biosciences (Heidelberg,G)
Boric acid	Merck (Darmstadt, G)
Bovine serum albumin (BSA)	Sigma (Deisenhofen, G)
Braun-H_2O (*Aqua ad iniectabilia* Braun)	Melsungen (Melsungen, G)
Bromophenol blue	Sigma (Deisenhofen, G)
ß-Mercaptoethanol (ß-ME)	Roth (Karlsruhe, G)
Deoxyribonucleotide triphosphate (dNTP)	Fermentas (St. Leon-Rot, G)
Dimethylsulfoxid (DMSO)	Sigma (Deisenhofen, G)
Dithiothreitol (0.1 M DTT)	Invitrogen (Karlsruhe, G)
Doxycycline (DOX)	Sigma (Deisenhofen, G)
Dulbeccos Modified Eagles Medium (DMEM)	Gibco (Eggenstein, G)
Eosin	Sigma (Deisenhofen, G)
Ethanol (EtOH)	Merck (Darmstadt, G)
Ethidium bromide (10 mg/ml)	Roth (Karlsruhe, G)
Ethylenediamine tetra-acetic acid-disodium salt (EDTA)	Sigma (Deisenhofen, G)
Fetal bovine serum (FBS)	Greiner (Frickenhausen, G)
Fetal calf serum (FCS)	Greiner (Frickenhausen, G)
Formaldehyde	Sigma (Deisenhofen, G)
Glycerol	Sigma (Deisenhofen, G)
Isopropanol	Carl Roth GmbH (Karlsruhe, G)
L-Glutamine (x100)	Invitrogen (Karlsruhe, G)
Hematoxylin	Sigma (Deisenhofen, G)
Hydrochloric acid (HCl)	Roth (Karlsruhe, G)
Magnesium chloride ($MgCl_2$)	Fermentas (St. Leon-Rot, G)

MethoCult M3434 medium	StemCell Technology (Vancouver, C)
Oligo dT	Fermentas (St. Leon-Rot, G)
Phosphate buffered saline (PBS)	PAN Biotech (Aidenbach, G)
Potassium chloride (KCl)	Roth (Karlsruhe, G)
Potassium hydro-phosphate ($KHOP_3$)	Roth (Karlsruhe, G)
Random hexamers	Fermentas (St. Leon-Rot, G)
Rat serum	Central animal facility (Mainz, G)
RPMI 1640	Life Technologies (Paisley, UK)
Sodium dodecyl sulfate (SDS)	Sigma (Deisenhofen, G)
Sodium chloride (NaCl)	Roth (Karlsruhe, G)
Sodium hydroxide (NaOH)	Sigma (Deisenhofen, G)
Sodium hydrogen phosphate ($NaHPO_3$)	Riedel de Haen (Seelze, G)
Sucrose	Roth (Karlsruhe, D)
SYBR Green I	Thermo Scientific (Epson, UK)
TRIS-(hydroxymethyl)-aminomethane (TRIS)	Roth (Karlsruhe, G)
Trypan blue	Sigma (Deisenhofen, G)
Trypsin/EDTA	PAN Biotech (Aidenbach, G)
Tween-20	Sigma (Deisenhofen, G)
Xylenecyanol	Sigma (Disenhofen, G)

2.1.2 Enzymes

Enzyme	**Company**
DNase I (2.5 Kunitz units/µl)	Qiagen (Hilden, G)
Proteinase K (0.5 mg/ml)	Merck (Darmstadt, G)
SuperScript Reverse Transcriptase II (200 units/µl)	Invitrogen (Karlsruhe, G)
Taq DNA Polymerase (5 units/µl)	Fermentas (St. Leon-Rot, G)
Thermo-Start DNA polymerase (1 unit/µl)	Thermo Scientific (Epson, UK)

2.1.3 Primers used for genotyping

Mice	Type	Primer	Sequence 5' to 3'
R26rtTA	k-i	FA	AAAGTCGCTCTGAGTTGTTAT
		RE	GGAGCGGGAGAAAATGGATATG
		RE SpliAcB	CATCAAGGAAACCCTGGACTACTG
AE	Transgene	AE1	ACCCTGCCCATCGCTTTCAA
		AE2	TCCACTCTTCTGCCCATTCT
Actin	HKG	FA (#201)	TCATCAGGTAGTCAGTGAGGTCGC
		RE (#202)	CACCACACCTTCTACAATGAGCTG
$RAG2^{-/-}$	k-o	RAG-A (antisense)	GGGAGGACACTCACTTGCCAGTA
		RAG-B (sense)	AGTCAGGAGTCTTCATTTCACTGA
		NEO	CGGCCGGAGAACCTGCGTGCAA

Abbreviations: R26rtTA, Rosa26 reverse tetracycline transactivator; k.i, knock-in; AE, AML1-ETO; HGK, house keeping gene; k.o, knock-out.

2.1.4 Molecular weight markers

Marker	Company
DNA Gene Ruler 100 bp	Fermentas (St. Leon-Rot, G)
DNA Gene Ruler 1 kb	Fermentas (St. Leon-Rot, G)

2.1.5 Kits

Kit	Company
Absolute QPCR SYBR Green Mix	Thermo Scientific (Epson, UK)
RNase-Free DNase Set	Qiagen (Hilden, G)
RNeasy Mini Kit	Qiagen (Hilden, G)

2.1.6 Consumables

Consumables	Company
Absolute QPCR seal	Thermo Scientific (Epson, UK)
BD Micro-Fine (1 ml, 30 Gx8 mm)	BD Biosciences (Heidelberg,G)
Cell culture plates (6-well, 96-well, 9 cm culture plates)	Greiner (Frickenhausen, G)
Cell strainer (40 µm nylon)	BD Falcon (Heidelberg,G)
Disposable plastic cuvettes	Braun (Melsungen, G)
Eppendorf tubes (1.5 and 2 ml safe-lock)	Eppendorf (Hamburg, G)
FACS-tubes (2 ml)	BD Biosciences (Heidelberg,G)
FACS-tubes (5 ml)	Sarstedt (Nümbrecht G)
Falcon tubes (sterile, 15 ml and 50 ml)	Greiner (Frickenhausen, G)
MACS columns (LD and LS)	MiltenyBiotec (Bergisch Gladbach, G)
Microscope slides Super Frost Plus	Menzel-Glaser (Braunschweig, G)
Microtainer K2E tubes	BD Biosciences (Heidelberg,G)
Mortar and pestle	Coorstek (Golden, USA)
Neulus needle (20, 21, 22 G)	Terumo (Leuven, G)
Neubauer counting chamber	Braun (Melsungen, G)
Pasteur pipettes	Roth (Karlsruhe, G)
PCR-Reaction tubes (0.2 ml Safe-Lock)	Eppendorf (Hamburg, G)
Petri dishes (sterile, 82 mm)	Greiner (Frickenhausen, G)
Qiashredder (50)	Qiagen (Hilden, G)
S&S-Rotrand-1x-Sterile filter (0.22 µm)	Schleicher&Schuell (Dassel, G)
Scalpel Cutfix (10)	Braun (Melsungen, G)
Sterile tips	Henke Sass Wolf (Tuttlingen, G)
SuperPlate Semi-Skirted PCR plate	Thermo Scientific (Epson, UK)
Syringe without needle (1 ml)	Terumo (Leuven, G)
Tips (200 µl, 1000 µl)	Greiner (Frickenhausen, G)
Vials (freezing cells)	Greiner (Frickenhausen, G)

2.1.7 Antibodies used against mouse blood cells

2.1.7.1 Antibodies used against differentiated blood cells

Antigen	Fluorochrome	Company	Alternative Name	Clone	Dilution
CD3	PE	Caltag		145-2C11	1:100
CD4	PE	BD	L3T4	GK1.5	1:100
CD8	PE	BD	Ly-2	53-6.7	1:100
CD8	APC	BD	Ly-2	53-6.7	1:100
CD11b	APC	BD	Mac-1; Integrin α_M	M1/70	1:200
CD11b	PE	BD	Mac-1; Integrin α_M	M1/70	1:200
CD11c	PE	Caltag		N418	1:100
CD19	PE	BD		1D3	1:100
CD23	PE	Southern		2G8	1:100
CD25	PE-Cy7	BD		PC61	1:100
CD41	PE	BD		MWReg30	1:100
CD44	APC	BD	Pgp-1, H-CAM, Ly-24	IM7	1:100
CD45R	PE	BD	B220	RA3-6B2	1:100
CD45R	APC	BD	B220	RA3-6B2	1:100
CD71	Biotin	Caltag	Transferrin R	R17 217.1.4	1:100
F4/80	PE-Cy7	Natutec		BM8	1:100
Gr-1	PE	BD	Ly-6C/ -6G	RB6-8C5	1:200
IgD	Bio	BD		AMS 9.1	1:100
IgM	APC	BD		II/41	1:100
Pan NK	PE	Caltag	DX5	DX5	1:100
NK1.1	APC	Caltag	DX5	DX5	1:100
TER119	PE	BD	Ly-76	TER119	1:100

Abbreviations: PE, phycoerythrin; APC, allophycocyanin; PE-Cy7, phycoerythrin-Cyanine 7; Bio, biotin.
Companies: Caltag (Invitrogen; Karlsruhe, G) G; BD Biosciences (Heidelberg, G), Natutec (Frankfurt, G).

2.1.7.2 Cocktail of antibodies used against differentiated blood cells

Antigen	Fluorochrome	Company	Composition	Clone	Dilution
Lineage cocktail	Pacific Blue	Natutec	CD3 CD45R/B220 CD11b TER-119 Ly-6G	17A2 RA3-6B2 M1/70 TER-119 RB6-8C5	1:50

Company: Natutec (Frankfurt, G).

2.1.7.3 Antibodies used against hematopoietic stem and progenitors cells

Antigen	Fluorochrome	Company	Altern. Name	Clone	Dilution
CD16/32	PE	BD	F_cII/IIIγ Receptor	2.4G2	1:100
CD34	PE	Caltag		RAM34	1:50
CD48	APC	Natutec	BCM1	HM48-1	1:500
CD90.1	APC	Natutec	Thy-1.1	HISR1	1:100
CD117	APC	Natutec	c-Kit	2B8	1:100
CD117	APC	BD	c-Kit	2B8	1:100
CD117	APC-Alexa750	Natutec	c-Kit	2B8	1:100
CD135	PE-Cy5	Natutec	Flk-2,Flt-3, Ly-72	A2F10	1:100
CD150	PE-Cy7	Biozol (Ak online)	SLAM-1	TC15-12,F12.2	1:200
IL7Rα	PE-Cy7	BD	CD127	A7R34	1:100
Sca-1	PE	Caltag	Ly.6A/E	D7	1:100
Sca-1	PE-Cy7	eBioscience	Ly.6A/E	D7	1:100

Abbreviations: PE, phycoerythrin; APC, allophycocyanin; PE-Cy7, phycoerythrin-Cyanine 7; APC-Alexa750, allophycocyanin-Alexa750, PE-Cy5, phycoerythrin-Cyanine 5 .
Companies: Caltag (Invitrogen; Karlsruhe, G) G; BD Biosciences (Heidelberg, G), Natutec (Frankfurt, G); Biozol (Eching, G); eBioscience (Frankfurt, G).

2.1.7.4 Antibodies used against CD45.2 and CD45.1 chimera mice

Antigen	Fluorochrome	Company	Alternative Name	Clone	Dilution
CD45.1	PE-Cy7	Natutec	SJL	A20	1:100
CD45.2	bio	BD	BD	104	1:100

Abbreviations: PE-Cy7, phycoerythrin-Cyanine 7; bio, biotin.
Companies: BD Biosciences (Heidelberg, G), Natutec (Frankfurt, G).

2.1.7.5 Antibodies used against biotin-labeled antibodies

Antigen	Fluorochrome	Company	Dilution
Sav	APC	Caltag	1:100
Sav	APC-Cy7	BD	1:100
Sav	PE-Cy5.5	BD	1:100
Sav	PE-Cy7	BD	1:100

Abbreviations: APC, allophycocyanin; APC-Cy7, allophycocyanin- Cyanine 7; PE-Cy5.5, phycoerythrin-Cyanine 5.5; PE-Cy7, phycoerythrin-Cyanine 7.
Companies: Caltag (Invitrogen; Karlsruhe, G); BD Biosciences (Heidelberg, G).

2.1.8 Microbead-labeled antibodies

Antigen	Company
CD90-microbead	MiltenyiBiotec
Anti-PE microbead	MiltenyiBiotec

Abbreviations: Anti-PE, anti-phycoerythrin.
Companies: MiltenyiBiotec (Bergisch Gladbach, G).

2.1.9 Dead cell exclusion solution

Staining Solution	Company	Dilution
7AAD	BD	1:100

Abbreviations: 7-amino-actinomycin D.
Company: BD Biosciences (Heidelberg, G).

2.1.10 Buffers

Buffers provided with the kits were used in the case of RNA isolation, RNA transcription and QPCR. All other buffers used are listed below.

Buffer	Composition
5 x FS buffer	Buffer with the SuperScript Reverse Transcriptase (Invitrogen)
10 x TBE buffer	108 g TRIS 55 g boric acid 40 ml 0.5 M EDTA pH 8.0 in 1 l ddH_2O pH 8.0 and sterile autoclaved
ACK Lysing Buffer	Red blood cells lysation Lonza Walkersville (Walkersville, USA)
DNase I stock solution	Lyophilized DNase I (1500 Kunitz units) dissolved in 550 µl RNase-free H_2O aliquoted and stored at -20 °C
DNase treatment	10 µl DNase solution 70 µl buffer RDD (provided in the RNase-Free DNase Set)
DNA gel loading buffer	0.25 % bromophenol blue 0.25 % xylencyanol 15 % glycerol in 10 ml ddH_2O
EDTA (0.5 M)	14.6 g EDTA in 100 ml ddH_2O pH 8.0 and sterile autoclaved
FACS buffer (modPBS)	10 % FCS in PBS
Giemsa solution	10 % Giemsa in distillated water
MACS buffer	0.5 % BSA 2 mM EDTA in PBS
Peripheral blood buffer	2 mM EDTA in PBS

Phosphate Buffered Saline (PBS)	8 g NaCl 0.2 g KCl 1.44 g $NaHPO_3$ 0.2 g $KHOP_3$ in 1 l ddH_2O pH 7.4 and autoclaved
Proteinase K solution	10 mg/ml in ddH_2O stored at -20°C
Rat serum solution	1:50 rat serum in PBS
Staining solution for flow cytometry	Antibody (1:100, 1:200, 1:500; see section 2.1.7.1 to 2.1.7.5) in 50 µl PBS
Tail mouse lysis buffer	0.05 % TRIS pH 8.0 0.02 % NaCl 0.1 % EDTA pH 7.4 1 % SDS 10 mg/ml Proteinase K
TRIS (1 M)	121.1 g TRIS in 1 l ddH_2O pH 6.8
Trypsin/EDTA	0.2 mM EDTA in PBS 0.025 %Trypsin autoclaved

2.1.11 Antibiotics

Antibiotic solution	**Composition**
Penicillin-Streptomycin (10000 units/ml)	Invitrogen (Karlsruhe, G)
Doxycycline treatment	3 mg/ml DOX 1 % sucrose in autoclaved water

2.1.12 Animals

Animals were kept under pathogen-free conditions in a 12 h light–dark cycle at 21.5 °C and 60 % relative humidity. All animal experiments were performed according to the guidelines and with approval of the local institutional animal care committee.

2.1.12.1 Animals origin

Mice	Origin
Transgenic tetO-AML1-ETO responder mouse line	Kindly provided by Dr. Dong-Er Zhang (Department of Pathology, Division of Biological Sciences, and Moores UCSD Cancer Center; University of California San Diego, USA).
Knock-in ROSA26-iM2 effector mouse line	Kindly provided by Prof. Dr. Rolf Sprengel (Max-Plank Institute for Medical Research; Heidelberg, G).
CD45.1/B6 mouse line	Kindly provided by Prof. Dr. Bernd Arnold (Department of Molecular Immunology, German Cancer Research Center; Heidelberg, G).
Immunodeficient RAG2$^{-/-}$ mouse line	Kindly provided by Dr. med. Edgar Schmitt (Institute for Immunology; Universitätsmedizin Mainz, G).

2.1.13 Cell culture materials

2.1.13.1 Cell lines

Cell lines	Origin
Human embryonic kidney cells (HEK 293)	Provided by Carsten Weiss (Institute of Toxicology, Universitätsmedizin Mainz, G).

Kasumi-1	Originally established from a pediatric AML-M2 patient carrying the t(8,21) chromosomal translocation. Kindly provided by Dr. med. Georg Heß (Universitätsmedizin Mainz, G).

2.1.13.2 Medium used for cell culture

Culture media	Composition
HEK 293 culture media	10 % FCS 1 % L-Glutamine 1 % penicillin-streptomycin (P/S) in DMEM media
Kasumi-1 culture media	10 % FBS in RPMI 1640 media

2.1.13.3 Medium used for freezing cell lines

Freezing media	Composition
Freezing media	10 % DMSO in FCS

2.1.14 Equipment

Equipment	Company
Adhesive Seal Applicator	Thermo Scientific (Epson, UK)
Autoclave	KSG Steriliser (Olching, G)
Balance BP 2215	Sartorius (Goettingen, G)
Bench centrifuge 5417 C, 5417 R and 5810R	Eppendorf (Hamburg, G)
Canon digital IXUS55	Canon (Tokyo, J)
Cell culture hood HLB2472	BIO-FLOW Technik (Meckenheim, G)
Cell culture incubator	Nunc (Wiesbaden, G)

Cell culture vortex	Heidolph (Kehlheim, G)
Deep freezer (-80°C)	Snijders (Tilburg, NL)
Electrophoresis power supply E844	Consort (Mainz, G)
Electrophoresis unit	Work-shop Johannes Gutenberg- Universität (Mainz, G)
FACSAria	BD (Heidelberg, G)
FACSCalibur	BD (Heidelberg, G)
FACSVentage	BD (Heidelberg, G)
Hematology Analyzer (ADVIA120)	Bayer (Leverkusen, G)
Heating block	Dri-Block DB-3A Techne (Cambridge, UK)
Laboratory centrifuge 400 R	Haraeus (Hanau, G)
Laboratory shaker	UNIMAX 2010 Heidolph (Kehlheim, G)
Liquid nitrogen tank	Air Liquide Kryotechnik GmbH (Düsseldorf, G)
LSRII Analyzer	BD (Heidelberg, G)
MACS Multi Stand	MiltenyBiotec (Bergisch Gladbach, G)
Mastercycler ep realplex^4 S	Eppendorf (Hamburg, G)
Microscope binocular Olympus CK2 and S2X9	Olympus (Hamburg, G)
Microscope ELWD	Nikon (Düsseldorf, G)
Millipore H_2O-production unit	Milli-Q plus Millipore (Eschborn, G)
NanoDrop 2000 device	Thermo Scientific (Epson, UK)
pH-Meter	Multical Typ 538 (Weilheim, G)
Pipettes (p-20, p-200, p-1000)	Gilson (Bad Camberg, G)
Pipetman	Hirschmann instrument (Eberstadt, G)
Pipette Discovery	Abimed (Langenfeld, G)
Red lamp	Electric Petra (Burgau, G)
Refrigerator 4 °C Profi line	Liebherr (Biberach an der Riss, G)
Refrigerator -20 °C Premium	Liebherr (Biberach an der Riss, G)
Thermo Mixer Compact	Eppendorf (Hamburg, G)
UV-Transluminator and video system	LTF Labortechnik (Wasserburg, G)
Vortex	Heidolph (Kehlheim, G)
Water bath	Grant Science Services (München, G)

2.1.15 Computers, printers and software

Computer, printer or software	Company
Acer notebook	Acer (Ahrensburg, G)
Adobe Illustrator CS	Adobe (San Jose, USA)
Adobe Photoshop CP	Adobe (San Jose, USA)
CellQuest Pro Software	BD (Heidelberg, G)
Cell^F Analysis Image Processing	Olympus (Hamburg, G)
DELL Optiplex GX620	DELL (Frankfurt, G)
EndNote Web 2.8	Thomoson Reuters (New York, USA)
FACSDiva Software	BD (Heidelberg, G)
FlowJo 8.8.4 Software	TreeStar (Ashland, USA)
GraphPad Software Prism	GraphPad (La Jolla, USA)
iWord, iPowerpoint	Office for Macintosh (USA)
Keynote and Numbers	Office for Macintosh, Apple (USA)
MacBookPro notebook	Macintosh, Apple (USA)
Microsoft Office	Windows XP (USA)
Multispecies Software	Bayer (Leverkusen, G)
NanoDrop 2000/200C Software	Thermo Scientific (Epson, UK)
QPCR Software	Eppendorf (Hamburg, G)
Printer DELL 3100	DELL (Frankfurt, G)
Primer Express	ABgene; Thermo Scientific (Epson, UK)
Printer *hp* Photosmart C4580	Hewlett-Packard (Böblingen, G)

2.2 Methods

2.2.1 Genotyping of mice

2.2.1.1 Genomic DNA extraction

Genomic DNA was extracted from mouse-tail biopsies. Approximately 1 cm of the tail was cut and subsequently incubated with 750 µl lysis buffer containing 30 µl Proteinase K (0.5 mg/ml) at 55 °C overnight until the tissue was completely enzymatically digested. Samples were vortexed for 10 min, 250 µl of 5 M NaCl was added and vortexed for 10 min. In order to discard unwanted debris, samples were pelleted at 14000 rpm for 10 min and 700 µl of the supernatant was transferred into a new tube. To each sample, 220 µl of isopropanol was added and the DNA was pelleted at 14000 rpm for 10 min. Next, the DNA pellet was washed twice with 500 µl of 70 % ethanol and centrifuged on 14000 rpm for 10 min. Finally, the pellet was resuspended in 50 µl ddH_2O and incubated for 30 min at 55 °C. In order to completely dissolve all DNA samples, DNA solutions were stored overnight at 4 °C before their use. The genomic DNA extracted from mouse-tail biopsies was diluted 1:25 and subsequently used for PCR-mediated genotyping.

2.2.1.2 Polymerase Chain Reaction (PCR)

The PCR method was used in order to amplify a specific DNA fragment (Mullis et al. 1990). The use of designed oligonucleotides (primers) allows amplifying of a particular DNA sequence. This method is based on cycling reactions divided in three steps: (i) melting of double strand DNA, (ii) primer annealing and (iii) synthesis of new DNA strands by DNA polymerase (elongation).

All PCR amplifications were performed as described by Saiki and colleagues (Saiki, Gelfund et al.1988) in an end volume of 25 µl. The setup for the amplification of DNA was established by modifying the magnesium concentration or the annealing temperature. PCR primers used for genotyping are described under 2.1.3.

The conditions from a standard PCR are shown bellow:

Reagent	Volume (µl)
1:10 10 x PCR buffer (-$MgCl_2$)	2.5
dNTP mix (0.2 mM each dNTP)	1
forward primer (10 pM)	1
reverse primer (10 pM)	1
DNA (1:25)	1
$MgCl_2$ (5 mM)	4-6
ddH_2O	14-12
Taq polymerase (5 u/µl)	0.5

The following PCR thermal cycling program was performed in an Eppendorf Mastercycler Gradient instrument:

	Temperature (°C)	Time	Number of cycles
Denaturation	94	4 min	1
Denaturation	94	1 min	30
Annealing	58-60	30-60 sec	
Extension	72	1 min	
Final elongation	72	8 min	1

Finally, the PCR product was loaded onto an agarose gel.

2.2.1.3 Electrophoresis of DNA

Electrophoresis can be used for separating DNA fragments according to their molecular weight. This technique operates with an electric field to separate the negatively charged DNA molecules in a gel matrix, with shorter DNA molecules moving faster than longer ones. The gel was composed of 2 % of agarose diluted in 1x TBE containing 7 µl / 100 ml of ethidium bromide solution (10 mg/ml). This mixture was boiled in a microwave

oven and subsequently filled into a gel tray that contained a comb at one side. When the gel cooled down, the comb was removed with several pockets remaining in the gel. For electrophoresis, the gel was immersed into a chamber filled with 1x TBE. Then, a DNA ladder (marker from 1 kb or 100 bp) was loaded onto the first well. In order to monitor the migration of the samples in the gel, PCR-products were mixed with a loading buffer containing bromophenol blue and then loaded onto the gel. The power supply was switched on and a 50 ml gel was run at 50 V. DNA fragments were finally visualized using an UV transilluminator and documented with the TF-video system.

2.2.2 Cell Culture Techniques

2.2.2.1 Culture of eukaryotic cell lines

Human Embryonic Kidney cells (HEK 293) were cultured in Dulbecco's modified Eagle's media (DMEM) supplemented with 10 % of heat inactivated (45 min, 56 °C) fetal calf serum (FCS), 1 % of penicillin/streptomycin (P/S), and 2 mM of L- glutamine at 37 °C in humidified air with 5 % CO_2. Cells were subcultured twice per week.
Kasumi-1 cells were cultured in RPMI 1640 media (Gibco) supplemented with 10 % heat inactivated (45 min, 56 °C) fetal bovine serum (FBS), grown at 37 °C, 5 % CO_2 and 90 % humidity. Cells were split 1:2 to 1:3 every three days.

2.2.2.2 Freezing cells

HEK 293 cells were trypsinized using 0.25 % Trypsin-EDTA and washed with DMEM media. Then, cells were counted as described in section 2.2.5.4 and pelleted by centrifugation at 1200 rpm for 5 min. Next, cells were resuspended in 1 ml freezing media (FCS 10% DMSO, 1 ml per 7.5 x 10^5 cells), kept at -80 °C overnight and finally stored in liquid nitrogen.
To freeze the not adherently growing Kasumi-1 cell line, cells were counted, pelleted by 1200 rpm for 5 min and washed with RPMI 1640 media. Next, cells were resuspended in 1 ml freezing media, kept at -80 °C overnight and finally stored in liquid nitrogen.

2.2.2.3 Recovery of frozen cells

Vials were placed in a 37 °C water bath. In order to avoid DMSO toxicity, cells were transferred into 15 ml Falcon tubes, washed with DMEM or RPMI medium and centrifuged at 1200 rpm for 10 min. Pellets were resuspended with growth medium and transferred in 10 cm-culture dishes.

2.2.3 Quantitative Reverse Transcriptase-Polymerase Chain Reaction (QPCR)

2.2.3.1 Total RNA extraction from cells

In all steps involving RNA handling an RNase-free working environment was maintained. Total RNA was extracted from cells with the RNeasy Mini Kit (Qiagen) according to the manufacturer instructions. In all cases, DNase I treatment was performed to avoid unwanted contamination of genomic DNA. Finally, RNA was diluted in 30 µl RNase free water. Isolated RNA was stored at -20 °C.

2.2.3.2 Determination of the RNA concentration

The RNA concentration was determined in 1.5 µl volume using a nanodrop device (NanoDrop 2000, Nanodrop 2000/2000C software, Thermo scientific). As a blank calibrator, RNase free water (1.5 µl) was loaded onto the optical pedestal. All samples were measured in the same way. The purity of the isolated RNA was estimated by calculating the E260/E280 ratio in each sample (greater than 1.8).

2.2.3.3 Reverse transcription of RNA

First strand cDNA synthesis was performed with the SuperScript Reverse Transcriptase II (Invitrogen). In order to be able to exclude contamination of genomic DNA, all reactions were carried out with and without reverse transcriptase. A first master mix was prepared with 0.5 µl of Oligo dT (100 µM; 0.5 µg/µl), 0.5 µl of random hexamers (100 µM; 0.2 µg/µl) and 1 µl of dNTPs mix (0.2 mM each). Next, a final volume of 12 µl was achieved

by adding total RNA (0.5-1 µg) and RNase free water. Samples were incubated at 65 °C for 5 min and chilled on ice for 2 min. A second master mix was prepared with 4 µl of 5 x FS buffer and 2 µl of 0.1 M DTT, and applied to each tube. Subsequently, 1 µl of SuperScript II was added into every other sample. Finally, tubes were incubated at 42 °C for 50 min and inactivation of the reverse transcriptase was performed by heating samples to 70 °C for 15 min. cDNA was diluted in 20-60 µl H_2O and stored at -20 °C.

2.2.3.4 Real Time Polymerase Chain Reaction (QPCR)

All PCR amplifications were performed in triplicate and in a 25 µl final volume reaction. Triplicate Master Mix 1 (MMix1) reactions were as follows:
MMix1 prepared for hypoxanthine guanine phosphoribosyl transferase (hprt; house keeping gene)

Reagent	**Volume (µl)**
Absolute QPCR SYBR Green Mix (1 x)	44
forward primer (hprt; 10 pM)	1.5
reverse primer (hprt; 10 pM)	1.5
H_2O	33

MMix1 prepared for AML1-ETO

Reagent	**Volume (µl)**
Absolute QPCR SYBR Green Mix (1 x)	44
forward primer (AML1-ETO; 10 pM)	1.5
reverse primer (AML1-ETO; 10 pM)	1.5
H_2O	33

Eight microliters of 1:10 diluted cDNA solution was added to MMix1 and 25 µl pipetted into a SuperPlate 96-well PCR Plate (Thermo Scientific). In order to avoid air bubbles,

PCR plates were shortly centrifuged on 1000 rpm for 1 min and bubbles were removed with a pipette. Finally, the PCR plate was sealed with an adhesive seal.
The setup of the reaction is shown in the representation below:

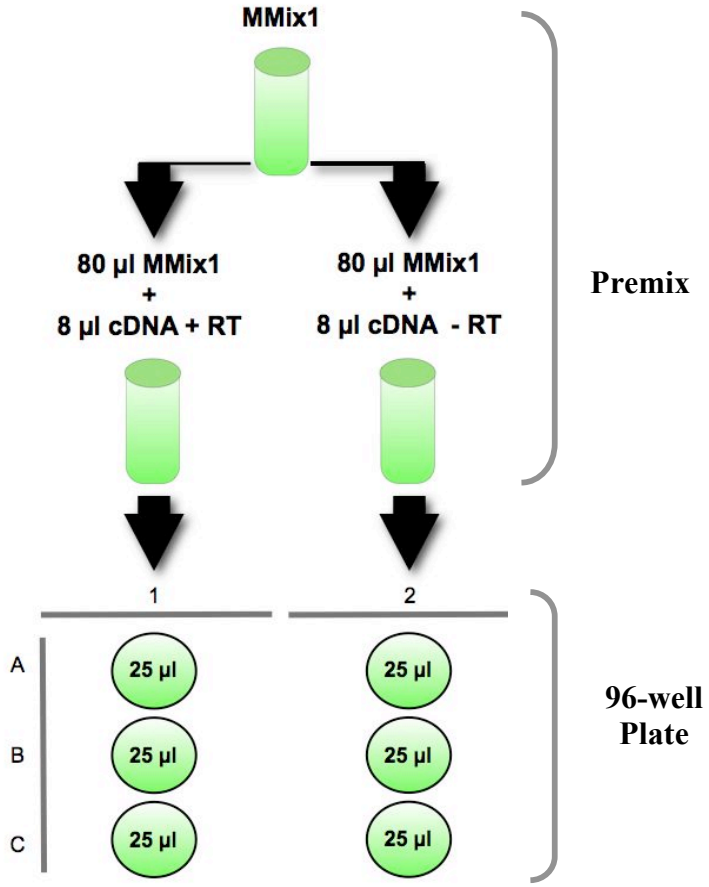

Figure 4: Schematic representation of a typical setup for the QPCR reaction
µl, microliters; RT, reverse transcriptase, MMix1, master mix 1

The following QPCR thermal cycling program was run on a Mastercycler ep realplex^4 S (Eppendorf):

	Temperature (°C)	Time	Number of cycles
Enzyme activation	95	15 min	1
Denaturation	95	15 sec	40
Annealing	55	30 sec	
Extension	72	30 sec	

To confirm the specificity of the reaction a melting curve analysis was performed after the amplification cycles:

	Temperature (°C)	Time	Number of cycles
Denaturation	95	30 sec	1
Starting temperature	60	30 sec	1
Melting step	60-95	15 sec	80

The fluorescent signal was monitored for each cycle (single reading at the end of the extension step) at 72 °C. The crossing point (Ct; cycle number at which the fluorescence exceeds the background signal) for each sample was determined with the second derivative maximum algorithm using an arithmetic baseline adjustment. The delta-delta Ct method was used for the relative quantification of mRNA levels (Schmittgen, 2001).

This method includes three calculation steps:

	Step	Formula
1	Normalization to Endogenous control	Ct Target gene- Ct Endogenous control = ΔCt
2	Normalization to Calibrator sample	ΔCt Sample- ΔCt Calibrator= ΔΔCt
3	Insertion of the normalized value	$2^{-\Delta\Delta Ct}$

2.2.3.5 Selection of QPCR primers

The cDNA of the human fusion protein for AML1-ETO was searched in the genomic NCBI data bank (NCBI; http://www.ncbi.nlm.nih.gov). In order to avoid amplification of AML1 or ETO wild type cDNA, one primer was selected from the AML1 coding region and the other from the ETO coding region (see picture bellow):

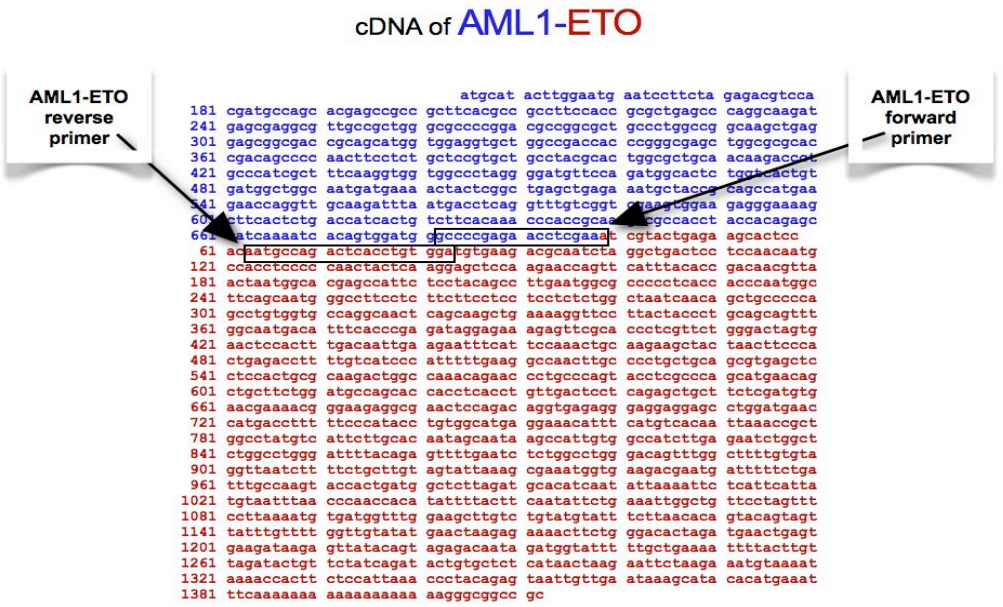

Figure 5: Human AML1-ETO nucleotid sequence (GenBank number AAB34819.2) showing the AML1-specific sequence in blue and the ETO-specific sequence in red
Primers are indicated.

QPCR primers were selected from the AML1-ETO cDNA with the help of the Program Primer Express (ABgene).

Hprt transcription was used as endogenous control. Hprt primers were kindly provided by Gorana Hollmann (Department of Molecular Immunology, German Cancer Research Center; Heidelberg, G).

2.2.3.6 QPCR primers

Lyophilized oligonucleotides were resuspended with ddH_2O and stored at 4 °C overnight. Primers were diluted to a final concentration of 10 pM/µl and stored at -20 °C.

Primers used for hprt and AML1-ETO amplification are represented bellow:

Primer	Sequence
Hprt forward	GCT CGA GAT GTC ATG AAG GAG AT
Hprt reverse	AGC AGG TCA GCA AAG AAC TTA TAG C

AML1-ETO forward	GCC CCG AGA ACC TCG AAA
AML1-ETO reverse	TCC ACA CGT GAG TCT GGC ATT

2.2.4 Induction of the tet-*on* system

In order to activate the expression of the conditional transgene, mice were treated with doxycycline (DOX). Three mg/ml of DOX and 1 % of sucrose was dissolved in autoclaved water and given to mice as a substitute of drinking water. Treated water was changed twice a week. Non-induced control mice were provided with normal drinking water.

2.2.5 Characterization of blood cell lineages from mice

2.2.5.1 Isolation of blood cells from mice

After sacrificing the mice by cervical dislocation, hematopoietic organs were removed and placed in cold modPBS on ice.

2.2.5.1.1 Isolation of bone marrow cells

Bone marrow cells were isolated from femur and tibia. Hind legs were dissected and the muscle tissue was removed using a scalpel and tissue paper. Cleaned bones were crushed with a pestle and a mortar. Cells were collected with a 1000 µl pipette and single-cell suspensions were obtained by passing the clumps through a 40 µm cell strainer. Finally, bone marrow cells were pelleted by centrifugation on 1200 rpm for 10 min.

2.2.5.1.2 Single-cell suspension from hematopoietic organs

Thymus, spleen and lymph node single-cell suspension were obtained by passing the whole organ through a 40 µm cell strainer using gentle pressure into cold modPBS. Cells were pelleted by centrifugation at 1200 rpm for 10 min.

2.2.5.2 Collection of peripheral blood from mice for flow cytometry

In order to obtain 100 µl of peripheral blood, a small cut was performed in the tail-vein of the mice. Whole blood was placed in Microtainer K2-EDTA-tubes (BD) and pelleted by centrifugation on 1200 rpm for 10 min. Erythrocytes were lysated as described in section 2.2.5.3 and cells were stained with 50 µl staining solution.

2.2.5.3 Lysis of erythrocytes

Erythrocytes from bone marrow, spleen and peripheral blood were lysated with a hypotonic lysis buffer, ACK buffer (Lonza). Cells were resuspended in 1-2 ml of lysis buffer, incubated for 3-5 min at room temperature, washed with PBS and finally, pelleted by centrifugation on 1200 rpm for 10 min.

2.2.5.4 Cell counting

Cells were diluted 1:100 or 1:1000 with Trypan blue, which is excluded by viable cells, in a 96-well-plate. 10 µl of each sample was used for cell counting in a Neubauer Chamber. Dead cells were excluded. The formula used for the calculation of total number of cells was the followed:

Formula	
Total number of cells (n)	$n= 10^4$ x dilution factor x volume (µl)

2.2.5.5 Differential blood parameters

Peripheral blood was obtained from a small cut performed in the mouse-tail vein. Whole blood was collected in Microtainer K2-EDTA-tubes (BD). In each case, 200 µl of whole blood and 100 µl of PBS/2 mM EDTA was transferred into a new tube. A blood cell count was performed using an automated hematological counter (Bayer ADVIA 120 Hematology Analyzer) with the mouse-specific software.

2.2.5.6 Preparation of peripheral blood smears

One drop of peripheral blood was collected with a yellow tip and placed on the extreme of a glass slide. A second slide was hold at an angle of 40-30° and put in contact with the drop. Pushing the top slide in one direction produced the final blood smear.

2.2.5.7 Giemsa staining of peripheral blood smears

Peripheral blood slides were fixed with 100 % of methanol for 30 seconds and subsequently washed with tap water. Smears were stained for 30 minutes with 10 % of freshly prepared Giemsa solution. Finally, peripheral blood smears were washed with tap water and air-dried.

2.2.5.8 Preparation of bone marrow smears and cytospins

Freshly prepared bone marrow cells were diluted to a final concentration of 0.5-1x10^5 cells per 200 µl of PBS. Samples were transferred in cytospin chambers (placed on microscope slides equipped with a two-hole paper filter) and centrifuged for 5 min on 500xg at room temperature. Smears were air-dried at least 1 h before staining.

2.2.5.9 Cell separation using Magnetic Activated Cell Sorting (MACS)

Cells were magnetically labeled with microbeads (50 nm in size) and separated using a magnetic field produced by the steel matrix of the MACS column, sitting in the MACS Separator. While the magnetically labeled cells are retained in the column, the unlabeled cells are contained in the flow through. To obtain the microbead-coated cells, MACS columns were removed, and the retained microbead-labeled cells were eluted.

2.2.5.9.1 Pan T-cell depletion using MACS

Freshly prepared bone marrow cells were isolated, erythrocytes were lysated and the total cell number was determined as described in sections 2.2.5.1, 2.2.5.3 and 2.2.5.4 respectively.

Next, cells were resuspended together with a solution of 10 µl of CD90 microbeads and 90 µl of MACS buffer per 10^7 cells. Cells were incubated for 20 min at 4 °C, then washed once in 1 ml of MACS buffer and resuspended in 500 µl MACS buffer per 10^8 cells. Single-cell preparations were obtained by passing suspensions through a 40 µm cell strainer.

For pan T-cell depletion, LS MACS columns (MiltenyiBiotec) were placed on a magnetic holder, and equilibrated with 2 ml of MACS buffer at room temperature. The flow-through was discarded and labeled cells were applied onto the column. Pan T-cells coupled with magnetic beads were retained in the column due to the magnetic field. Columns were rinsed with 3 x 1 ml of MACS buffer at room temperature, flow-through was collected and pooled by centrifugation at 1200 rpm for 10 min. As a quality control, a sample from each depleted fraction was taken and analyzed for purity using a FACSCalibur instrument (BD) as described in section 2.2.8.1. The efficiency of the depletion was in all cases greater than 90 %.

2.2.5.9.2 Purification of blood cells by indirect labeling

Freshly prepared bone marrow cells were isolated, erythrocytes were lysated and total cell number was determined as described in sections 2.2.5.1, 2.2.5.3 and 2.2.5.4 respectively.

Next, cells were resuspended in PE conjugated antibodies against B220 or CD3 or Ter119 or Gr-1 or CD11b. One µl of each antibody (1:100) was used per 1 x 10^6 cells. After 20 min incubation at 4 °C, cells were washed with PBS and centrifuged at 1200 rpm for 10 min. Subsequently, pellets were resuspended in a mixture of 10 µl of anti-PE microbeads and 100 µl of MACS buffer per 10^7 cells. Cells were incubated for 20 min at 4 °C, washed once in 1 ml of MACS buffer and resuspended in 500 µl MACS buffer per 10^8 cells. Single-cell preparations were obtained by passing the suspension through a 40 µm sieve. For positive selection, LD columns (MiltenyiBiotec) were placed on a

magnetic holder. Columns were pre-conditioned by equilibrating with 2 ml of MACS buffer at room temperature. Flow-through was discarded and labeled cells were applied onto the column. Columns were rinsed with 3 x 1 ml of MACS buffer at room temperature and the flow-through was discarded. Columns were removed from the magnetic field and rinsed with MACS buffer. Positive-labeled cells were collected in the flow-through and pelleted by centrifugation at 1200 rpm for 10 min. As a quality control, a sample from each eluted fraction was taken and analyzed for purity using a FACSCalibur instrument (BD) as described in section 2.2.8.1. The efficiency of the positive selection was in all cases greater than 90 %.

2.2.6 Bone marrow transplantation

2.2.6.1 Bone marrow transplantation

B6/CD45.1 or immunodeficient RAG2$^{-/-}$ mice were used as recipients and were irradiated with 950 or 450 rad respectively. Four to six hours after radiation bone marrow transplantation was performed. Bone marrow cells from donor mice were isolated, erythrocytes were lysated and cells were counted as described in sections 2.2.5.1, 2.2.5.3 and 2.2.5.4 respectively. To avoid a graft-versus-host reaction, T-cells were depleted with CD90 microbeads as described in section 2.2.5.9.1. Depleted bone marrow cells were counted and washed three times with PBS. Finally, 5 x 10^5 cells were mixed with 500 µl PBS and injected into mouse-tail veins. As a control, several mice were injected with PBS. All control mice died within 14 days after irradiation.

2.2.6.2 Confirmation of bone marrow reconstitution

Between six and eight weeks after transplantation, reconstitution was checked by flow cytometry. Mice were bled and erythrocytes were lysated as described in section 2.2.5.2. Subsequently, cells were labeled with fluorochrome-coupled CD4, CD8 and B220 antibodies as described in section 2.2.5.3 and percentages of T and B cells in peripheral blood were measured with a FACSCalibur instrument (BD).

2.2.7 Colony Forming Unit assay

Freshly prepared bone marrow cells were obtained as described in section 2.2.5.1. Bone marrow cells (1 x 10^4) were mixed with 1 ml of semi-solid MethoCult M3434 medium (Stem Cell technologies) and plated on a 6-well-plate. Colonies were counted after eight days using an inverted microscope (Nikon ELWD 0.3). Colonies were classified in three types CFU- colony-forming unit granulocyte/erythroid/macrophage/megakaryocyte (GEMM), colony-forming unit granulocyte/macrophage (CFU-GM), burst-forming unit erythroid (BFU-E) and scored according to the manufacturer's instructions. Representative images from BFU-E, CFU-GM and CFU-GEMM provided by StemCell Technologies are depicted in Figure 6.

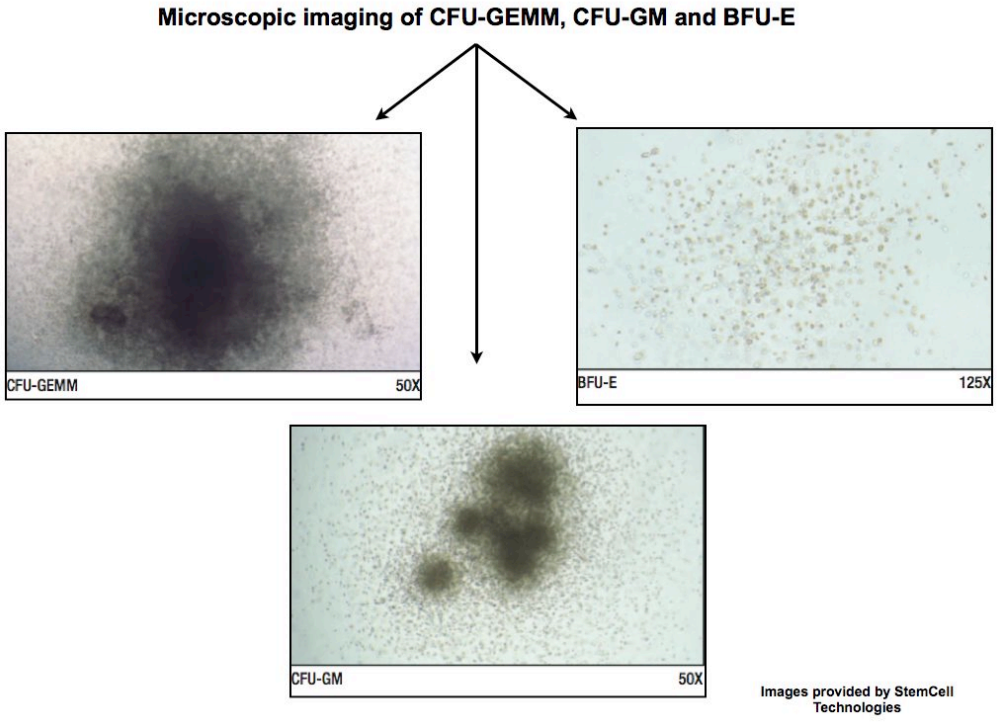

Figure 6: Colony forming assay
Representative images depicting CFU-GEMM, CFU-GM and BFU-E colonies provided by the StemCell Technologies manual.
CFUs, colony-forming units; CFU-GEMM, colony-forming unit granulocyte/erythroid/macrophage/ megakaryocyte; CFU-GM, colony-forming unit granulocyte/macrophage; BFU-E, burst-forming unit Erythroid.

2.2.8 Fluorescence Activated Cell Sorting (FACS)

2.2.8.1 Preparation of cells for FACS analysis

A number of 5 x 10^6 cells were resuspended and incubated with 1:50 rat serum for 15 min to avoid unspecific staining. Cells were washed with modPBS, centrifuged at 1200 rpm for 10 min and resuspended in 50 µl staining solution. Antibodies used were fluorochrome-coupled or biotinylated, diluted in PBS in 50 µl volume reactions. The dilution factor was depended on the fluorescence emission of the antibody as represented in section 2.1.7. Next, cells were incubated at 4 °C for 30 min. After labeling, excess of antibody was removed by washing cells with modPBS followed by centrifugation at 1200 rpm for 10 min. In case biotinylated antibodies were used, streptavidin (coupled with a selected fluorochrome) was used in the second staining step, followed by 30 min incubation time at 4 °C, washed with modPBS and pelleted at 1200 rpm for 10 min. Finally, cells were resuspended with 250 µl modPBS and analyzed with a FACSCalibur, FACSAria or BD LSRII Analyzer (BD).

2.2.8.2 Preparative isolation of cells using FACS

Cells were prepared as described in section 2.2.8.1 and kindly sorted by Dipl. Ing Julia Altmaier (FACS Core Facility; Universitätsmedizin Mainz, G) using a FACSVantage instrument (BD).

2.2.8.3 Collection and analysis of FACS data

Several programs were used for the collection and the analysis of the data. For acquisition of data on the FACSCalibur and FACSVantage instruments (BD) the CellQuest Pro software (BD) was used. In order to acquire data from the LSRII Analyzer and the FACSAria instruments (BD) the FACSDiva (BD) software was used. Subsequently, the FlowJo software (TreeStar) was employed for the downstream analysis and representation of the collected data.

2.2.8.4 Biostatistics and scientific graphing

Biostatistics analysis and the subsequent data representation were performed with the SPSS and the GraphPad Prism software (GraphPad Software, La Jolla, USA) using a MacBookPro notebook (Macintosh, Apple) or an Acer notebook (Ahrensburg, G).

2.2.9 Microscopy

2.2.9.1 Colony forming unit assay (CFUs) documentation

Colonies were counted after eight days using an inverted microscope (Nikon ELWD 0.3) according to the manufacturer's instructions (MiltenyiBiotec).

2.2.9.2 Blood and bone marrow smears documentation

Blood and bone marrow smears were documented using an Olympus BX50 W I microscope. Pictures were collected and digitally documented using the Olympus BX50 W I microscope. Finally, images were processed using the NIH ImageJ software and Adobe Photoshop CS.

2.2.10 Histopathology

2.2.10.1 Isolation of organs from mice

After sacrificing the mice by cervical dislocation, thymus, spleen, lymph node, lung, liver, brain, tongue, intestine, colon and skin were removed and placed in freshly prepared 2.5 % formaldehyde.

2.2.10.2 Histopathological analysis

Fixed organs were embedded in paraffin. Sections were stained with hematoxylin and eosin according to standard protocols or analyzed for apoptosis using the TUNEL assay as described in section 2.2.10.3. Images were generated using a standard diagnostic BX45

Microscope equipped with a C4040 digital camera (both Olympus, Hamburg, Germany) and Photoshop 7.0 (Adobe Systems, San Jose, CA). Histopathological analysis and interpretation of the data was kindly performed by Prof. Dr. Toni Lehr (Institute for Pathology, Lausanne, Switzerland) or Dr. Andreas Kreft (Universitätsmedizin Mainz, Germany).

2.2.10.3 Hematoxylin and Eosin staining of hematopoietic organs

Hematoxylin stains nucleic acids and thus results in blue staining of nuclei. Eosin nonspecifically stains proteins, resulting in cytoplasm and extracellular matrix appearing in pink. Hematoxylin and Eosin staining of hematopoietic organs was performed by Prof. Dr. Toni Lehr (Institute for Pathology, Lausanne, Switzerland) or Dr. Andreas Kreft (Universitätsmedizin Mainz, Germany).

2.2.10.4 TUNEL assay

Organ sections were analyzed using the TdT-mediated dUTP nick end labeling assay (Apo-BRDU; BD Biosciences Pharmingen, San Diego, CA) according to the manufacturer's instructions and were kindly performed and interpreted by Prof. Dr. Toni Lehr (Institute for Pathology, Lausanne, Switzerland).

3 RESULTS

3.1 Conditional AML1-ETO activation with the R26/AE mouse model directs generalized expression to HSC, progenitors and differentiated blood cells

In order to determine the *in vivo* consequences of AML1-ETO fusion protein expression for hematopoiesis, compound ROSA26-iM2/tetO-AML1-ETO (R26/AE) mice were generated allowing the conditional expression of AML1-ETO under the control of the ROSA26 (R26) locus (Soriano, 1999; Zambrowicz et al., 1997).

The R26 mouse model was generated by Wörtge and colleagues in Heidelberg and characterized by the support of our group in Mainz (Wörtge et al., 2010). This knock-in mouse line contains the iM2 reverse tetracycline-dependent transactivator-coding region and a tet-responsive humanized green fluorescence protein (hGFP) gene inserted into the R26 gene locus (Figure 7). The transgenic tetO-AML1-ETO mouse line includes the tetracycline-binding domain just upstream from the minimal promoter of the human cytomegalovirus driving transcription of AML1-ETO (Figure 7). AML1-ETO transgenic mice were kindly provided by Dr. Dong-Er Zhang and have been previously described (Rhoades et al., 2000). In aggregate, the compound R26/AE mouse model uses the tet on/off system to conditionally induce transgene expression (Gossen and Bujard, 2002). In this system, doxycycline (DOX), which is a derivate of tetracycline, is dissolved in water and given to mice as a substitute of normal drinking water. As shown in Figure 7 in the presence of DOX, AML1-ETO is conditionally activated whereas mice receiving normal drinking water will not express the transgene.

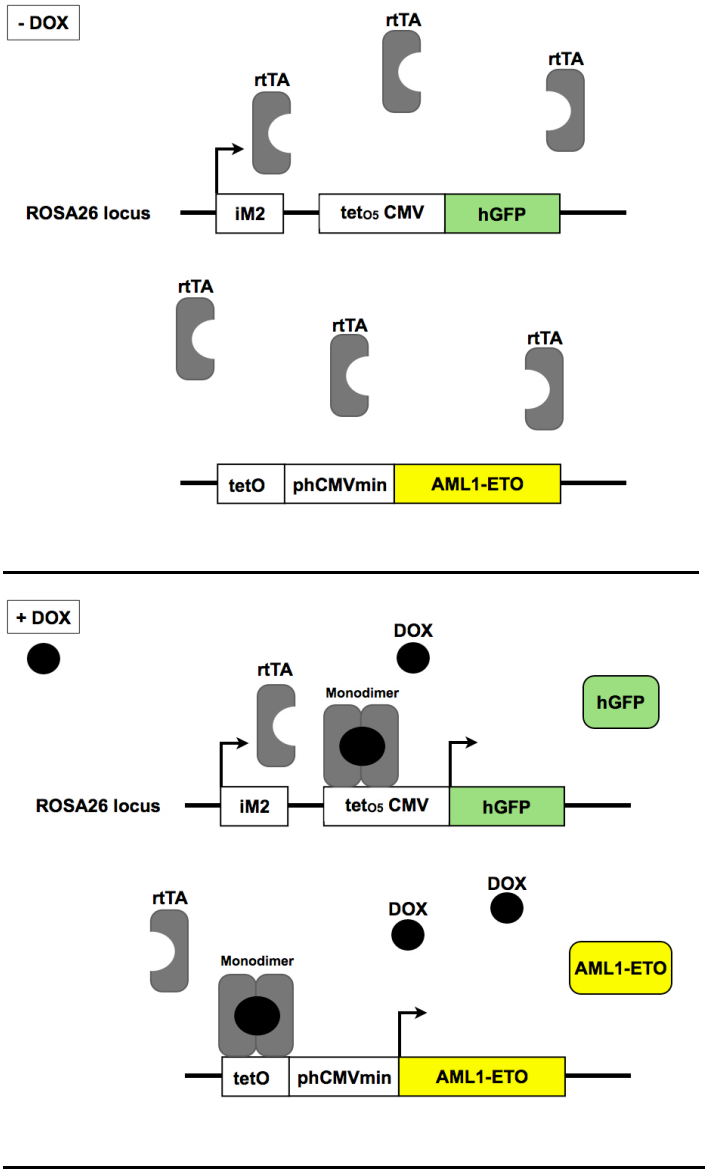

Figure 7: Schematic representation of the R26/AE mouse model that uses the tet on conditional induction system for AML1-ETO transgene expression

In the absence of doxycycline (-DOX) the reverse tetracycline transactivator (rtTA) cannot interact with the tetracycline-binding site and hGFP and AML1-ETO are not expressed. By contrary, when doxycycline is added, rtTA molecules can form monodimers and interact to the tetO binding sites and activate transcription of hGFP and AML1-ETO.

-DOX, absence of doxycycline; +DOX, presence of doxycycline; iM2, reverse tetracycline-dependent transactivator coding region; tetO5 CMV, tetracycline binding domain and cytomegavirus promoter; hGFP, green fluorescence protein; tetO, tetracycline binding domain; phCMVmin, minimal promoter of human cytomegaviurs.

Real-time quantitative PCR (QPCR) was performed to check the switchability and to discard any leakiness of the tet on system. Moreover, it was important to test if the R26 locus will direct conditional transgene expression to different hematopoietic lineages and to determine the relative level of AML1-ETO transcripts for each cell type. For the QPCR experiment, total RNA was extracted from the human Kasumi-1 cell line, and from whole bone marrow extracted from non-induced and AML1-ETO-induced R26/AE mice. Equally, sorted hematopoietic stem cells and immature progenitors, purified B- and T-cells, erythrocytes, megakaryocytes, macrophages and granulocytes were used as a source of mRNA. In order to be able to exclude any contamination with genomic DNA,

all reactions were carried out with and without reverse transcriptase. Finally, QPCR reactions of each sample were run in triplicate and three independent experiments were performed for each cell type. The delta-delta Ct method was chosen for the relative quantification of mRNA levels (Schmittgen, 2001). This method takes the cycle number into account at which the fluorescence exceeds the background signal (Ct) from the gene to be studied, which is then normalized to a selected housekeeping gene (ΔCt). Thus, different amounts of cDNA can be normalized between the samples. Finally, the ΔCt value is normalized to a calibrator sample (ΔΔCt). The statistical representation of the data represents the value calculated using the formula $2^{-\Delta\Delta Ct}$, where ΔΔCt is $Ct^{Kasumi\text{-}1}$- ($Ct^{AML1\text{-}ETO}$- Ct^{hprt}). In all cases hprt was used as housekeeping gene for normalization. In order to compare the levels of AML1-ETO mRNA in the R26/AE mouse model to a generally used standard, the Kasumi-1 cell line was used as a calibrator. Kasumi-1 cells were originally established from a seven-year-old Japanese boy with AML subtype M2 in relapse and after bone marrow transplantation (Asou et al., 1991).

To demonstrate the switchability and the lack of leakiness of the system, whole bone marrow from R26/AE mice, treated for three days with DOX, and bone marrow cells from genetically identical animals, fed with normal drinking water, were isolated and levels of AML1-ETO transcripts were measured using QPCR. As shown in Figure 8, no detectable levels of AML1-ETO transcripts were present in non-induced bone marrow. As expected, bone marrow cells from induced R26/AE animals showed detectable AML1-ETO transcription. To establish if the R26 locus will direct conditional transgene expression to different hematopoietic lineages, progenitors and hematopoietic stem cells (LKS; $lineage^-$, c-Kit^+, Sca-1^+), B-cells (B220), T-cells (CD3), erythrocytes (Ter119), megakaryocytes (CD41), macrophages (CD11b) and granulocytes (Gr-1) from AML1-ETO-induced R26/AE mice were analyzed. As shown in Figure 8 all tested lineages expressed AML1-ETO mRNA. Erythrocytes and granulocytes showed higher AML1-ETO transcription levels than Kasumi-1 cells. Meanwhile, compared to Kasumi-1 cells, lower levels of AML1-ETO mRNA were found in LKS and CD11b cells. Finally, megakaryocytes, B- and T-cells showed the lowest levels of AML1-ETO transcription when compared to Kasumi-1 cells. Taken together, these data confirm that AML1-ETO expression in R26/AE mice was switchable and completely dependent on the presence of DOX. All blood cell lineages analyzed, including hematopoietic stem and progenitors cells, transcribed AML1-ETO, and the measured mRNA levels were comparable to those

found in the Kasumi-1 cell line. Therefore, it is to be concluded that the R26/AE mouse is a powerful experimental model that can be used to investigate the role of the AML1-ETO fusion protein *in vivo*.

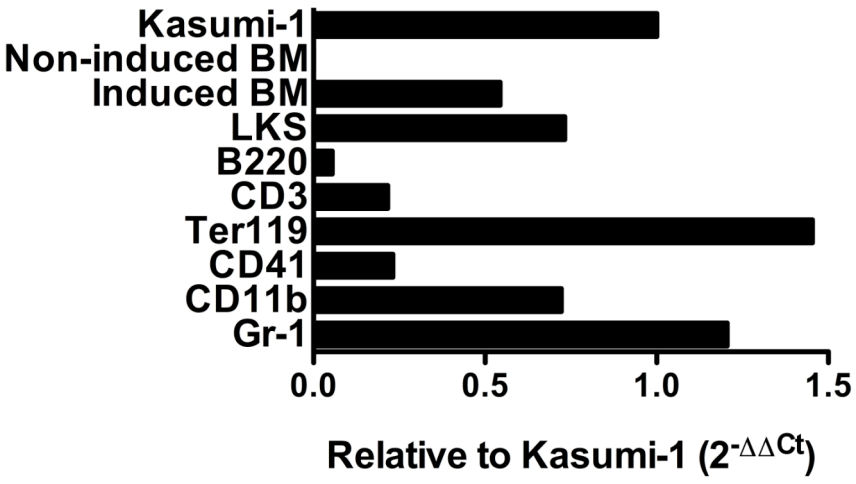

Figure 8: Real time PCR analysis
Statistical representation of values calculated using the delta delta Ct method. $2^{-\Delta\Delta Ct}$ is calculated by $\Delta\Delta Ct = Ct^{Kasumi-1} - (Ct^{AML1-ETO} - Ct^{hprt})$ where Ct is the cross point at which the fluorescence exceeds the background signal. BM, bone marrow; LKS, $lineage^-$, $c\text{-}Kit^+$, $Sca\text{-}1^+$ cells; B220, B-cells; CD3, T-cells; Ter119, erythrocytes; CD41, megakaryocytes; CD11b, macrophages; Gr-1, granulocytes.

3.2 Generalized expression of the AML1-ETO fusion protein in bi-transgenic R26/AE mice leads to rapid lethality

To evaluate the effect of aberrant AML1-ETO protein expression in R26/AE mice, a group of 18 mice was treated with doxycycline (Figure 9A; +DOX). In addition, a genetically identical group of 18 animals was kept on normal drinking water (Figure 9A; -DOX). The Kaplan-Meier survival curve (Figure 9B) shows the percentage of alive mice following AML1-ETO induction. Unexpectedly, after just ten days of AML1-ETO expression, only 50 % of the mice were still alive. Mice that expressed the AML1-ETO fusion protein rapidly lost weight and showed less mobility. Additionally, epidermal hyperplasia was observed in AML1-ETO-expressing mice (data not shown). The control group fed with normal drinking water remained healthy during the whole experiment. Because of the close relationship of the AML1-ETO fusion protein to AML disease, it

was decided to focus the analysis on hematopoietic organs, hematopoietic stem cells, progenitors and differentiated blood cells.

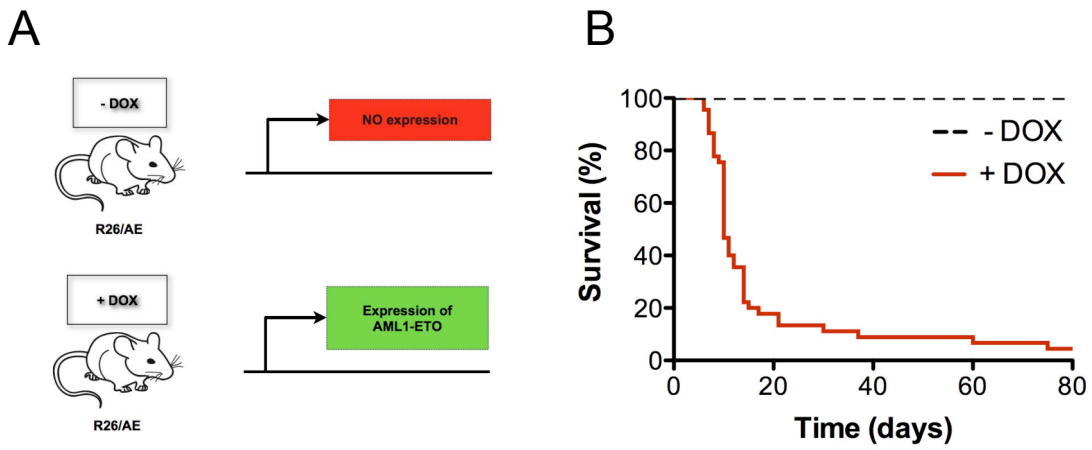

Figure 9: Conditional AML1-ETO expression in R26/AE mice and Kaplan-Meier curve showing the effect of generalized AML1-ETO expression on overall survival.
(A) Representation of R26/AE model that uses the tetracycline on/off conditional induction system for transgene expression.
(B) Kaplan-Meier survival curve.
R26/AE, Rosa26/AML1-ETO mice; -DOX, without doxycycline; +DOX, with doxycycline.

3.3 Aberrant expression of the AML1-ETO fusion protein promotes thymic atrophy, splenomegaly and enlargement of the lymph nodes

In order to identify phenotypical differences between hematopoietic organs from R26/AE mice expressing AML1-ETO protein and the control group, thymus, spleen and lymph nodes were removed, weighted and photographically documented.

In Figure 10, an organ weight diagram of R26/AE mice fed with normal drinking water is represented by white boxes (-DOX) and black boxes show the organ weight of R26/AE mice exposed to DOX for fourteen days (+DOX). Representative pictures from the thymus, the spleen and the lymph node are shown in the upper part of the Figure 10. After fourteen days of AML1-ETO expression, the thymus presented a dramatic reduction in size and weight compared to control mice. Furthermore, spleen and lymph nodes were significantly bigger when compared to non-induced organs. These results indicated that the expression of AML1-ETO fusion protein in R26/AE mice promotes a size reduction of the thymus, splenomegaly and enlargement of the lymph nodes.

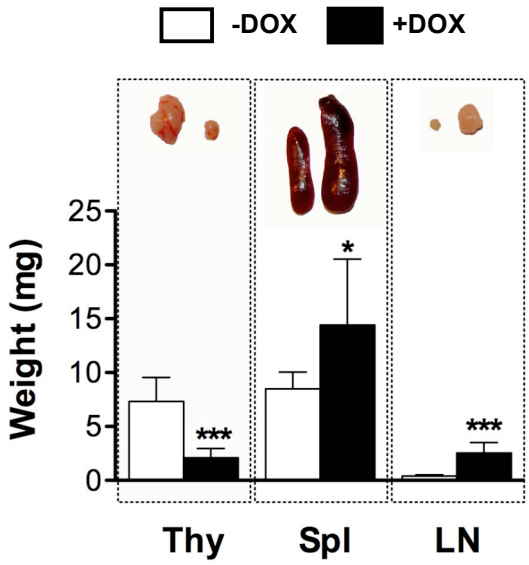

Figure 10: Representative images and statistical representation of the organ-weights in thymus, spleen and lymph nodes from AML1-ETO-expressing and control mice
-DOX, without doxycycline; +DOX, with doxycycline; Thy, thymus; Spl, spleen; LN, lymph node; *p<0.05; ***p<0.001. The bar diagrams represent the mean weight values ± standard deviations from at least eight mice in each group.

3.4 Short-term AML1-ETO expression dysregulates peripheral blood parameters

To further investigate the consequences of aberrant AML1-ETO protein expression for blood cells, a peripheral blood analysis with at least eight mice in each group was performed. Mice were bled from the tail vein and blood was collected in Microtainer K2E tubes (BD). Finally, blood was diluted in peripheral blood buffer and peripheral blood counts were determined in the Institute of Clinical Chemistry and Laboratory Medicine at the Medical Center of Johannes-Gutenberg University of Mainz, using an ADVIA120 Hematology Analyzer running on the Multispecies Software (Bayer, Leverkusen, Germany). The statistical representations of the obtained results are shown in Figure 11. The peripheral blood analysis indicated a significant drop in white blood cells (WBC) and lymphocytes (LY) and a dramatic increase in neutrophils (NE) and basophils (BA). Meanwhile, a moderate decrease of monocytes (MO) and platelets (PLT) together with a significant increase in numbers of large myeloperoxidase-unstained cells (LUC) was observed. Eosinophils (EO), red blood cells (RBC) and hemoglobin (HB) levels appeared normal when compared to those obtained from the control group. In

aggregate, AML1-ETO expression in R26/AE mice promoted a pronounced drop in WBC, LY, MO and PLT numbers and an increase in NEs, BAs and LUCs.

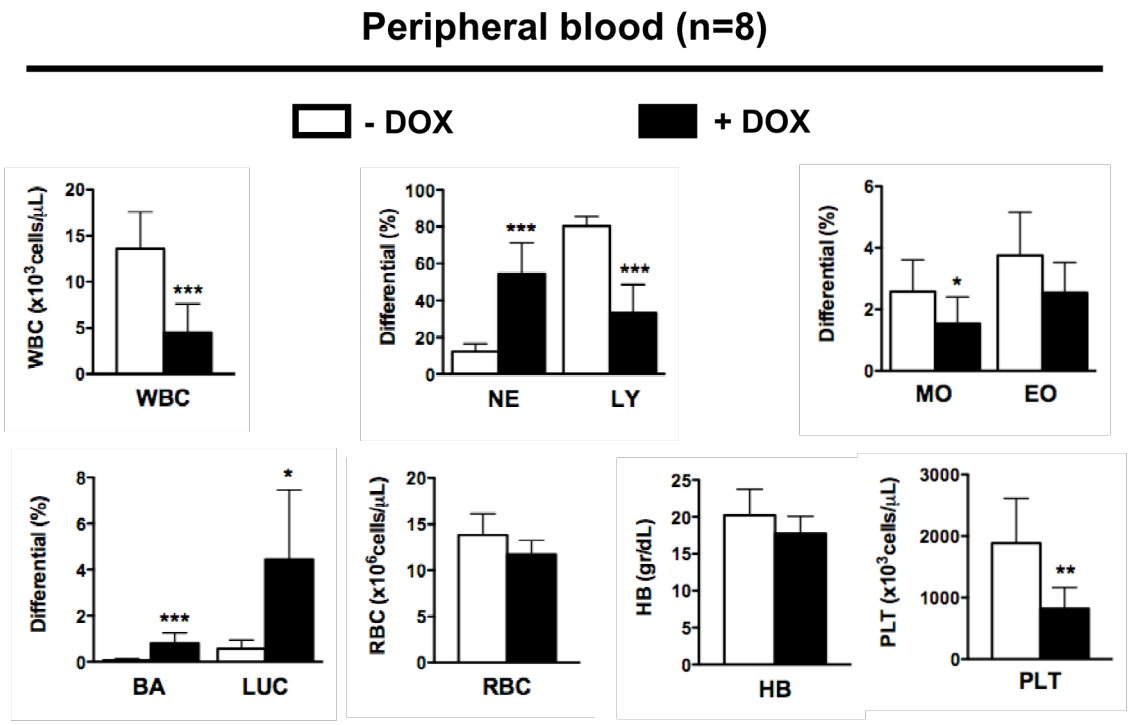

Figure 11: Peripheral blood analysis of AML1-ETO-expressing and control mice
Peripheral blood parameters of R26/AE mice fed with normal drinking water are represented as white boxes (-DOX), and the values of R26/AE mice that expressed the AML1-ETO fusion protein are depicted as black boxes (+DOX). The bar diagrams represent the mean values of peripheral blood parameters ± standard deviations. -DOX, without doxycycline; +DOX, with doxycycline; n, number of mice; WBC, white blood cells; NE, neutrophils; LY, lymphocytes; MO, monocytes; EO, eosinophils; BA, basophils; LUC, large unstained cells; RBC, red blood cells; HB, hemoglobin; PLT, platelets; *p<0.05; **p<0.01; ***p<0.001.

3.5 Histopathology

3.5.1 Histopathology of the thymus, the spleen and the lymph node

In order to determine the consequences of constitutive AML1-ETO expression for the morphology of hematopoietic organs, a histopathological analysis was performed. Thymus, spleen and lymph nodes were removed from R26/AE mice, treated with DOX and from genetically identical mice, fed with normal drinking water. Next, organs were fixed in 2.5 % formaldehyde, embedded in paraffin, and sections stained with hematoxylin and eosin. The histopathological analysis and the interpretation of the data

were done by Prof. Dr. Toni Lehr (Institute of Pathology, Lausanne, Switzerland) or Dr. Andreas Kreft (Medical Center of Johannes-Gutenberg University, Mainz, Germany).

3.5.1.1 Thymus

Histopathological analysis of the thymus revealed a profound perturbation in the overall structure of this organ. As shown in Figure 12, microscopic analysis (x4 and x40) indicated that the cortico-medullary compartmentalization in AML1-ETO-expressing thymus was entirely lost (Figure 12C and D). In addition, the brown fat, which normally surrounds the hilus region in abundance, was markedly reduced and atrophic in AML1-ETO-induced mice (Figure 12C). Regarding the analysis of higher magnifications (x40), it emerged that the thymus of AML1-ETO-expressing mice showed massive apoptosis (Figure 12D). Taken together, the thymus structure of AML1-ETO-expressing mice was considerably perturbed and showed an increase in apoptotic cells.

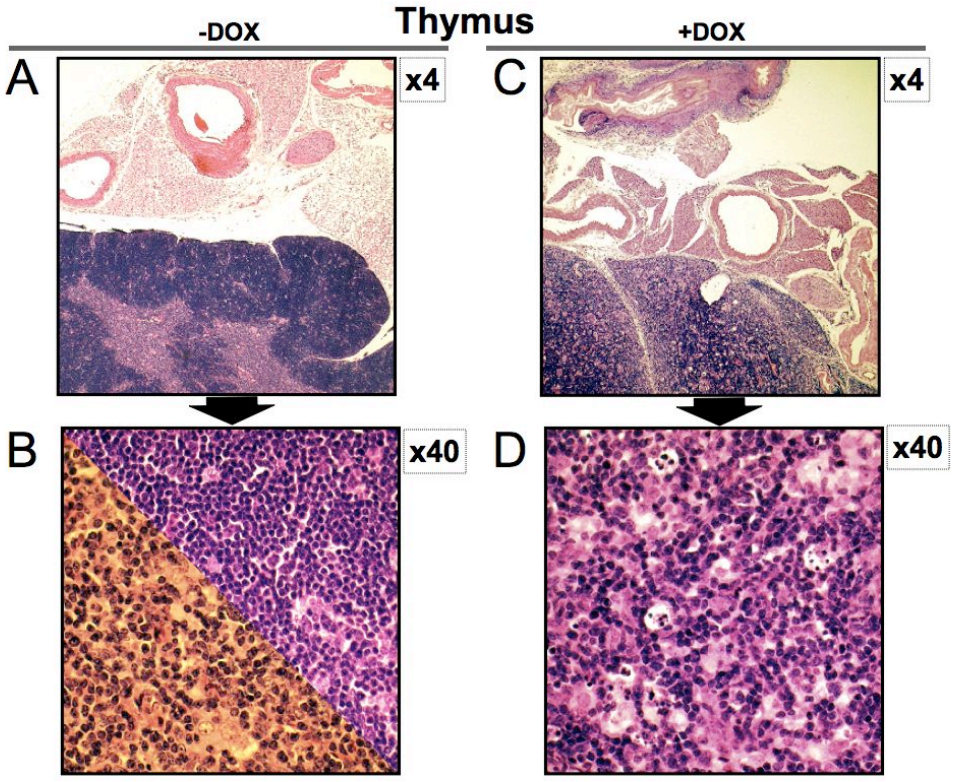

Figure 12: Hematoxylin and eosin staining of representative thymus sections from AML1-ETO-expressing mice (right) and controls (left)
(A) Hematoxylin and eosin staining of a representative thymus section from a non-induced-R26/AE mouse. **(B)** Higher magnification of a hematoxylin and eosin staining of a representative thymus section from a non-induced-R26/AE mouse.

(C) Hematoxylin and eosin staining of a representative thymus section from an AML1-ETO-expressing mouse. Note the loss of the cortex-medullary compartmentalization and the surrounding fat tissue.
(D) Higher magnification of a hematoxylin and eosin staining of a representative thymus from an AML1-ETO-expressing mouse. Note the loss of the cortex-medullary compartmentalization and the increase in apoptotic cells.
The magnification of each section is indicated on the right. -DOX, without doxycycline; +DOX, with doxycycline.

3.5.1.2 Spleen

Histopathological analysis of the spleen revealed that induction of AML1-ETO resulted in a profound change in normal spleen architecture characterized by a loss of the demarcation between red and white pulp (Figure 13C) when compared to the control (Figure 13A). Furthermore, the germinal centers of the spleen, which were clearly discernible within the white pulp of control mice (Figure 13A), became completely amorphous in induced animals (Figure 13C). Moreover, higher magnification showed an increase of apoptotic cells in AML1-ETO-expressing mice (Figure 13D) when compared to non-induced animals (Figure 13B).

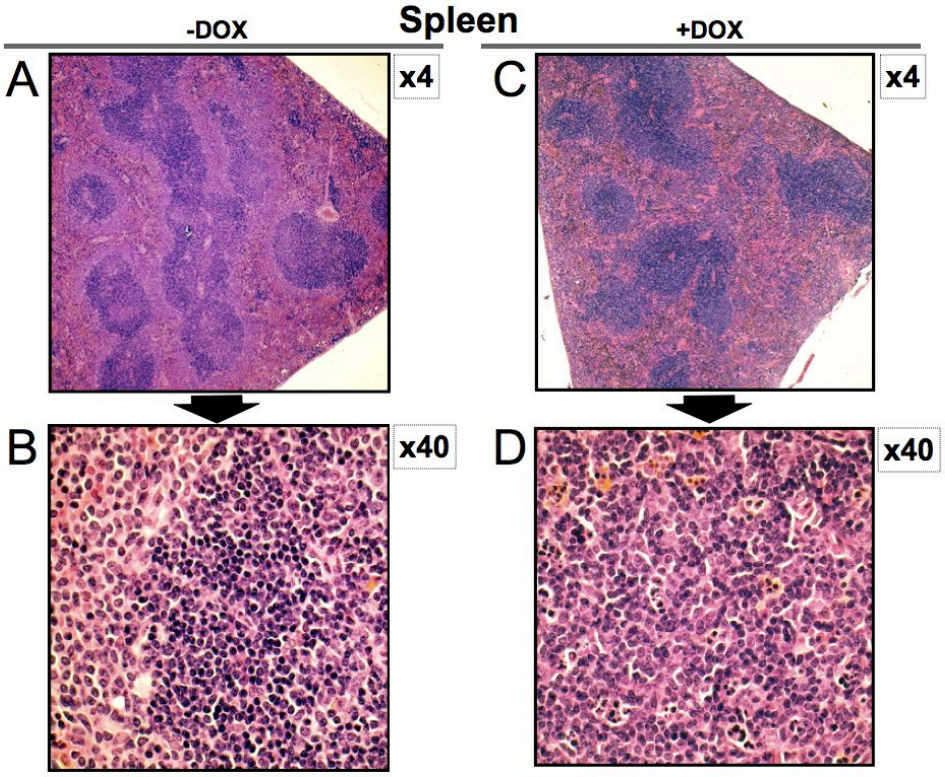

Figure 13: Hematoxylin and eosin staining of representative spleen sections from AML1-ETO-expressing mice (right) and controls (left)
(A) Hematoxylin and eosin staining of a representative spleen section from a non-induced R26/AE mouse.
(**B)** Higher magnification of a hematoxylin and eosin staining of a representative spleen section from a non-induced R26/AE mouse.

(C) Hematoxylin and eosin staining of a representative spleen section from an AML1-ETO-expressing mouse. Note the amorphous structure of the germinal centers within the white pulp.
(D) Higher magnification of a hematoxylin and eosin staining of a representative spleen section from an AML1-ETO-expressing mouse. Note the higher incidence in apoptotic cells.
The magnification of each section is indicated on the right. -DOX, without doxycycline; +DOX, with doxycycline.

3.5.1.3 Lymph nodes

Microscopic inspection of the lymph nodes revealed the complete transformation of the germinal centers with a compacted marginal region surrounding a central core, which contained more loosely packed cells in AML1-ETO-expressing mice (Figure 14C). Of note was the striking lack of periganglionic fat tissue in the induced state (Figure 14C). Moreover, higher magnification showed an increase of apoptotic cells in AML1-ETO-expressing (Figure 14D) compared to non-induced animals (Figure 14B).

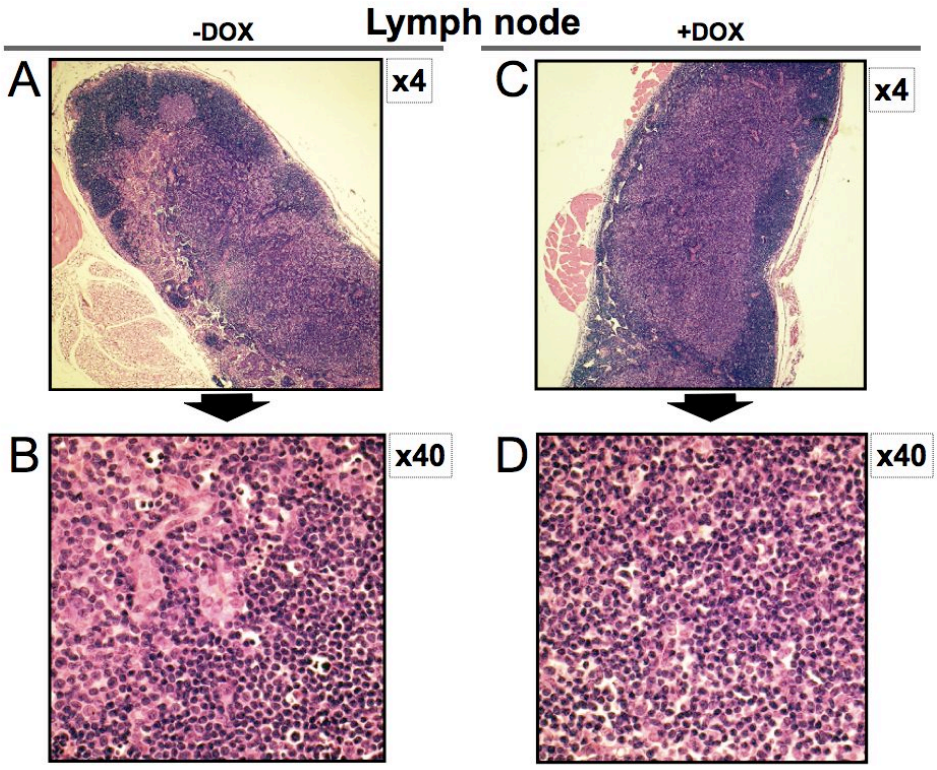

Figure 14: Hematoxylin and eosin staining of representative lymph node sections from AML1-ETO-expressing mice (right) and controls (left)
(A) Hematoxylin and eosin staining of a representative section from the lymph node of a R26/AE non-induced mouse.
(B) Higher magnification of a hematoxylin and eosin staining of a representative section from the lymph node of a non-induced R26/AE mouse.

(C) Hematoxylin and eosin staining of a representative section from the lymph node of an AML1-ETO-induced mouse.
(D) Higher magnification of a hematoxylin and eosin staining of a representative section from the lymph node of an AML1-ETO-induced mouse.
The magnification of each section is indicated on the right. -DOX, without doxycycline; +DOX, with doxycycline.

In aggregate, the histopathological analysis indicated that hematopoietic organs undergo rapid modification after conditional expression of the AML1-ETO transgene for fourteen days.

3.6 Flow cytometric analysis reveals a profound perturbation of normal hematopoiesis

Because of the close relationship between the AML1/RUNX1 protein and blood disorders, like familial platelet disorders, myeloproliferative disease and AML (De Braekeleer et al., 2009; Harada and Harada, 2009), it was important to analyze changes in normal hematopoiesis after enforced AML1-ETO expression. In order to specifically characterize different blood cell populations, including hematopoietic stem cells and progenitors, flow cytometry was used.

3.6.1 Erythropoiesis is compromised in AML1-ETO-expressing mice

Erythroid maturation was monitored following the Lodish flow cytometry analysis protocol. In the past, the group of Prof. Harvey Lodish published that using anti-CD71 and anti-Ter119 antibodies, four stages of erythroid-maturation can be identified (Socolovsky et al., 2001). Following this method, the most immature erythroid cells are the proerythroblasts, described as $CD71^{+}/Ter119^{low}$ (see Figure 15, quadrant I) followed by the basophilic erythroblasts, defined by $CD71^{+}/Ter119^{+}$ expression (quadrant II). In addition, the late baso- and chromatophilic erythroblasts are found within the $CD71^{low}/Terr19^{+}$ population (quadrant III) and the most mature red blood cell population including reticulocytes and orthochromatophilic erythroblasts, is defined by $CD71^{-}/Ter119^{+}$ expression (quadrant IV). Using these criteria, the analysis of erythropoiesis after fourteen days of AML1-ETO expression in bi-transgenic R26/AE mice (+DOX;

right plot) revealed a significant reduction in basophilic- (II) and late baso- and chromatophilic erythroblasts (III) and an increase in orthochromatophilic erythroblast (IV) when compared to the control group (-DOX; left plot). The statistical analyses of relative (Figure 15B) and absolute percentages (Figure 15C) of red blood cell maturation patterns (I to IV) are represented as bar diagrams where maturation stages from R26/AE mice fed with normal drinking water are shown as white boxes (-DOX) and R26/AE mice that expressed the AML1-ETO fusion protein are depicted as black boxes (+DOX). These results indicated that erythropoiesis is profoundly disturbed in AML1-ETO-induced mice, apparent by a reduced number in basophilic erythroblasts (II) and late baso- and chromatophilic erythroblasts (III) and an increase in number of orthochromatophilic erythroblast (IV).

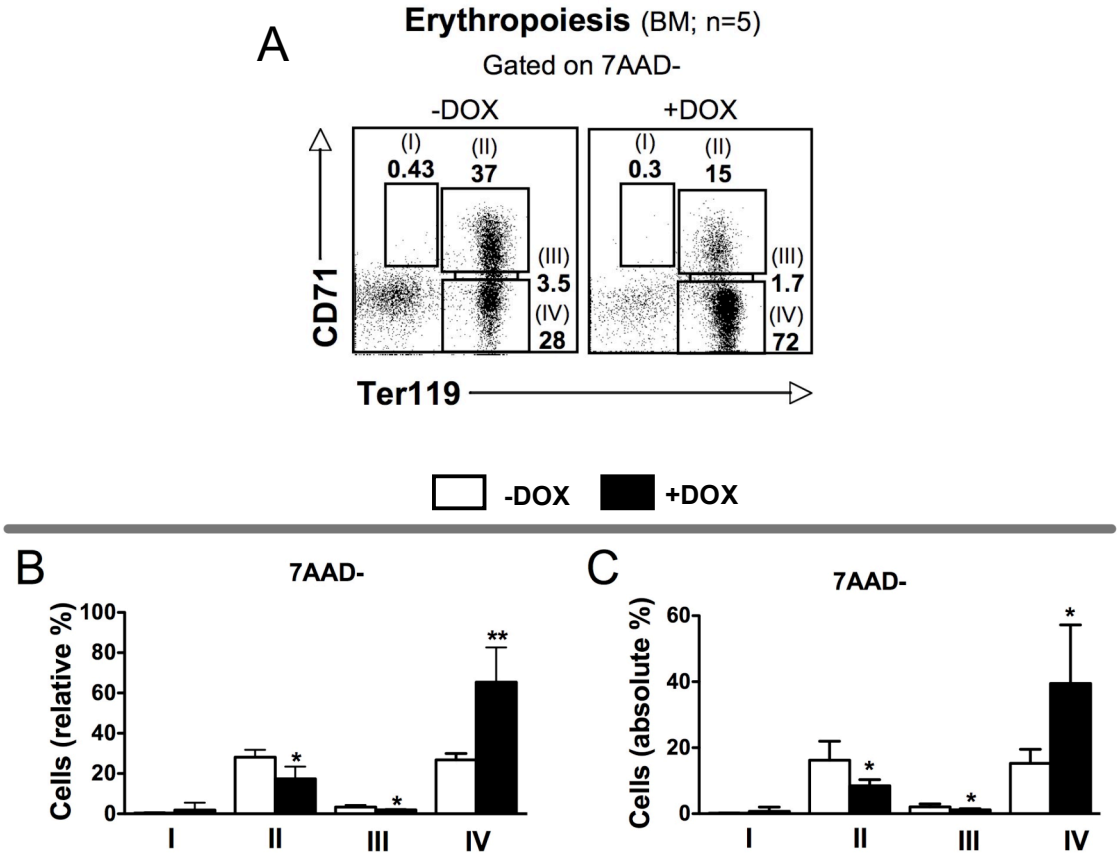

Figure 15: FACS analysis of erythropoiesis
(A) Representative dot plots depicting red blood cell maturation patterns (I to IV) from a control (left plot) and an AML1-ETO-induced mouse (right plot).
(B) Bar diagrams showing relative percentages of red blood cell maturation stages from non-induced (-DOX, white boxes) and AML1-ETO-induced mice (+DOX, black boxes).
(C) Bar diagrams showing absolute percentages of red blood cell maturation stages from non-induced (-DOX, white boxes) and AML1-ETO-induced mice (+DOX, black boxes).

BM, bone marrow; n, number of animals; 7AAD, 7-amino-actinomycin; -DOX, without doxycycline; +DOX, with doxycycline; I, proerythroblasts; II; basophilic erythroblasts; III; late basophilic erythroblasts and chromatophilic erythroblasts; IV, orthochromatophilic erythroblasts; *p<0.05; **p<0.01. Dead cells were excluded by 7AAD staining. The bar diagrams represent the mean values of relative or absolute cell percentages ± standard deviations from at least five mice in each group.

3.6.2 Flow-cytometry analysis of megakaryocytes

In order to analyze the consequences of AML1-ETO expression for megakaryocytes in the bone marrow, more immature and mature populations of megakaryocytes were experimentally determined using c-Kit and CD41 surface markers. Immature megakaryocytes are defined by c-Kit$^+$/CD41$^+$ and mature megakaryocytes fall within the c-Kit$^-$/CD41$^+$population (Salek-Ardakani et al., 2009). As shown in Figure 16 representative flow cytometric dot plots are depicted for a control mouse (16A; -DOX) and for an AML1-ETO-expressing mouse (16A; +DOX). Bone marrow cells from AML1-ETO-expressing mice displayed a pronounced increase in c-Kit$^+$/CD41$^+$ cells when compared to control mice. However, the c-Kit$^-$/CD41$^+$ population did not show any significant changes in either relative or absolute percentages (Figure 16B and C). In aggregate, aberrant short-term expression of AML1-ETO protein promoted an increase in immature megakaryocytes but not in mature megakaryocytes in the bone marrow.

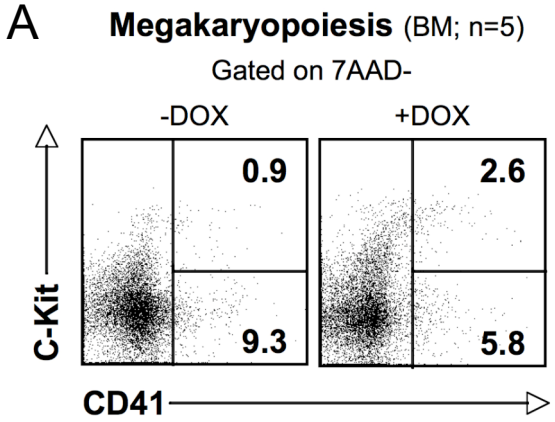

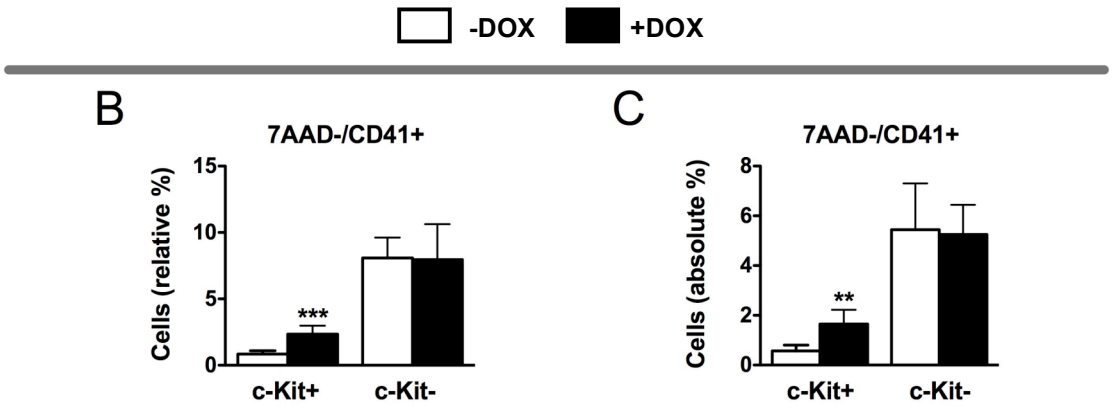

Figure 16: FACS analysis of immature (c-Kit$^+$/CD41$^+$) and mature megakaryocytes (c-Kit$^-$/CD41$^+$)
(A) Representative dot plots depicting immature (upper right quadrant) and mature megakaryocytes (lower right quadrant) from a control (left plot) and an AML1-ETO-induced mouse (right plot).
(B) Bar diagrams showing relative percentages of immature (c-Kit$^+$) and mature megakaryocytes (c-Kit$^-$) from non-induced (-DOX, white boxes) and AML1-ETO-induced mice (+DOX, black boxes).
(C) Bar diagrams showing absolute percentages of immature (c-Kit$^+$) and mature megakaryocytes (c-Kit$^-$) from non-induced (-DOX, white boxes) and AML1-ETO-induced mice (+DOX, black boxes).
BM, bone marrow; n, number of animals; 7AAD, 7-amino-actinomycin; -DOX, without doxycycline; +DOX, with doxycycline; **p<0.01; ***p<0.001. Dead cells were excluded by 7AAD staining. The bar diagrams represent the mean values of relative or absolute percentages ± standard deviations from at least five mice in each group.

3.6.3 AML1-ETO-expressing mice show a perturbation of granulopoiesis in bone marrow and spleen

Under normal circumstances, granulopoiesis occurs in the bone marrow. Additionally, a small percentage of granulocytes are also present in the spleen (Basu et al., 2004; Strauss-Ayali et al., 2007). To further study the granulocyte behavior in aberrantly AML1-ETO-expressing mice, CD11b and Gr-1 antibodies were used to distinguish between granulocytic progenitors (CD11b$^+$/Gr-1^{low}) and mature granulocytes (CD11b$^+$/Gr-1^{high}) in the bone marrow (Figure 17A). In addition, splenic granulocytes (CD11b$^+$/Gr-1$^+$) were analyzed (Figure 17B). The statistical analyses of relative (Figure 17C and E) and absolute percentages (Figure 17D and F) of immature (Gr-1^{low}) and mature granulocytes (Gr-1^{high}) in the bone marrow and granulocytes in the spleen (CD11b$^+$/Gr-1$^+$) are represented as bar diagrams. Flow cytometry revealed a significant expansion in absolute and relative numbers of granulocytic progenitors in the bone marrow and of granulocytes in the spleen (Figure 17A and B). However, a significant reduction in absolute and relative numbers of more mature granulocytes in the bone

marrow was observed. Together, mice expressing the AML1-ETO fusion protein showed an increase in granulocytic progenitors (Gr-1^{low}) in the bone marrow and an overall expansion of splenic granulocytes (CD11b^{+}/Gr-1^{+}). Moreover, a significant decrease in mature granulocytes (Gr-1^{high}) in the bone marrow was observed.

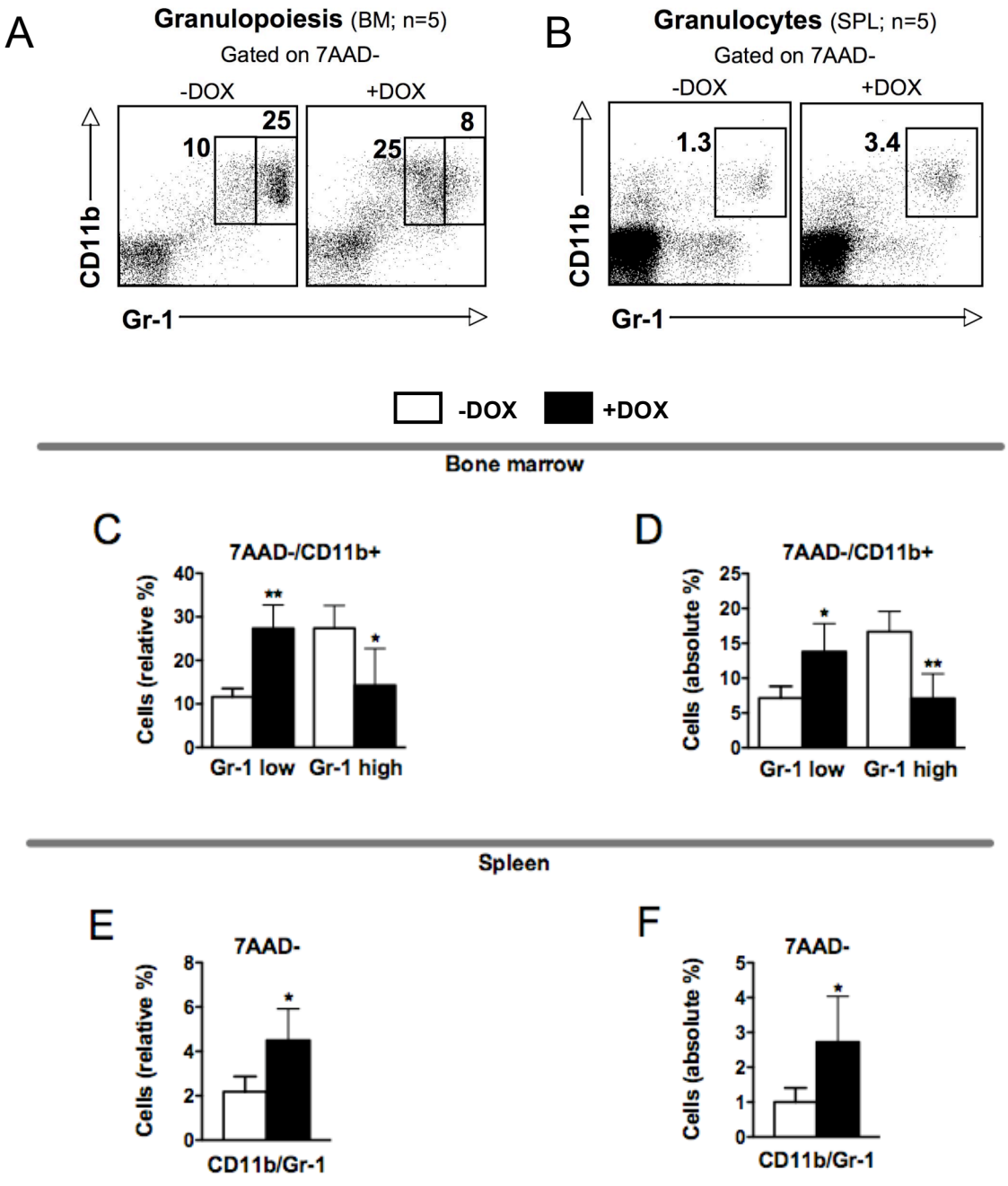

Figure 17: FACS analysis of granulopoiesis in the bone marrow and in the spleen
(A) Representative dot plots depicting granulocytic progenitors (Gr-1^{low}) and mature granulocytes (Gr-1^{high}) in the bone marrow from a control (left plot) and an AML1-ETO-induced mouse (right plot).
(B) Representative dot plots depicting splenic granulocytes from a control (left plot) and an AML1-ETO-induced mouse (right plot).

(C) Bar diagrams showing relative percentages of immature (Gr-1^{low}) and mature granulocytes (Gr-1^{high}) from non-induced (-DOX, white boxes) and AML1-ETO-induced mice (+DOX, black boxes).
(D) Bar diagrams showing absolute percentages of immature (Gr-1^{low}) and mature granulocytes (Gr-1^{high}) from non-induced (-DOX, white boxes) and AML1-ETO-induced mice (+DOX, black boxes).
(E) Bar diagrams showing relative percentages of splenic granulocytes from non-induced (-DOX, white boxes) and AML1-ETO-induced mice (+DOX, black boxes).
(F) Bar diagrams showing absolute percentages of splenic granulocytes from non-induced (-DOX, white boxes) and AML1-ETO-induced mice (+DOX, black boxes).
BM, bone marrow; SPL, spleen; n, number of animals; 7AAD, 7-amino-actinomycin; -DOX, without doxycycline; +DOX, with doxycycline; *p<0.05; **p<0.01. Dead cells were excluded by 7AAD staining. Mean values of relative or absolute percentages ± standard deviations from at least five mice in each group were depicted as bar diagrams.

3.6.4 B- and T-cells are compromised after short-term constitutive expression of AML1-ETO protein

To clarify the consequences of aberrant AML1-ETO expression for B- and T-cells *in vivo*, both populations were analyzed following a fourteen-day AML1-ETO induction.

3.6.4.1 Analysis of bone marrow B-cells

B-cell synthesis takes place in the bone marrow. However, there are also “old” B-cells that re-circulate in this tissue. Using B220 and CD19 surface markers, these two B-cell populations can be distinguished. Newly synthesized B-cells can be identified by $B220^{+}/CD19^{low}$ and re-circulating B-cells are described by $B220^{+}/CD19^{high}$ surface marker expression. Figure 18A depicts a representative flow cytometric dot plot of a control mouse (-DOX) and an AML1-ETO-expressing mouse (+DOX). The statistical analyses of relative (Figure 16B) and absolute percentages (Figure 18C) of newly synthesized ($CD19^{low}$) and re-circulating B-cells ($CD19^{high}$) are represented in bar diagrams. Following aberrant expression of AML1-ETO protein, both $B220^{+}/CD19^{high}$ and $B220^{+}/CD19^{low}$ cell populations dropped in absolute and relative numbers when compared to the control group. In conclusion, short-term expression of AML1-ETO protein in R26/AE mice caused a drastic reduction in numbers of B-cells in the bone marrow compartment.

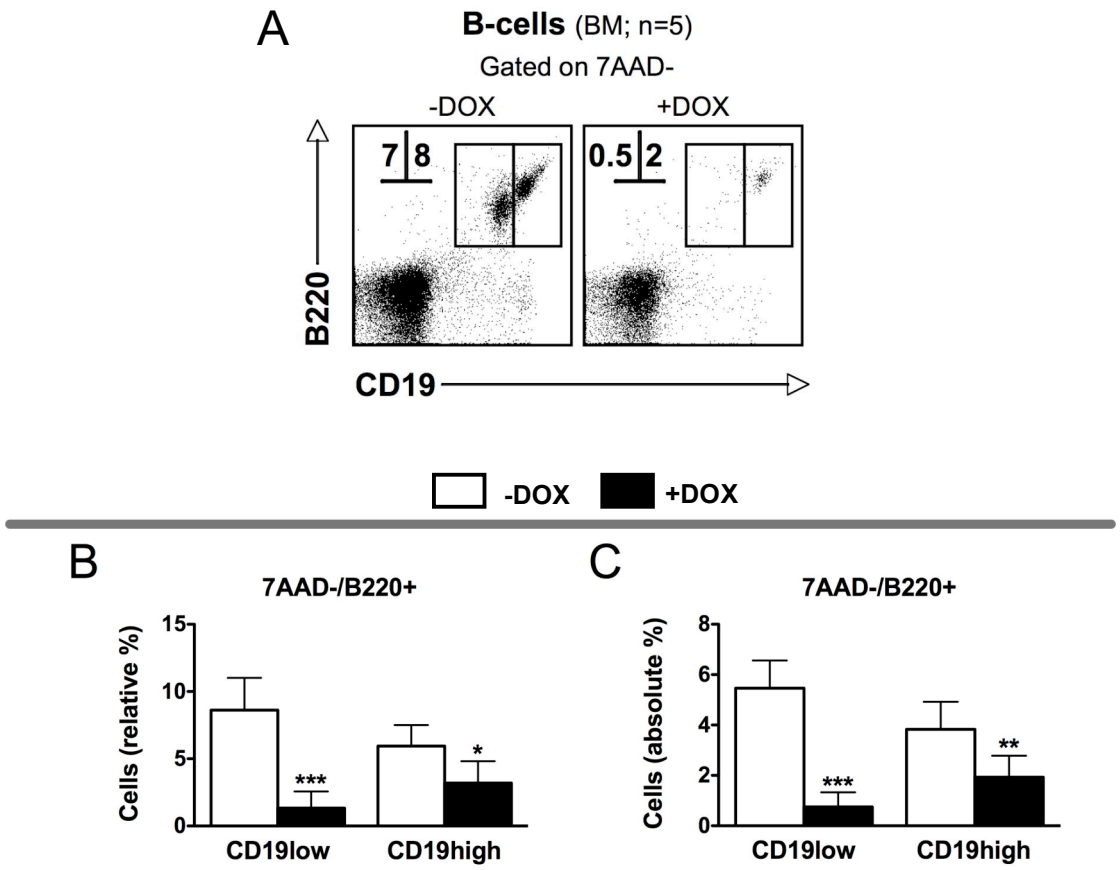

Figure 18: FACS analysis of re-circulating ($B220^{+}/CD19^{high}$) and newly produced B-cells ($B220^{+}/CD19^{low}$)
(A) Representative dot plots depicting re-circulating ($CD19^{high}$) and newly produced B-cells ($CD19^{low}$) of a control (left plot) and an AML1-ETO-induced mouse (right plot).
(B) Bar diagrams showing relative percentages of re-circulating ($CD19^{high}$) and newly produced B-cells ($CD19^{low}$) from non-induced (-DOX, white boxes) and AML1-ETO-induced mice (+DOX, black boxes).
(C) Bar diagrams showing absolute percentages of re-circulating ($CD19^{high}$) and newly produced B-cells ($CD19^{low}$) from non-induced (-DOX, white boxes) and AML1-ETO-expressing mice (+DOX, black boxes).
BM, bone marrow; n, number of animals; 7AAD, 7-amino-actinomycin; -DOX, without doxycycline; +DOX, with doxycycline; *p<0.05; **p<0.01; ***p<0.001. Dead cells were excluded by 7AAD staining. The bar diagrams represent the mean values of relative or absolute percentages ± standard deviations from at least five mice in each group.

3.6.4.2 Analysis of thymic T-cells

Histopathological analysis of the thymus showed a profound perturbation of the normal organ structure and a higher presence of apoptotic cells (Figure 12). Based on these results, it had to be answered if T-cell maturation was affected or not. Under normal conditions, T-cell progenitors migrate from the bone marrow and subsequently enter the thymus through the cortex to start maturation (Schwarz and Bhandoola, 2006). These

cells are double negative for CD4 and CD8 (DN) markers. During maturation, T-cell progenitors proceed through three distinct developmental stages, characterized by the up- and down-regulation of two markers, namely CD44 and CD25. Thus DN1 ($CD4^-/CD8^-/CD44^+/CD25^-$), DN2 ($CD4^-/CD8^-/CD44^+/CD25^+$) and DN3 ($CD4^-/CD8^-/CD44^-/CD25^+$) thymocytes can be distinguished. After T-cell-receptor (TCRαβ) rearrangement, these cells undergo a positive selection, where only T-cells whose TCR recognize self-major histocompatibility complex (MHCs) molecules can survive. Next, T-cells that react too strongly to self-MHCs are eliminated (negative selection). At this stage, T-cells express CD4 and CD8 surface markers (double positive, DP) and finally CD4 or CD8 markers are down-regulated and CD4 or CD8 single positive cells are emerging in the thymus (Hoffman et al., 1996; Owen and Jenkinson, 1992; Sakano, 1996; Takahama et al., 1992; Willerford et al., 1996).

Representative flow cytometric dot plots of T-cell maturation steps are depicted for control mice (Figure 19A and B; -DOX) and AML1-ETO-expressing mice (Figure 19A and B; +DOX). As seen in Figure 19A, C and D, DN3 T-cells significantly decreased in relative and absolute numbers, and DN1 cells increased in absolute numbers but not in relative percentages when compared to control values. Meanwhile, DP cells were profoundly reduced in absolute and relative percentages. In addition, CD4 and CD8 single positive T-cells decreased in relative numbers when compared to the control group. However, $CD4^+$ T-cells remained normal in absolute percentage and $CD8^+$ cells increased in number (Figure 19B, E and F). Based on these results it is to be concluded that the process of T-cell maturation in AML1-ETO-expressing mice is profoundly altered. Given the drastic reduction in DN3 thymocytes, which was accompanied by a nearly complete reduction in CD4/CD8 DP cells, it is very likely that AML1-ETO expression was incompatible with normal DN maturation and TCRαβ rearrangement in the thymus.

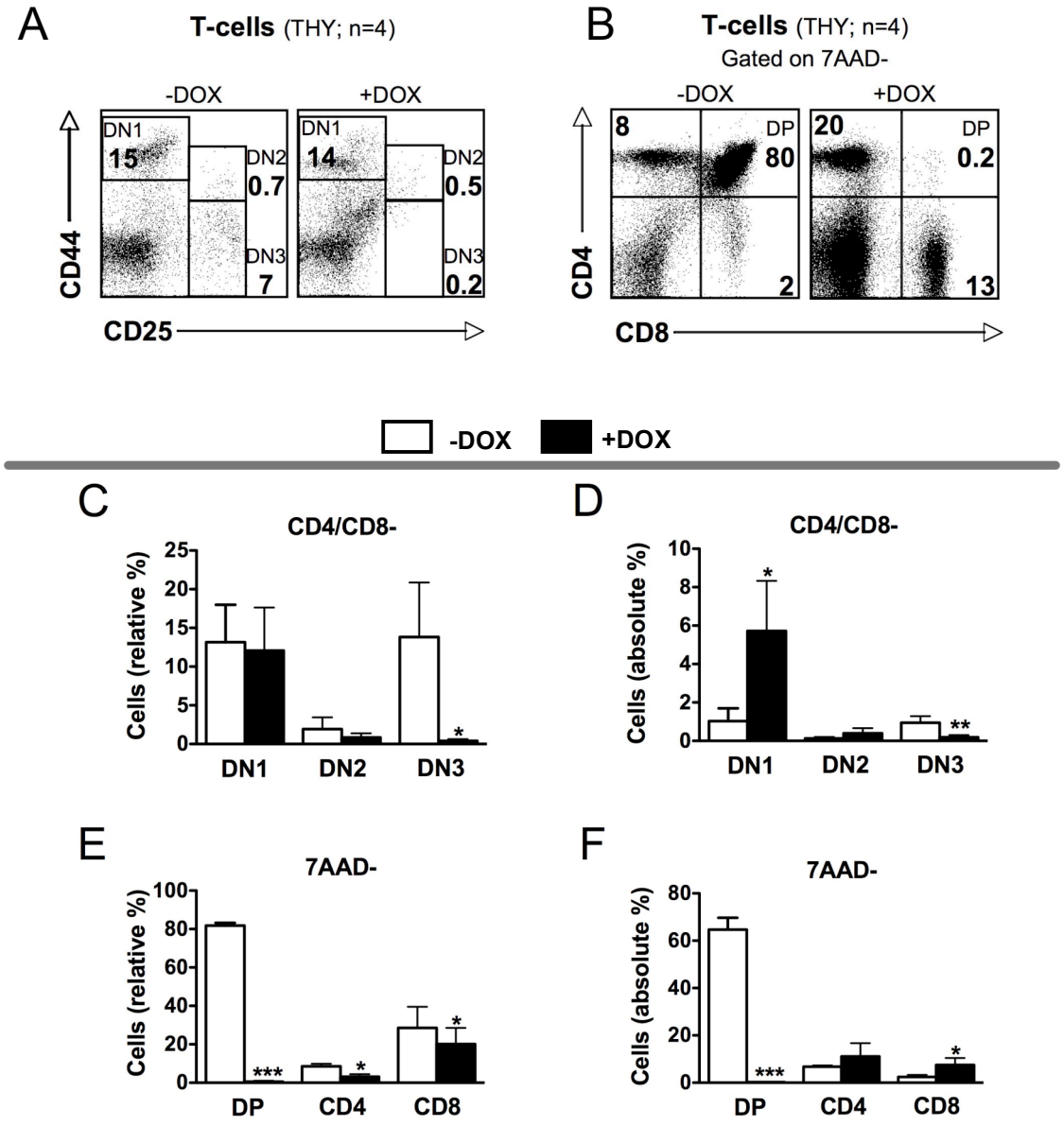

Figure 19: FACS analysis of T-cell maturation in the thymus

(A) Representative dot plots depicting the initial steps of T-cell maturation in the thymus (DN1 to DN3) from a control (left plot) and an AML1-ETO-induced mouse (right plot).

(B) Representative dot plots depicting the final steps of T-cell maturation in the thymus (DP, $CD4^+$, and $CD8^+$) from a control (left plot) and an AML1-ETO-induced mouse (right plot).

(C) Bar diagrams showing relative percentages of the initial steps of T-cell maturation in the thymus (DN1 to DN3) from non-induced (-DOX, white boxes) and AML1-ETO-induced mice (+DOX, black boxes).

(D) Bar diagrams showing absolute percentages of the initial steps of T-cell maturation in the thymus (DN1 to DN3) from non-induced (-DOX, white boxes) and AML1-ETO-induced mice (+DOX, black boxes).

(E) Bar diagrams showing relative percentages of the final steps of T-cell maturation in the thymus (DP, $CD4^+$ and $CD8^+$) from non-induced (-DOX, white boxes) and AML1-ETO-induced mice (+DOX, black boxes).

(F) Bar diagrams showing absolute percentages of the final steps of T-cell maturation in the thymus (DP, $CD4^+$ and $CD8^+$) from non-induced (-DOX, white boxes) and AML1-ETO-induced mice (+DOX, black boxes).

DN1, $CD4^-/CD8^-$, double negative 1 cells; DN2, $CD4^-/CD8^-$, double negative 2 cells; DN3, $CD4^-/CD8^-$, double negative 3 cells; DP, $CD4^+/CD8^+$, double positive cells, THY, thymus; n, number of animals; 7AAD, 7-amino-actinomycin; -DOX, without doxycycline; +DOX, with doxycycline; *p<0.05; **p<0.01;

***p<0.001. Mean values of relative or absolute percentages ± standard deviations from at least four mice in each group are represented as bar diagrams. Dead cells were excluded by 7AAD staining.

3.6.5 Abnormal increase of LKS cells in the bone marrow of AML1-ETO-expressing mice

Lineage negative, c-Kit$^+$ and Sca-1$^+$ cells are also known as LKS cells. This population includes hematopoietic stem cells (HSCs) and more committed progenitors (Uchida and Weissman, 1992). To enrich for HSCs and immature progenitors, mature blood cell lineage markers like CD3 (T-cells), B220 (B-cells), Gr-1 (granulocytes), CD11b (macrophages), TER119 (erythrocytes) or CD11c (dendritic cells) are used for negative selection. In addition, LKS cells specifically express c-Kit and Sca-1 surface markers. Thus it is possible to gate cells that are negative for lineage markers (lin$^-$) but positive for the c-Kit and the Sca-1 marker. In Figure 20A representative flow cytometric contour plots of LKS cells are depicted for a control mouse (Figure 20A; -DOX) and an AML1-ETO-expressing mouse (Figure 20A; +DOX). Acquired cells were negatively gated for lineage markers (data not shown) and positively gated for c-Kit and Sca-1 as shown in Figure 20A. A more than a three-fold expansion was observed in relative numbers of LKS cells from R26/AE induced mice (Figure 20A, +DOX) when compared to the control group (Figure 20A, -DOX). Additionally, a similar increase in absolute numbers of LKS cells was apparent. In conclusion, AML1-ETO expression in mice promoted a remarkable increase in absolute and relative numbers of HSCs/progenitors.

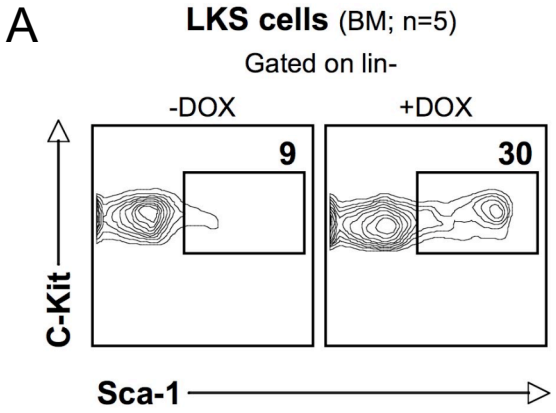

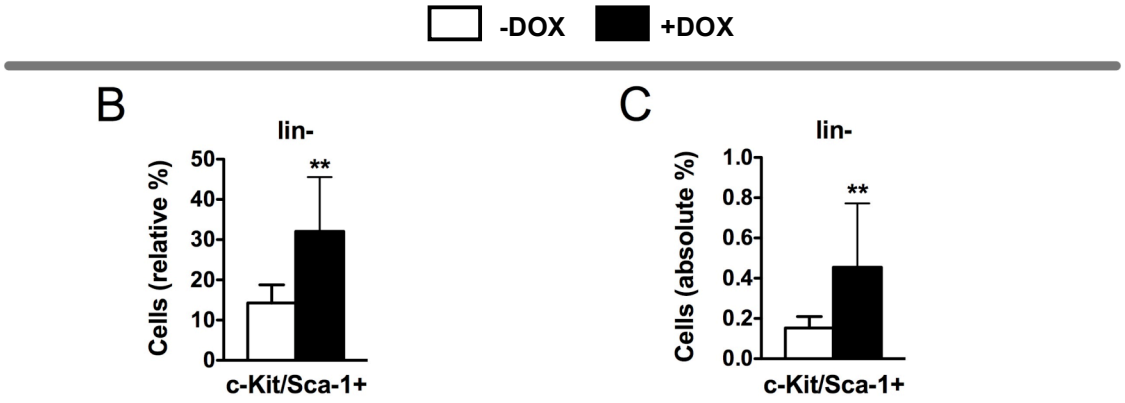

Figure 20: FACS analysis of LKS cells
(A) Representative contour plots depicting LKS cells from a control (left plot) and an AML1-ETO-induced mouse (right plot).
(B) Bar diagrams showing relative percentages of LKS cells from non-induced (-DOX, white boxes) and AML1-ETO-induced mice (+DOX, black boxes).
(C) Bar diagrams showing absolute percentages of LKS cells from non-induced (-DOX, white boxes) and AML1-ETO-induced mice (+DOX, black boxes).
LKS, lineage$^-$/c-Kit$^+$/Sca-1$^+$**;** BM, bone marrow; n, number of animals; lin-, negative for lineage; -DOX, without doxycycline; +DOX, with doxycycline; **p<0.01. The bar diagrams represent the mean values of relative or absolute percentages ± standard deviations from at least five mice in each group.

3.7 Generation of chimeric mice to restrict AML1-ETO expression to blood cells

Bi-transgenic R26/AE mice showed a dramatic phenotype after fourteen days of DOX-exposure. Given the generalized transcription activity of the R26 locus, all organs except the brain are bound to express AML1-ETO (Wörtge et al., 2010). Therefore, it was difficult to appropriately interpret the high lethality rates and the rapidly induced histopathological and hematological phenotypes observed in AML1-ETO-expressing mice. Moreover, in AML patients the AML1-ETO fusion protein is only expressed in hematopoietic cells (Miyamoto et al., 1996; Miyamoto et al., 2000). In order to mimic the situation occurring in AML-M2 patients harboring the t(8;21) chromosome translocation, R26/AE bone marrow cells were adoptively transferred into immunodeficient RAG2$^{-/-}$ mice. RAG2$^{-/-}$ mice lack of functional B- and T-cells as a result of homozygous deletion of the Recombination Activating Gene 2 (Fugmann et al., 2000; Shinkai et al., 1992). Subsequently, the experimental generation of these chimeric mice allowed to specifically restrict AML1-ETO expression to hematopoietic stem cells, progenitors and

differentiated blood cells. In addition, the use of RAG2$^{-/-}$ mice can prevent host versus host reaction.

Bone marrow cells from non-induced R26/AE mice were adoptively transferred into conditioned RAG2$^{-/-}$ mice. To first evaluate the adequate dose of γ-radiation, only PBS was injected into a total number of six irradiated RAG2$^{-/-}$ mice. Mice belonging to this control group died within two weeks. Eight weeks after R26/AE bone marrow transplantation, reconstitution was determined by analyzing T-cells from peripheral blood using flow-cytometry (data not shown). From all generated chimeric mice (R26/AE/RAG2$^{-/-}$), 90 % showed a robust reconstitution (data not shown). Reconstituted mice were then divided into two groups. In each resulting cohort, 25 mice were either fed with normal drinking water (control group, -DOX) or treated with DOX, resulting in blood cell-autonomous expression of AML1-ETO protein (+DOX). The experimental setup and the DOX-dependent AML1-ETO activation is illustrated in Figure 21A and B.

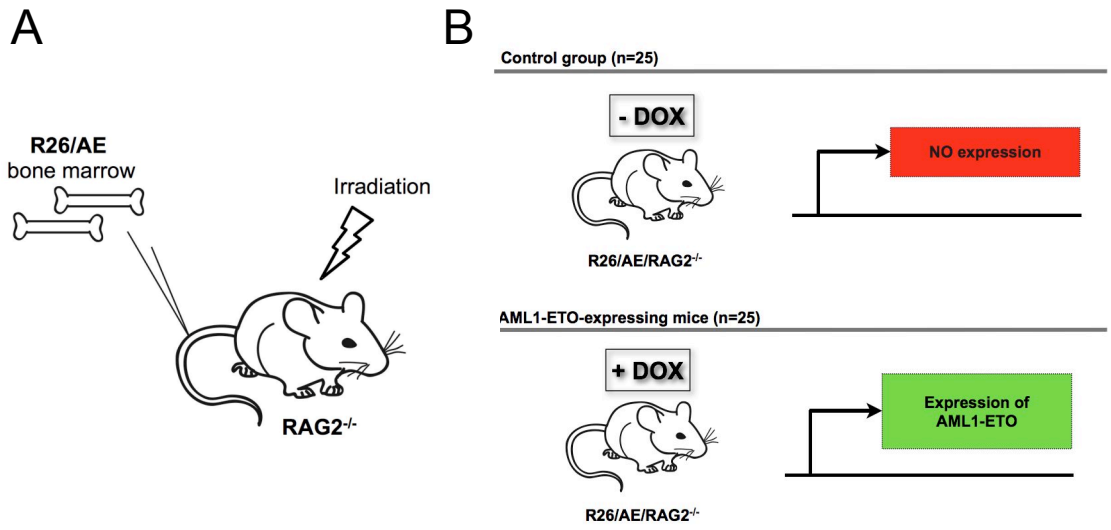

Figure 21: Schematic representation of the adoptive transfer model and conditional AML1-ETO expression in R26/AE/RAG2$^{-/-}$ chimeric mice
(A) Schematic representation of the adoptive transfer of bone marrow cells from R26/AE mice into conditioned RAG2$^{-/-}$ animals.
(B) Representation of R26/AE/RAG2$^{-/-}$ model that uses the tetracycline on/off conditional induction system for transgene expression.
RAG2$^{-/-}$, Recombination Activated Gene 2 knock-out; R26/AE, ROSA26-rtTA/tetO-AML1-ETO.

3.8 Long-term AML1-ETO expression reduces overall mobility patterns and dysregulates peripheral blood parameters

In order to determine if AML1-ETO-expressing R26/AE/RAG2$^{-/-}$ chimeras were sick, mobility, weight and general appearance were regularly inspected. Interestingly, no significant changes were found in mobility patterns or phenotypical appearance between non-exposed and DOX-exposed R26/AE/RAG2$^{-/-}$ mice during the first eight to nine months of AML1-ETO induction. However, after nine months of AML1-ETO expression, AML1-ETO-induced animals started to lose weight and showed less mobility when compared to the control group. To minimal invasively confirm any hematological abnormalities, a peripheral blood analysis was performed at monthly intervals. To this end, AML1-ETO-expressing and control mice were bled from the tail vein and blood parameters were determined. The statistical representation of these experiments is shown in Figure 22.

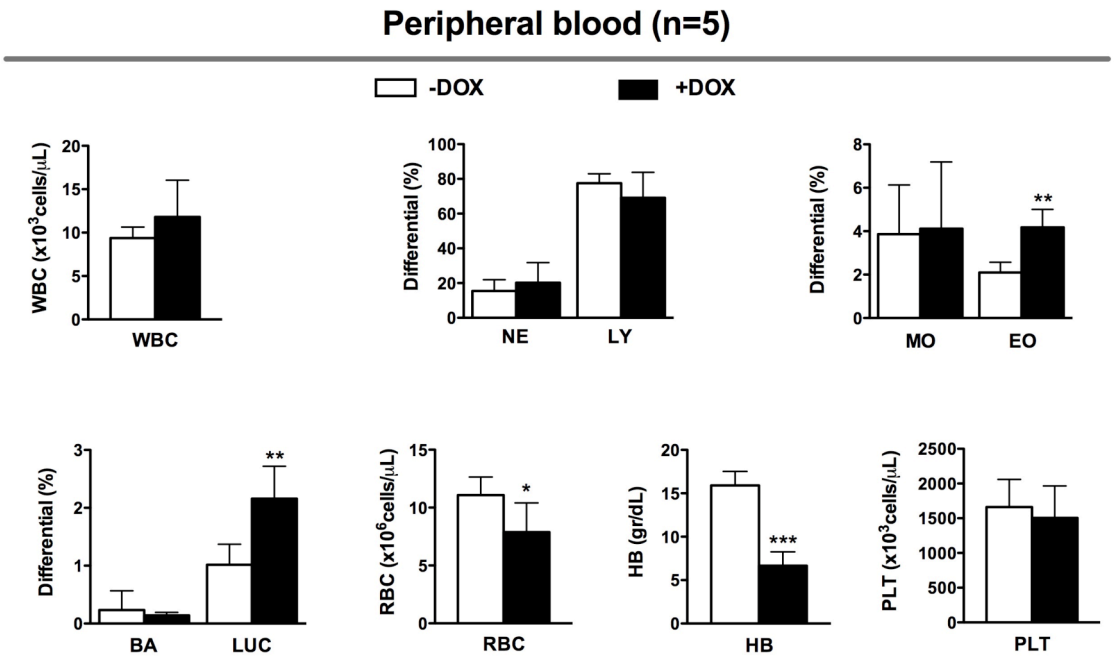

Figure 22: Peripheral blood analysis of AML1-ETO-expressing R26/AE/RAG2$^{-/-}$and control mice

-DOX, without doxycycline; +DOX, with doxycycline; n, number of mice; WBC, white blood cells; NE, neutrophils; LY, lymphocytes; MO, monocytes; EO, eosinophils; BA, basophils; LUC, large unstained cells; RBC, red blood cells; HB, hemoglobin; PLT, platelets; *p<0.05; **p<0.01; ***p<0.001. The bar diagrams represent the mean values of peripheral blood parameters ± standard deviations from at least five mice in each group.

Peripheral blood analysis revealed a dramatic increase in eosinophils (EO) and large myeloperoxidase-negative unstained cells (LUC). Meanwhile, a moderate decrease of red blood cells (RBC) was observed. Moreover, peripheral blood analysis indicated that levels of hemoglobin dropped remarkably when compared to the control group. However, white blood cell (WBC), neutrophil (NE), lymphocyte (LY), monocyte (MO) and platelet (PLT) levels remained normal in AML1-ETO-activated animals. Taken together, cell autonomous expression of AML1-ETO protein promoted a pronounced drop in RBC and HB levels and increased EOs and LUCs.

3.9 Peripheral blood smears and bone marrow cytospins reveal aberrant erythrocytes and an expansion of granulocytes

Microscopic analysis of blood films from induced mice indicated that AML1-ETO expression promoted aberrant red blood cell morphology (see black arrows in Figure 23B). Compared to the non-induced peripheral erythrocytes (Figure 23A), red blood cells of AML1-ETO-expressing mice showed a striking variation in diameter, heterogeneity of hemoglobin content as well as some variation in shape. In addition, AML1-ETO-expressing bone marrow cytospins, showed more granulopoiesis (see black arrows in Figure 23D) when compared to the control group (Figure 23C). However, no signs of blasts were noted. These data demonstrated that blood-restricted AML1-ETO expression promoted anisocytosis, polychromasia and poikilocytosis of peripheral erythrocytes that was accompanied by abnormal rates of granulopoiesis but no expansion of myeloblasts. The lack of myeloblasts in the bone marrow of AML1-ETO-expressing mice demonstrated that these animals did not have leukemia.

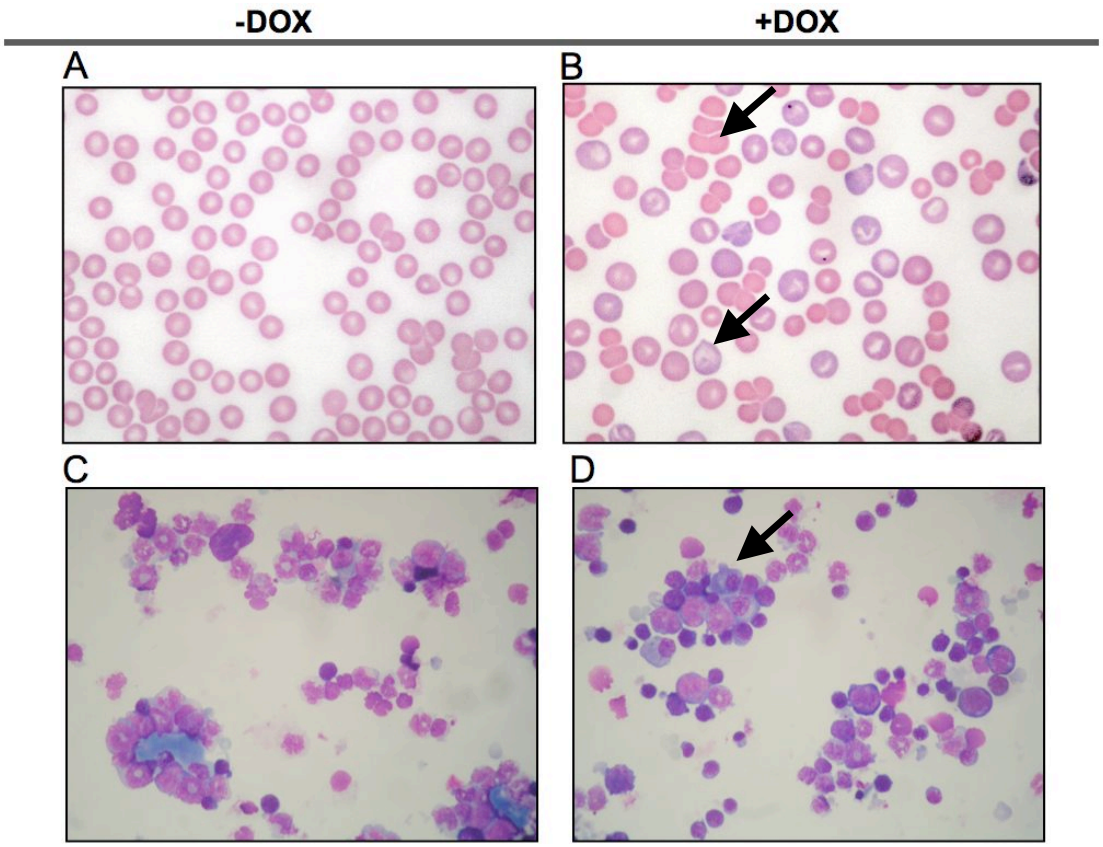

Figure 23: Giemsa staining of blood and bone marrow films
(A) Giemsa staining of a representative peripheral blood smear from a non-induced mouse (-DOX)
(B) Giemsa staining of a representative peripheral blood smear from an AML1-ETO-expressing mouse (+DOX). Of note the variation in diameter and in shape of erythrocytes indicated with black arrows.
(C) Giemsa staining of a representative bone marrow cytospin from a non-induced mouse (-DOX)
(D) Giemsa staining of a representative bone marrow cytospin from an AML1-ETO-expressing mouse (+DOX). Of note the increased granulopoiesis indicated with a black arrow.
-DOX, without doxycycline; +DOX, with doxycycline. Black arrows indicate the observed abnormalities.

3.10 AML1-ETO expression in R26/AE/RAG2$^{-/-}$ mice leads to splenomegaly and to size reduction of the thymus and lymph nodes

Since AML1-ETO-expressing R26/AE/RAG2$^{-/-}$ mice presented abnormalities in peripheral blood values (Figure 22), it was important to determine if phenotypical differences were observed between hematopoietic organs from AML1-ETO-induced and control mice. Therefore, thymus, spleen and lymph nodes were removed, weighted and photographically documented. In Figure 24, the organ weight diagram of chimeric R26/AE mice fed with normal drinking water is represented by white boxes (-DOX) and black boxes show the organ-weight of mice exposed to DOX for nine months (+DOX).

Representative pictures from the thymus, the spleen and the lymph node are shown in the upper part of the Figure 24. The organs of control mice are depicted on the left and organs from induced chimeric animals are shown on the right. After nine months of AML1-ETO expression, the thymus and the lymph nodes showed a dramatic reduction in size and weight when compared to the control group. Furthermore, splenomegaly was observed in AML1-ETO-expressing animals. These results indicated that AML1-ETO induction promoted a size reduction of the thymus and lymph nodes, accompanied by a marked splenomegaly. These data thus provided direct evidence that cell-autonomous expression of AML1-ETO had a strong influence on the structure and cellularity of hematopoietic organs.

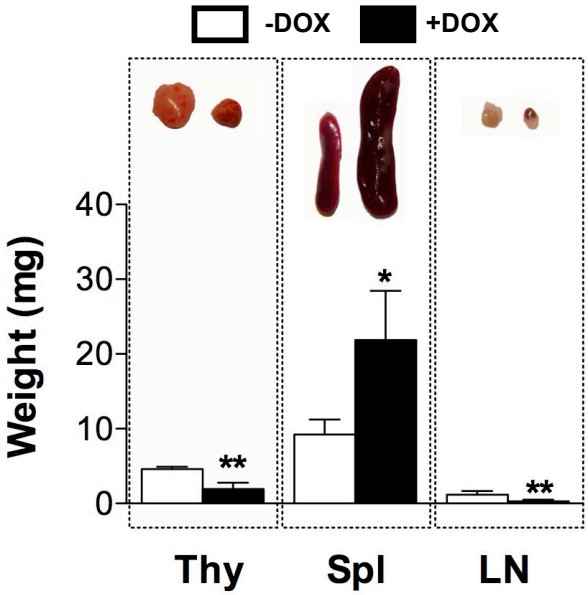

Figure 24: Representative images and statistical representation of the thymus, spleen and lymph node weights from AML1-ETO-expressing and control mice
-DOX, without doxycycline; +DOX, with doxycycline; Thy, thymus; Spl, spleen; LN, lymph nodes; *p<0.05; **p<0.01. The bar diagrams represent the mean weight values ± standard deviations from at least five mice in each group.

3.11 Histopathology

3.11.1 Histopathology of the thymus, the spleen and the lymph nodes

In order to determine the consequences of long-term AML1-ETO expression for the morphology of hematopoietic organs, a histopathological analysis was performed.

Thymus, spleen and lymph nodes were removed from non-induced and induced R26/AE/RAG2$^{-/-}$ mice. Organs were fixed in 2.5 % formaldehyde, embedded in paraffin, and sections were stained with hematoxylin and eosin. The histopathological analysis and the interpretation of the data was done by Prof. Dr. Toni Lehr (Institute of Pathology, Lausanne, Switzerland) or Dr. Andreas Kreft (Medical Center of Johannes-Gutenberg University, Mainz, Germany).

3.11.1.1 Histopathology of the spleen

Previously, as seen in Figure 24 DOX-exposed mice presented a marked splenomegaly. Interestingly, histological analysis of spleens from AML1-ETO-induced mice revealed an increase in erythropoiesis within the red pulp (Figure 25D). An additional difference between induced and control spleens was that the demarcation between red and white pulp became less apparent in AML1-ETO expressing animals. However, the overall architecture of the white pulp remained normal in these animals (Figure 25C).

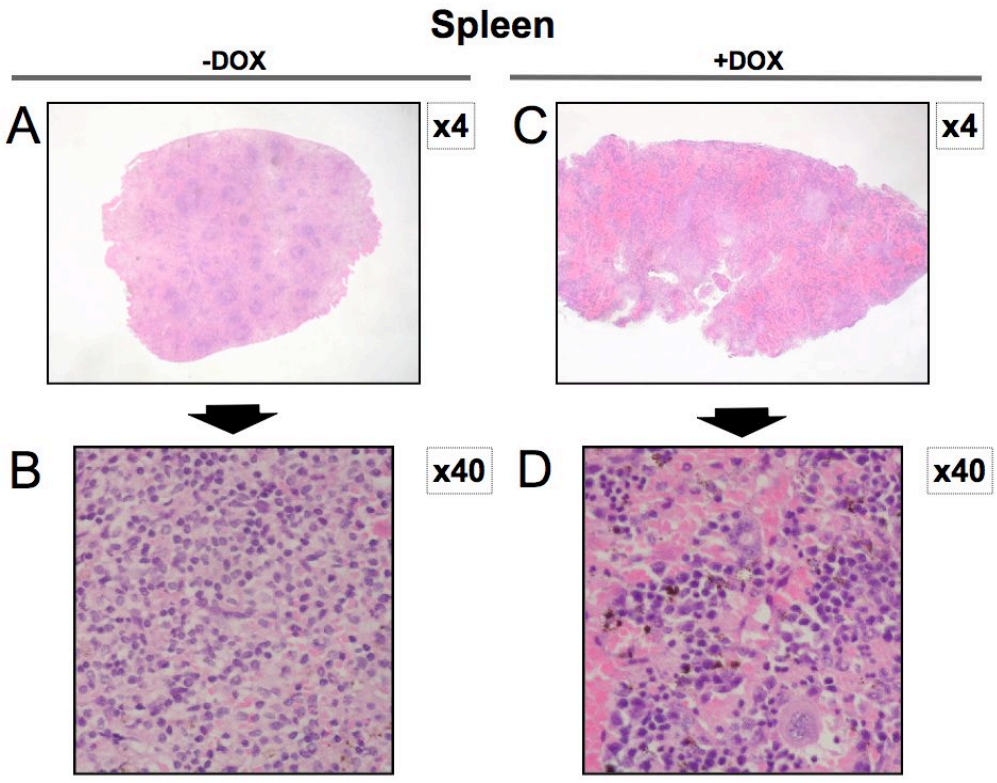

Figure 25: Hematoxylin and eosin staining of representative spleen sections from AML1-ETO-expressing mice (right) and controls (left)

(A) Hematoxylin and eosin staining of a representative spleen section from a non-induced R26/AE/RAG2$^{-/-}$ mouse.
(**B)** Higher magnification showing the hematoxylin and eosin staining of a representative spleen section from a non-induced R26/AE/RAG2$^{-/-}$ mouse.
(C) Hematoxylin and eosin staining of a representative spleen section from an AML1-ETO-expressing mouse.
(D) Higher magnification showing the hematoxylin and eosin staining of a representative spleen section from an AML1-ETO-expressing mouse. Note the higher incidence of erythroid clusters.
The magnification of each section is indicated on the right. -DOX, without doxycycline; +DOX, with doxycycline.

3.11.1.2 Histopathology of the thymus

As seen in Figure 24 the thymus of AML1-ETO-expressing mice was reduced in size. Despite its reduced size, this organ revealed a normal organization of cortex and medulla with no obvious histological differences between induced and control mice (Figure 26A and C). Higher magnification of thymic sections from AML1-ETO-expressing animals did not reveal any abnormalities when compared to the control group (Figure 26B and D). Taken together, despite its size reduction, thymic morphology was not affected. Equally, higher magnifications did not reveal any obvious morpho-pathological changes in AML1-ETO-induced animals (Figure 26D).

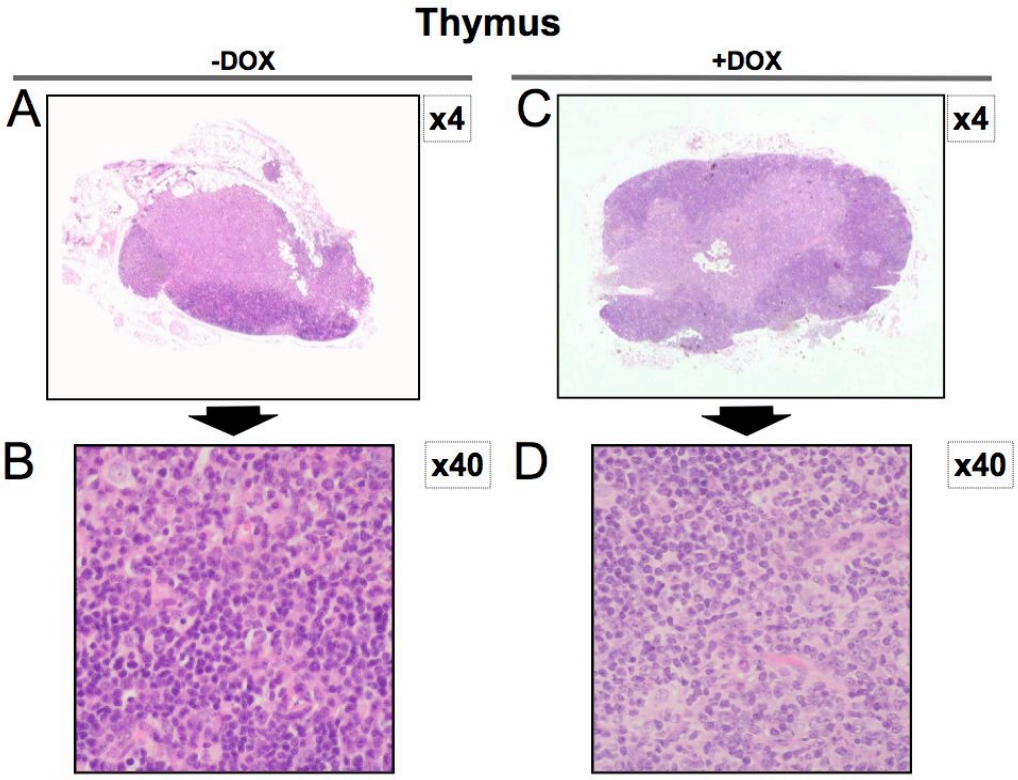

Figure 26: Hematoxylin and eosin staining of representative thymus sections from a control (-DOX) and an AML1-ETO-expressing animal
(A) Hematoxylin and eosin staining of a representative thymus section from a non-induced-R26/AE/RAG2$^{-/-}$ mouse.
(B) Higher magnification of a hematoxylin and eosin staining of a representative thymus section from a non-induced- R26/AE/RAG2$^{-/-}$ mouse.
(C) Hematoxylin and eosin staining of a representative thymus section from an AML1-ETO-expressing mouse.
(D) Higher magnification of a hematoxylin and eosin staining showing a representative thymus from an AML1-ETO-expressing mouse.
The magnification of each section is indicated on the right.

3.11.1.3 Histopathology of the lymph nodes

As seen in Figure 24, the lymph nodes from long-term AML1-ETO-expression mice were decreased in size. However, the architecture of the lymph nodes was essentially intact in AML1-ETO-expressing mice when compared to the control group (Figure 27A and C). Similar results were obtained by analyzing higher magnifications of the lymph nodes sections where no alterations were observed between AML1-ETO-induced mice and control (Figure 27D and B). These results indicated that AML1-ETO expression led to a size reduction but not to morpho-pathological changes in AML1-ETO-expressing animals.

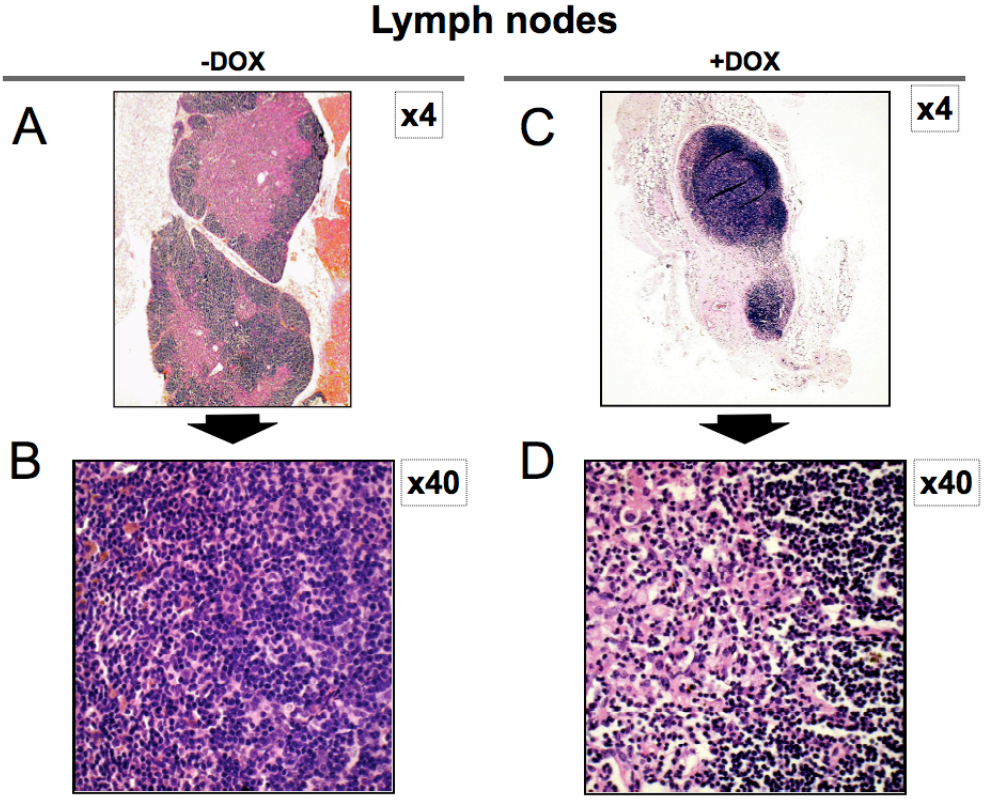

Figure 27: Hematoxylin and eosin staining of representative lymph node sections from AML1-ETO-expressing mice (right) and controls (left)
(A) Hematoxylin and eosin staining of a representative section from the lymph node of a non-induced R26/AE/RAG2$^{-/-}$ mouse.
(B) Higher magnification of hematoxylin and eosin staining of a representative section from the lymph node of a non-induced R26/AE/RAG2$^{-/-}$ mouse.
(C) Hematoxylin and eosin staining of a representative section from the lymph node of an AML1-ETO-induced mouse.
(D) Higher magnification of hematoxylin and eosin staining of a representative section from the lymph node of an AML1-ETO-induced mouse.
The magnification of each section is indicated on the right. -DOX, without doxycycline; +DOX, with doxycycline.

This data provided experimental evidence that cell-autonomous AML1-ETO expression in hematopoietic cells promoted atrophy of the thymus and the lymph nodes with no apparent histo-pathological changes and induced splenomegaly accompanied by increased erythropoiesis.

3.12 Terminal dUTP nick-end labeling assay (TUNEL) of the thymus and the lymph nodes

Given the reduction in size of the thymus and the lymph nodes it was of interest to determine if in these organs a higher incidence of apoptosis was present. Therefore, TUNEL assays were performed. The TUNEL assay is a common method for detecting DNA fragmentation that results from apoptotic signaling cascades. The assay relies on the presence of nicks in the DNA which can be identified by terminal deoxynucleotidyl transferase, an enzyme that will catalyze the addition of dUTPs that are secondarily labeled with a marker. It may also label cells that have suffered severe DNA damage (http://www.roche-applied-science.com).

3.12.1 TUNEL staining of thymus sections

Thymus sections were stained, microscopically analyzed and photographically documented. TUNEL assays revealed no differences between thymic sections from non-induced and AML1-ETO-expressing mice (Figures 28A and C). Equally, higher magnifications of the thymus from AML1-ETO-induced animals did not show any

apparent increase of apoptotic cells (compare amount of TUNEL-positive brown cells between Figure 28B and D). The histopathological analysis and the interpretation of the data were done by Prof. Dr. Toni Lehr (Institute of Pathology, Lausanne, Switzerland).

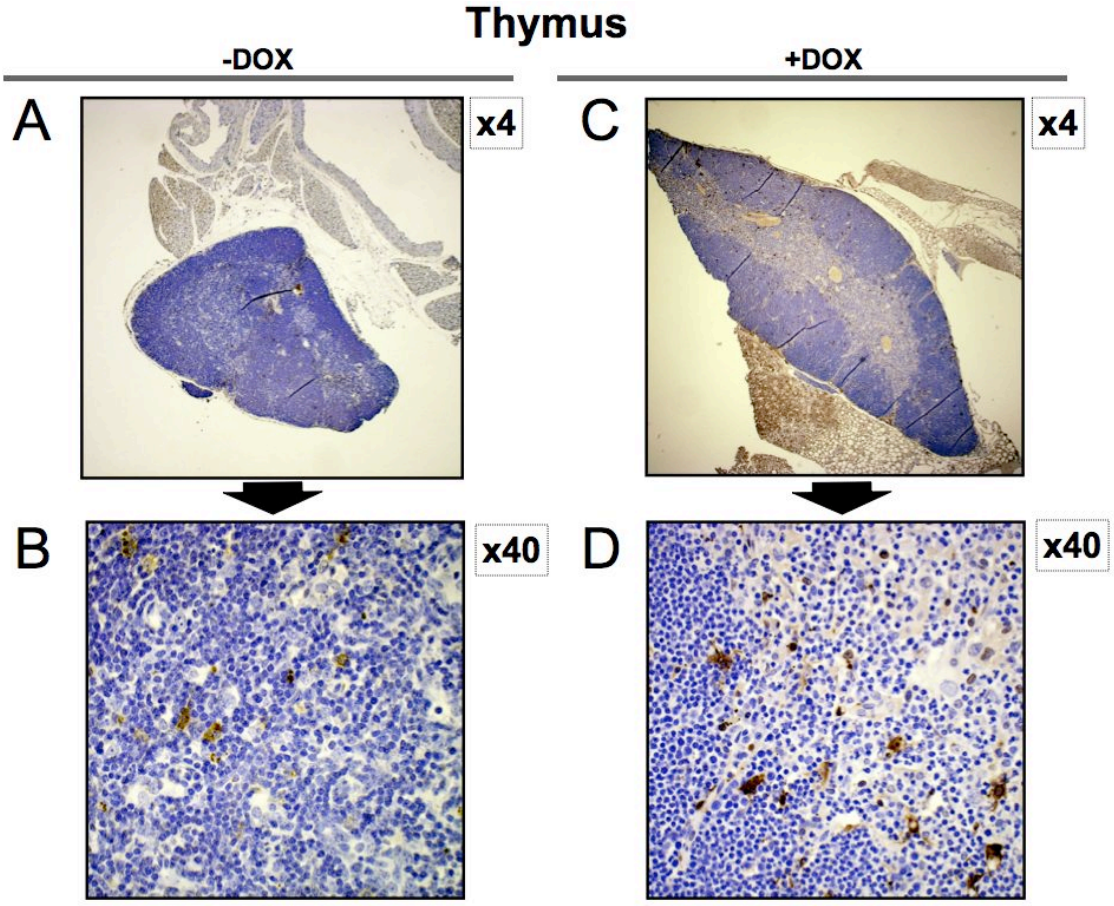

Figure 28: TUNEL staining of representative thymus sections from AML1-ETO-expressing mice (right) and controls (left)
(A) TUNEL assay of a representative thymus section from a non-induced mouse.
(B) Higher magnification of a TUNEL staining showing a representative thymus section from a non-induced- mouse. TUNEL-positive brown cells to be noticed.
(C) TUNEL staining of a representative thymus section from an AML1-ETO-induced animal.
(D) Higher magnification of a TUNEL staining showing a representative thymus section from an AML1-ETO-expressing mouse. TUNEL-positive brown cells to be noticed.

3.12.2 TUNEL staining of lymph nodes

Apoptosis rates were determined in the lymph nodes from non-induced and AML1-ETO-induced animals using the TUNEL assay. Lymph node sections were prepared as described (Section 3.11.1). TUNEL analyses revealed no apparent variations

between lymph node sections from AML1-ETO-expressing and control animals (Figure 29A and C). In addition, higher magnification of lymph node sections from AML1-ETO-expressing mice showed no alterations in the number of apoptotic cells when compared to the control group (brown TUNEL-positive cells in Figure 29B and D). It is to be concluded that AML1-ETO expression did not increase apoptosis in the lymph nodes.

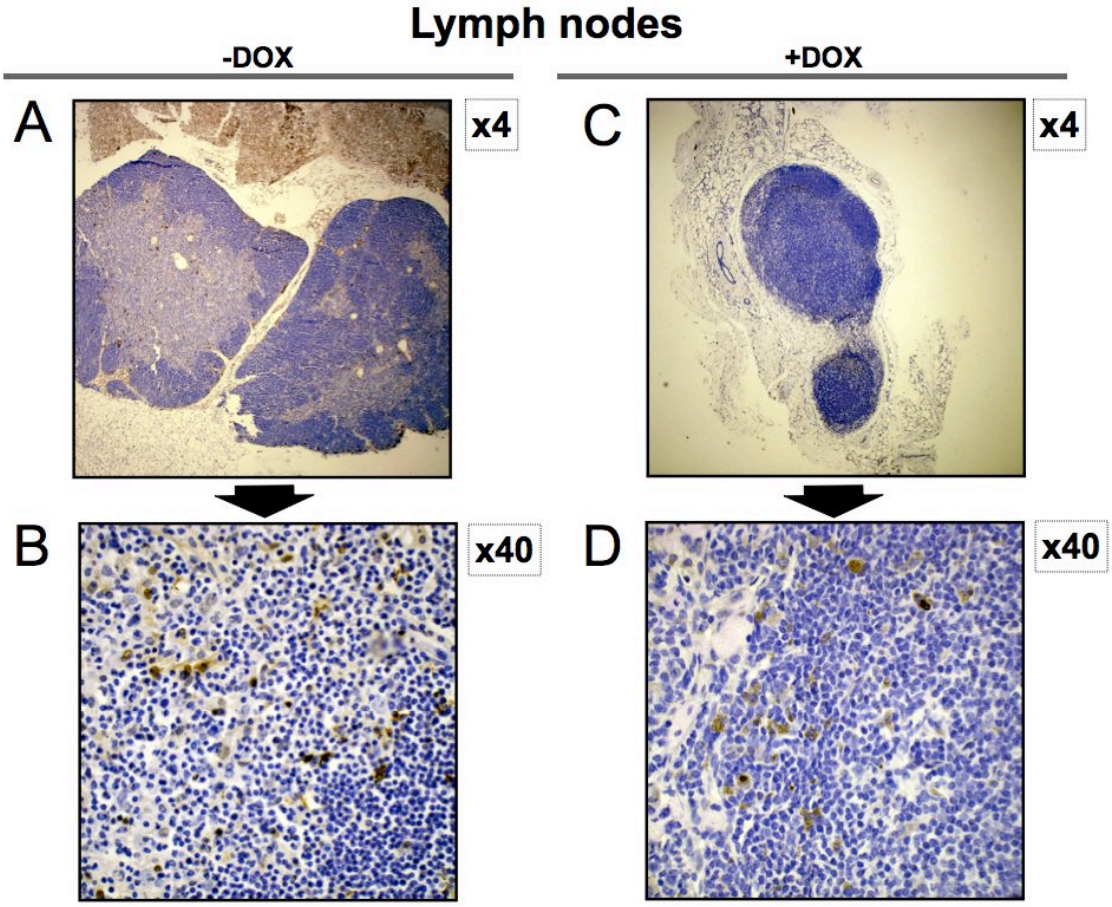

Figure 29: TUNEL staining of representative lymph nodes sections from AML1-ETO-expressing mice (right) and controls (left)
(A) TUNEL assay of a representative lymph node section from a non-induced mouse.
(B) Higher magnification of a TUNEL staining showing a representative lymph node section from a non-induced- mouse. Note TUNEL-positive brown cells.
(C) TUNEL staining of a representative lymph node section from an AML1-ETO-induced animal.
(D) Higher magnification of a TUNEL staining showing a representative lymph node section from an AML1-ETO-expressing mouse. Note TUNEL-positive brown cells.

3.13 Flow cytometric analysis of blood cell-autonomous AML1-ETO expression reveals a complete modulation of normal hematopoiesis

Since the appearance and the weight of hematopoietic organs were strongly affected by long-term AML1-ETO expression (Figure 24), the impact of AML1-ETO activation for different hematopoietic lineages, progenitors and HSCs was analyzed using flow-cytometry.

3.13.1 Perturbed erythropoiesis in AML1-ETO-expressing mice

The observed anemia in peripheral blood values of AML1-ETO-expressing mice (Figure 22) suggested an impairment of normal hematopoiesis. Therefore, it was of interest to determine how erythropoiesis was affected in the bone marrow of long-term AML1-ETO-expressing mice. Erythroid maturation was monitored following the Lodish flow cytometric protocol (Socolovsky et al., 2001). As described in section 3.6.1, four different developmental stages (indicated by Roman numbers) can be identified using CD71 and Ter119 surfaces markers: $CD71^{+}/Ter119^{low}$ (see Figure 30A, quadrant I); $CD71^{+}/Ter119^{+}$ (quadrant II); $CD71^{low}/Terr19^{+}$ population (quadrant III); $CD71^{-}/Ter119^{+}$ expression (quadrant IV). Using these criteria, the analysis of erythropoiesis after nine months of AML1-ETO expression (+DOX; right), revealed a remarkable increase in absolute and relative numbers of proerythroblasts (I) and a significant reduction in orthochromatophilic erythroblast (IV). However, basophilic- (II) and late baso- and chromatophilic erythroblasts (III) remained normal. In Figure 30 representative flow cytometric dot plots of bone marrow erythropoiesis are depicted for a control mouse (28A; -DOX) and an AML1-ETO-expressing mouse (28A; +DOX). The statistical analyses of relative (Figure 30B) and absolute percentages (Figure 30C) of different red blood cell maturation fractions (I to IV) are represented as bar diagrams. The results obtained in this experiment indicated that consistent with the peripheral blood values, erythropoiesis was profoundly disturbed in AML1-ETO-induced mice, exemplified by an increase in proerythroblasts and a reduction in orthochromatophilic erythroblasts (Figure 30A; I and IV).

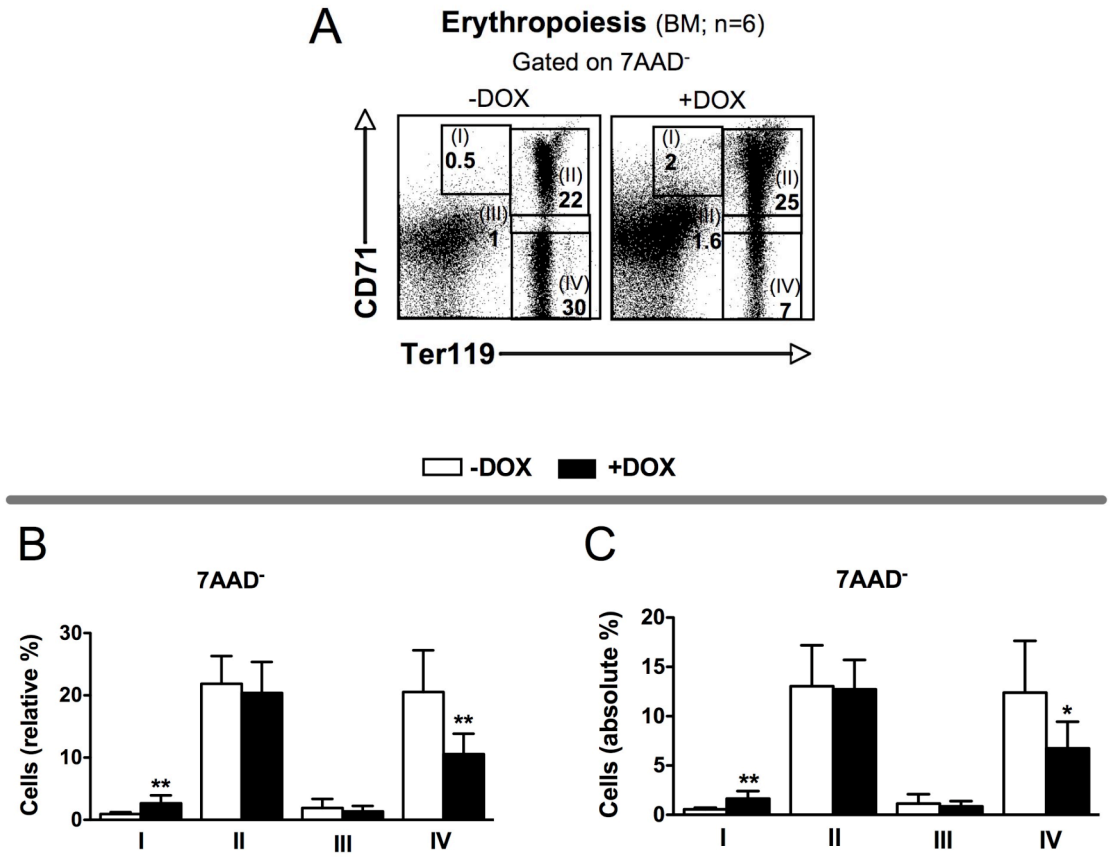

Figure 30: FACS analysis of bone marrow erythropoiesis
(A) Representative dot plots depicting red blood cell maturation stages (I to IV) from a control (left plot) and a R26/AE/RAG2$^{-/-}$-induced mouse (right plot).
(B) Bar diagrams showing relative percentages of different red blood cell maturation steps from non-induced (-DOX, white boxes) and AML1-ETO-induced mice (+DOX, black boxes).
(C) Bar diagrams showing absolute percentages of different red blood cell maturation stages from non-induced (-DOX, white boxes) and AML1-ETO-induced mice (+DOX, black boxes).
BM, bone marrow; n, number of animals; 7AAD, 7-amino-actinomycin; -DOX, without doxycycline; +DOX, with doxycycline; I, proerythroblasts; II; basophilic erythroblasts; III; late basophilic erythroblasts and chromatophilic erythroblasts; IV, orthochromatophilic erythroblasts; *p<0.05; **p<0.01. The bar diagrams depicted the mean values of relative or absolute percentages ± standard deviations from at least six mice in each group. Dead cells were excluded by 7AAD staining.

3.13.2 Analysis of megakaryocytes

To evaluate the consequences of blood-restricted AML1-ETO expression for megakaryocytes in the bone marrow, immature and mature populations of megakaryocytes were evaluated using flow-cytometry. Immature megakaryocytes are defined by c-Kit$^+$/CD41$^+$ expression and mature megakaryocytes fall within c-Kit$^-$/CD41$^+$ population (Salek-Ardakani et al., 2009). As shown in Figure 31 both immature and

mature megakaryocytes were not affected in relative numbers (Figure 31A and B). However, mature megakaryocytes were increased in absolute values. Representative flow cytometric dot plots for this experiment are depicted for a control mouse (A; -DOX) and an AML1-ETO-expressing mouse (A; +DOX). To summarize, long-term expression of AML1-ETO in R26/AE/RAG2$^{-/-}$ mice did not promote significant changes in megakaryopoiesis when compared to the control group, with the exception of a slight increase noted in absolute numbers of mature megakaryocytes.

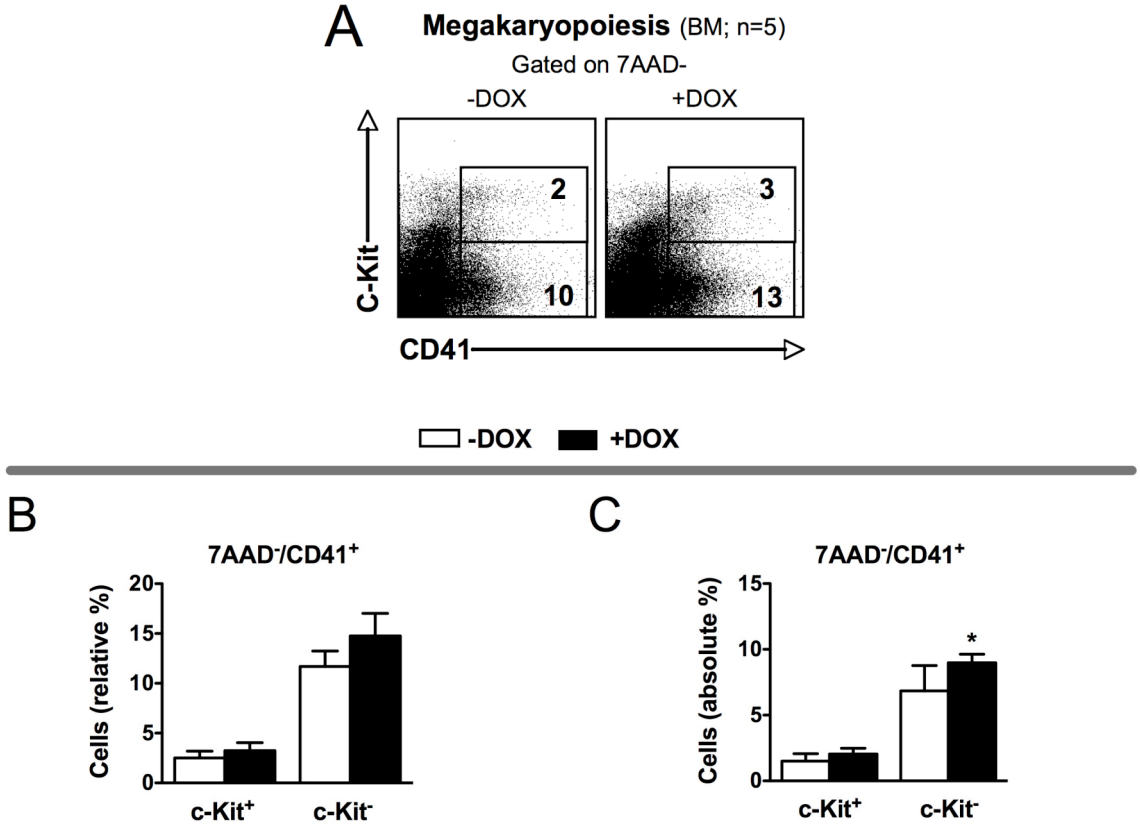

Figure 31: FACS analysis of immature (c-Kit$^+$/CD41$^+$) and mature megakaryocytes (c-Kit$^-$/CD41$^+$)

(A) Representative dot plots depicting immature (upper right quadrant) and mature megakaryocytes (lower left quadrant) from a control (left plot) and an AML1-ETO-induced mouse (right plot).

(B) Bar diagrams showing relative percentages of immature (c-Kit$^+$) and mature megakaryocytes (c-Kit$^-$) from non-induced (-DOX, white boxes) and AML1-ETO-induced mice (+DOX, black boxes).

(C) Bar diagrams showing absolute percentages of immature (c-Kit$^+$) and mature megakaryocytes (c-Kit$^-$) from non-induced (-DOX, white boxes) and AML1-ETO-induced mice (+DOX, black boxes).

BM, bone marrow; n, number of animals; 7AAD, 7-amino-actinomycin; -DOX, without doxycycline; +DOX, with doxycycline; *p<0.05. Dead cells were excluded by 7AAD staining. Mean values of relative or absolute percentages ± standard deviations from at least five mice in each group were depicted as bar diagrams.

3.13.3 Long-term AML1-ETO expression leads to changes in bone marrow granulopoiesis

Since enforced AML1-ETO-expression was reported to lead to myeloproliferative disease in mice (de Guzman et al., 2002; Fenske et al., 2004; Grisolano et al., 2003; Nishida et al., 2006) it was of importance to determine if AML1-ETO-expressing R26/AE/RAG2$^{-/-}$ mice produced a similar phenotype as noted in these models. Therefore, bone marrow samples were incubated with CD11b and Gr-1 antibodies distinguishing between granulocytic progenitors (CD11b^{+}/Gr1^{low}) and mature granulocytes (CD11b^{+}/Gr1^{high}; Figure 32A). Flow cytometry analyses after nine months following AML1-ETO induction revealed a significant expansion in absolute and relative numbers of granulocytic progenitors and mature granulocytes (Figure 32B and C). These data clearly demonstrated that enforced AML1-ETO expression promoted an increase in both immature and mature stages of granulopoiesis.

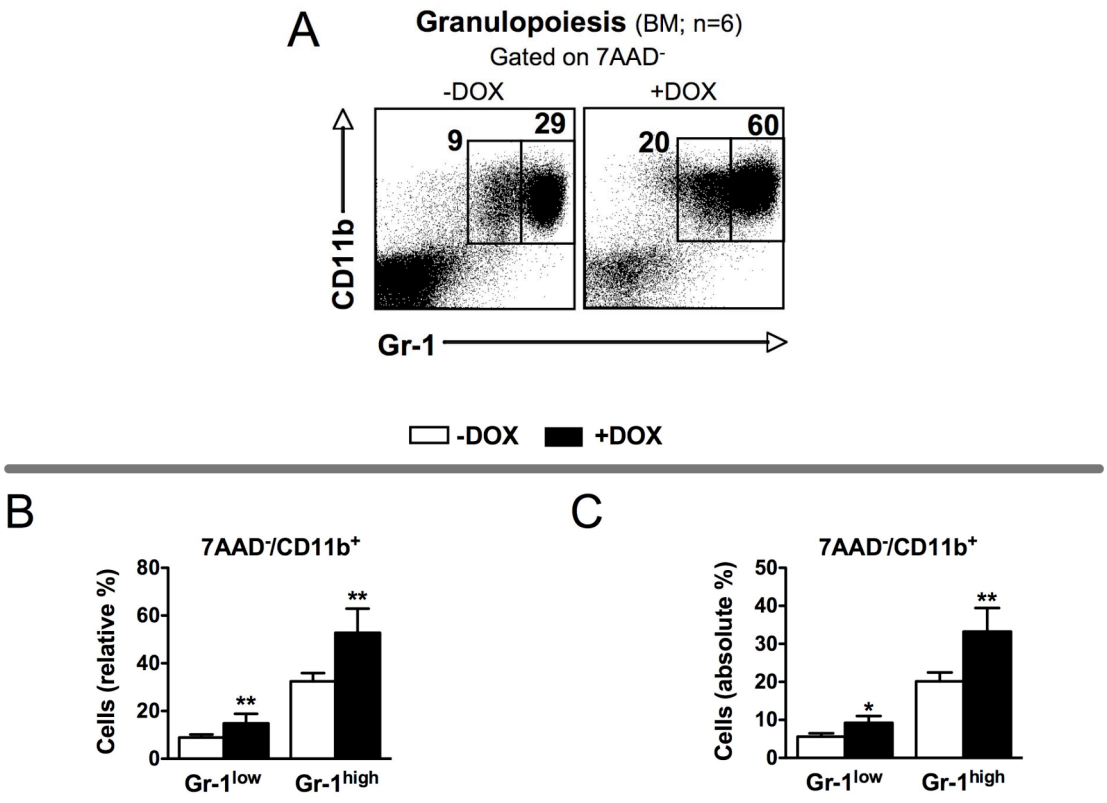

Figure 32: FACS analysis of granulopoiesis in the bone marrow
(A) Representative dot plots depicting granulocytic progenitors and mature granulocytes in the bone marrow of a control (left plot) and an AML1-ETO-induced mouse (right plot).
(B) Bar diagrams showing relative percentages of immature (Gr-1^{low}) and mature granulocytes (Gr-1^{high}) from non-induced (-DOX, white boxes) and AML1-ETO-expressing mice (+DOX, black boxes).

(C) Bar diagrams showing absolute percentages of immature (Gr-1^{low}) and mature granulocytes (Gr-1^{high}) from non-induced (-DOX, white boxes) and AML1-ETO-expressing mice (+DOX, black boxes).
BM, bone marrow; n, number of animals; 7AAD, 7-amino-actinomycin; -DOX, without doxycycline; +DOX, with doxycycline; *p<0.05; **p<0.01. Bar diagrams represent the mean values of relative or absolute percentages ± standard deviations from at least six mice in each group. Dead cells were excluded by 7AAD staining.

3.13.4 AML1-ETO expression induces no changes in immature and mature blasts within the bone marrow

Since microscopic inspection of bone marrow smears showed normal blasts counts in AML1-ETO-expressing mice (Figure 23), it was of interest to confirm these findings using flow-cytometry. The aim of this experiment was to analyze the percentage of blasts in the bone marrow and to determine if AML1-ETO-induced animals presented leukemia. Following the FAB and WHO definition the presence of 20-30 % blasts in the bone marrow is a sign of leukemia (Vardiman et al., 2009). Zuber and colleagues defined immature blasts as B220$^-$/CD3$^-$/Ter119$^-$/Sca-1$^-$/F4/80^{low}/c-Kit$^+$/CD11b$^-$/Gr-1$^-$ and mature blasts as B220$^-$/CD3$^-$/Ter119$^-$/Sca-1$^-$/F4/80^{low}/c-Kit$^+$/CD11b$^+$/Gr-1^{low} (Zuber et al., 2009).

As shown in Figure 33A, no differences between immature blasts from control and DOX-exposed animals were observed. Similar results were obtained for mature blasts, which remained normal when compared to the control group (Figure 33B). In addition, these findings were in accordance with the absence of increased blast counts in AML1-ETO expressing bone marrow preparations seen upon microscopic inspection (Figure 23). In summary, elevated levels of granulopoiesis in the bone marrow of AML1-ETO expressing mice were not accompanied by an increase in immature and mature blasts demonstrating the absence of leukemia in long-term induced animals.

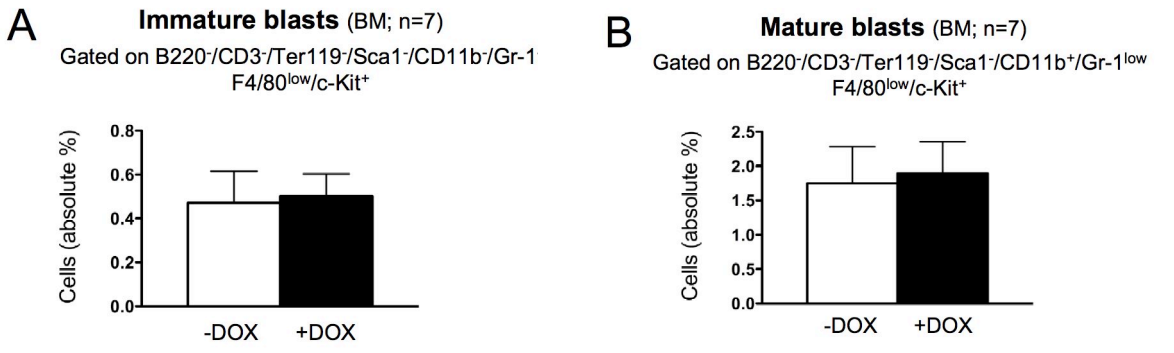

Figure 33: Analysis of immature and mature blasts using flow cytometry
(A) Bar diagrams showing absolute percentages of immature blasts from non-induced (-DOX, white boxes) and AML1-ETO-expressing mice (+DOX, black boxes).
(B) Bar diagrams showing absolute percentages of mature blasts from control (-DOX, white boxes) and AML1-ETO-induced animals (+DOX, black boxes).
BM, bone marrow; n, number of animals; -DOX, without doxycycline; +DOX, with doxycycline; The bar diagrams represent the mean values of absolute percentages ± standard deviations from at least seven mice in each group. Surface markers expression is indicated for each group.

3.13.5 Cell-autonomous expression of AML1-ETO protein impedes normal lymphoid maturation

In order to determine the consequences of long-term AML1-ETO expression in lymphoid cells, B- and T-cell development was analyzed using flow-cytometry.

3.13.5.1 Flow-cytometric analysis of B-cells in bone marrow and spleen

Normally, initial B-cell development occurs in the bone marrow and then, immature B-cells migrate to the spleen where they develop to mature B-cells (Abdou and Abdou, 1973; Abdou and Richter, 1970). In order to determine if B-cell development was affected by AML1-ETO expression, pre- and pro-, immature and re-circulating B-cells were analyzed using the B220 and the IgM surface markers. Pre- and pro- B-cells can be defined by $B220^{+}/IgM^{-}$ (Figure 34A; quadrant I) surface markers. Furthermore, immature B-cells fall within the $B220^{low}/IgM^{+}$ population (Figure 34A; quadrant II) and re-circulating B-cells can be described as $B220^{high}/IgM^{+}$ cells (Figure 34A; quadrant III). With regard to mature splenic B-cells, this population is positive for B220 and IgM surface markers. In this study it was of interest to determine if B-cell development was disturbed by the blood-restricted expression of AML1-ETO protein. As shown in Figure 34, pre- and pro- (I), immature (II) and re-circulating B-cells (III) significantly decreased in absolute and relative numbers in AML1-ETO-expressing mice (Figure 34A, C and D; +DOX). In addition, a slight reduction in relative and absolute numbers of splenic B-cells was observed in DOX-exposed animals when compared to the control group (Figure 34B, E and F; +/- DOX). Taken together, long-term expression of AML1-ETO in chimeric mice perturbed normal B-cell development already at early stages (pre- and pro- B-cells) and an overall reduction of B-cells in the bone marrow and the spleen was noticed.

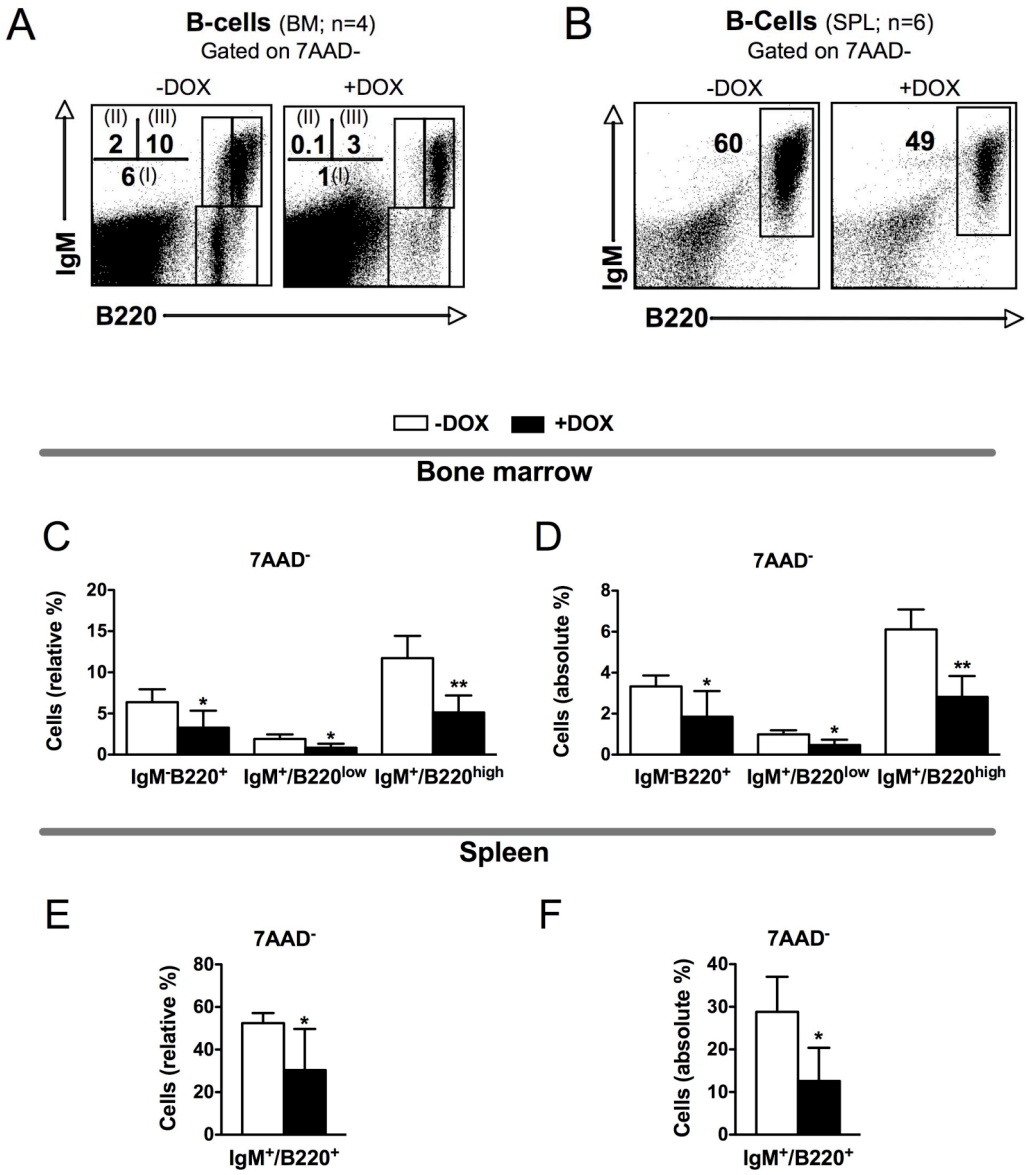

Figure 34: FACS analysis of B-cells in the bone marrow and in the spleen

(A) Representative dot plots depicting B-cell maturation in the bone marrow of a control (left plot) and an AML1-ETO-induced mouse (right plot).

(B) Representative dot plots depicting B-cells in the spleen of a control (left plot) and an AML1-ETO-induced mouse (right plot).

(C) Bar diagrams showing relative percentages of different B-cell populations from non-induced (-DOX, white boxes) and AML1-ETO-expressing mice (+DOX, black boxes).

(D) Bar diagrams showing absolute percentages of different B-cell populations from non-induced (-DOX, white boxes) and AML1-ETO-expressing mice (+DOX, black boxes).

(E) Bar diagrams showing relative percentages of B-cells in the spleen from non-induced (-DOX, white boxes) and AML1-ETO-induced mice (+DOX, black boxes).

(F) Bar diagrams showing absolute percentages of B-cells in the spleen from non-induced (-DOX, white boxes) and AML1-ETO-induced mice (+DOX, black boxes).

I, pre and pro B-cells; II, immature B-cells, III, re-circulating B-cells; BM, bone marrow; SPL, spleen; n, number of animals; 7AAD, 7-amino-actinomycin; -DOX, without doxycycline; +DOX, with doxycycline; *p<0.05; **p<0.01; ***p<0.001. Mean values of relative or absolute percentages ± standard deviations from at least four mice in each group are depicted as bar diagrams. Dead cells were excluded by 7AAD staining.

3.13.5.2 Analysis of T-cell maturation

Under normal circumstances T-cell maturation takes place in the thymus. T-cell maturation steps were determined by the use of CD44, CD25, CD4 and CD8 antibodies (see section 3.6.4.2). The initial stages of T-cell maturation are DN1, DN2 and DN3 and they can be defined as $CD4^-/CD8^-/CD44^+/CD25^-$, $CD4^-/CD8^-/CD44^+/CD25^+$ and $CD4^-/CD8^-/CD44^-/CD25^+$ populations. Subsequent steps of T-cell development are the DP, the CD4 and the CD8 single positive cells, which are defined as $CD4^+/CD8^+$, $CD4^+$ and $CD8^+$ populations. Representative dot plots depicting the DN1 to the DN3 T-cell maturation stages and the DP to single CD4 or CD8 T-cells are show in Figure 35A and B. Analysis of the data revealed that DN1 and DN2 thymocytes remained unchanged in absolute and relative numbers when compared to control mice. However, AML1-ETO expression resulted in a decrease of DN3 ($CD44^-/CD25^+$) thymocytes. With regard to later T-cell developmental stages, double-positive (DP, $CD4^+/CD8^+$) cells were markedly reduced in absolute and relative numbers in AML1-ETO-expressing mice (Figure 35B). Meanwhile, CD4 and CD8 single positive cells remained normal when compared to the control group (Figure 35B). In summary, AML1-ETO expression resulted in a decrease of DN3 ($CD44^-/CD25^+$) thymocytes indicating an impaired transition from the DN2 to the DN3 stage in the thymus. Furthermore, double-positive (DP, $CD4^+/CD8^+$) T-cells were markedly reduced in AML1-ETO-expressing mice (Figure 35B, E and F). These results indicated an obvious alteration in normal T-cell development following aberrant AML1-ETO expression in $R26/AE/RAG2^{-/-}$ mice.

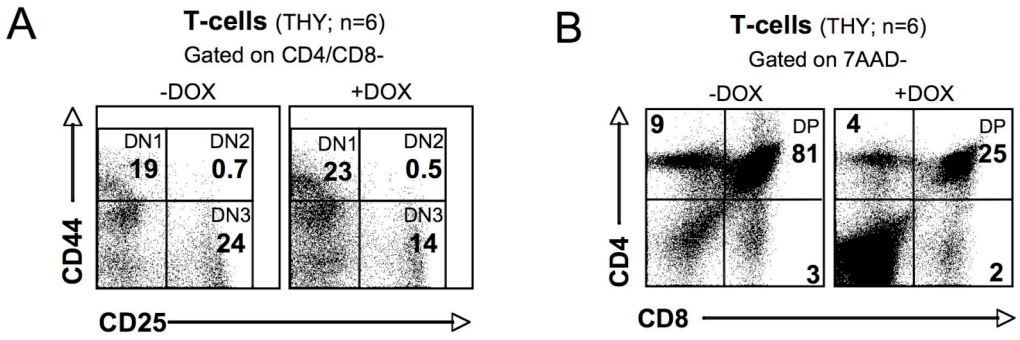

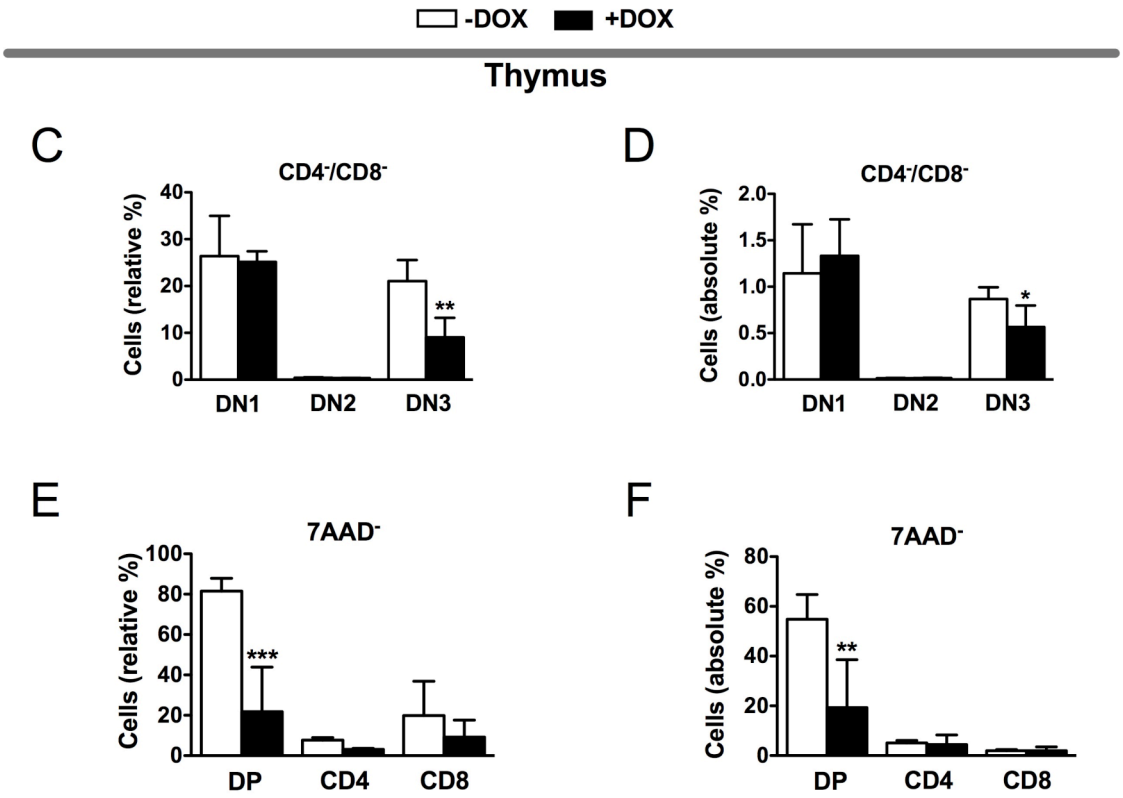

Figure 35: FACS analysis of T-cell maturation in the thymus

(A) Representative dot plots depicting the initial steps of T-cell maturation in the thymus (DN1 to DN3) of a control (left plot) and an AML1-ETO-induced mouse (right plot).

(B) Representative dot plots depicting the final steps of T-cell maturation in the thymus (DP, $CD4^+$ and $CD8^+$) of a control (left plot) and an AML1-ETO-induced mouse (right plot).

(C) Bar diagrams showing relative percentages of the first steps of T-cell maturation in the thymus (DN1 to DN3) from non-induced (-DOX, white boxes) and AML1-ETO-expression mice (+DOX, black boxes).

(D) Bar diagrams showing absolute percentages of the initial steps of T-cell maturation in the thymus (DN1 to DN3) from non-induced (-DOX, white boxes) and AML1-ETO-expression mice (+DOX, black boxes).

(E) Bar diagrams showing relative percentages of the final steps of T-cell maturation in the thymus (DP, $CD4^+$ and $CD8^+$) from non-induced (-DOX, white boxes) and AML1-ETO-induced mice (+DOX, black boxes).

(F) Bar diagrams showing absolute percentages of the final steps of T-cell maturation in the thymus (DP, $CD4^+$ and $CD8^+$) from non-induced (-DOX, white boxes) and AML1-ETO-induced mice (+DOX, black boxes).

DN1, $CD4^-/CD8^-$, double negative 1 cells; DN2, $CD4^-/CD8^-$, double negative 2 cells; DN3, $CD4^-/CD8^-$, double negative 3 cells; DP, $CD4^+/CD8^+$, double positive cells, THY, thymus; n, number of animals; 7AAD, 7-amino-actinomycin; -DOX, without doxycycline; +DOX, with doxycycline; *p<0.05; **p<0.01; ***p<0.001. Dead cells were excluded by 7AAD staining. The bar diagrams represent the mean values of relative or absolute percentages ± standard deviations from at least four mice in each group. Surfaces parameters are indicated for each group.

3.13.6 AML1-ETO expression promotes high extra-medullary activity in the spleen

The increase of non-differentiated large cells (LUC) in blood cell counts (Figure 22) together with the observed splenomegaly (Figure 24) and the higher incidence of erythroid clusters within the red pulp of DOX-exposed R26/AE/RAG2$^{-/-}$ mice (Figure 25), suggested an abnormal extra-medullary activity in the spleen. To carefully analyze these findings, it was of importance to determine the relative and absolute numbers of erythroid-progenitors, myeloid populations and LKS cells in the spleen.

3.13.6.1 Expression of AML1-ETO protein impairs an increase in splenic erythropoiesis

Since AML1-ETO expression in R26/AE/RAG2$^{-/-}$ mice led to splenomegaly (Figure 24), it was of interest to determine if any differences in splenic erythroid progenitors were observed between non-induced and AML1-ETO-expressing mice. Firstly, spleens were removed from mice, mature erythrocytes were lysated and cells were stained with CD71 and TER119 antibodies. Then, the double positive population (CD71^{+}/TER119^{+}) containing erythroid progenitors was analyzed. In Figure 36 flow cytometric dot plots for erythroid progenitors are depicted for a control (Figure 36A; -DOX) and an AML1-ETO-expressing mouse (Figure 36A; +DOX). As shown in Figure 36, a more than three-fold increase in absolute and relative numbers of erythroid progenitors was observed in AML1-ETO-expressing mice when compared to the control group. Therefore, it was to be concluded that the expression of AML1-ETO in R26/AE/RAG2$^{-/-}$ mice promoted an increase in extra-medullary erythropoiesis.

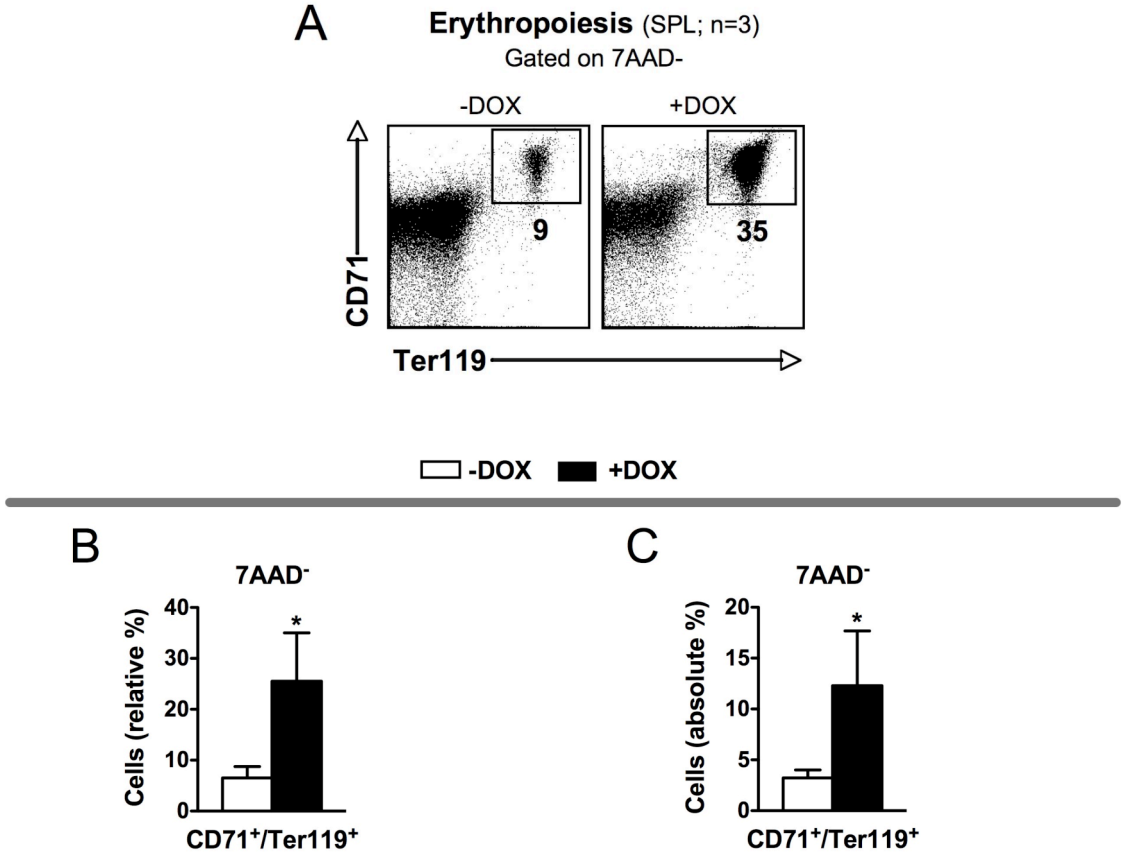

Figure 36: FACS analysis of erythroid progenitors in the spleen
(A) Representative dot plots depicting erythroid progenitors in the spleen from a control (left plot) and an AML1-ETO-induced mouse (right plot).
(B) Bar diagrams showing relative percentages of the $CD71^+/TER119^+$ population from non-induced (-DOX, white boxes) and AML1-ETO-expressing mice (+DOX, black boxes).
(C) Bar diagrams showing absolute percentages of the $CD71^+/TER119^+$ population from non-induced (-DOX, white boxes) and AML1-ETO-expressing mice (+DOX, black boxes).
SPL, spleen; n, number of animals; 7AAD, 7-amino-actinomycin; -DOX, without doxycycline; +DOX, with doxycycline; *p<0.05; **p<0.01. Mean values of relative or absolute percentages ± standard deviations from at least three mice in each group represented as bar diagrams. Dead cells were excluded by 7AAD staining.

3.13.6.2 Long-term AML1-ETO expression in R26/AE/RAG2$^{-/-}$ mice leads to an increase in splenic granulocytes

Given the enhanced granulopoiesis seen in the bone marrow of AML1-ETO-expressing R26/AE/RAG2$^{-/-}$ mice (Figure 32), it was important to determine if any differences were to be observed with regard to extra-medullary granulocytes. Therefore, the granulocytic population from the spleen was enumerated using CD11b and Gr-1 antibodies. Figure 37 depicts representative flow cytometric dot plots of granulocytes for

a control mouse (Figure 37A; -DOX) and an AML1-ETO-expressing mouse (Figure 37A; +DOX). In correlation with the increase in granulocytes found in the bone marrow of AML1-ETO-expressing animals, granulocytes were also expanded in the spleen demonstrating that blood-restricted AML1-ETO expression led to the expansion of granulocytes not only in the bone marrow compartment but also in the spleen.

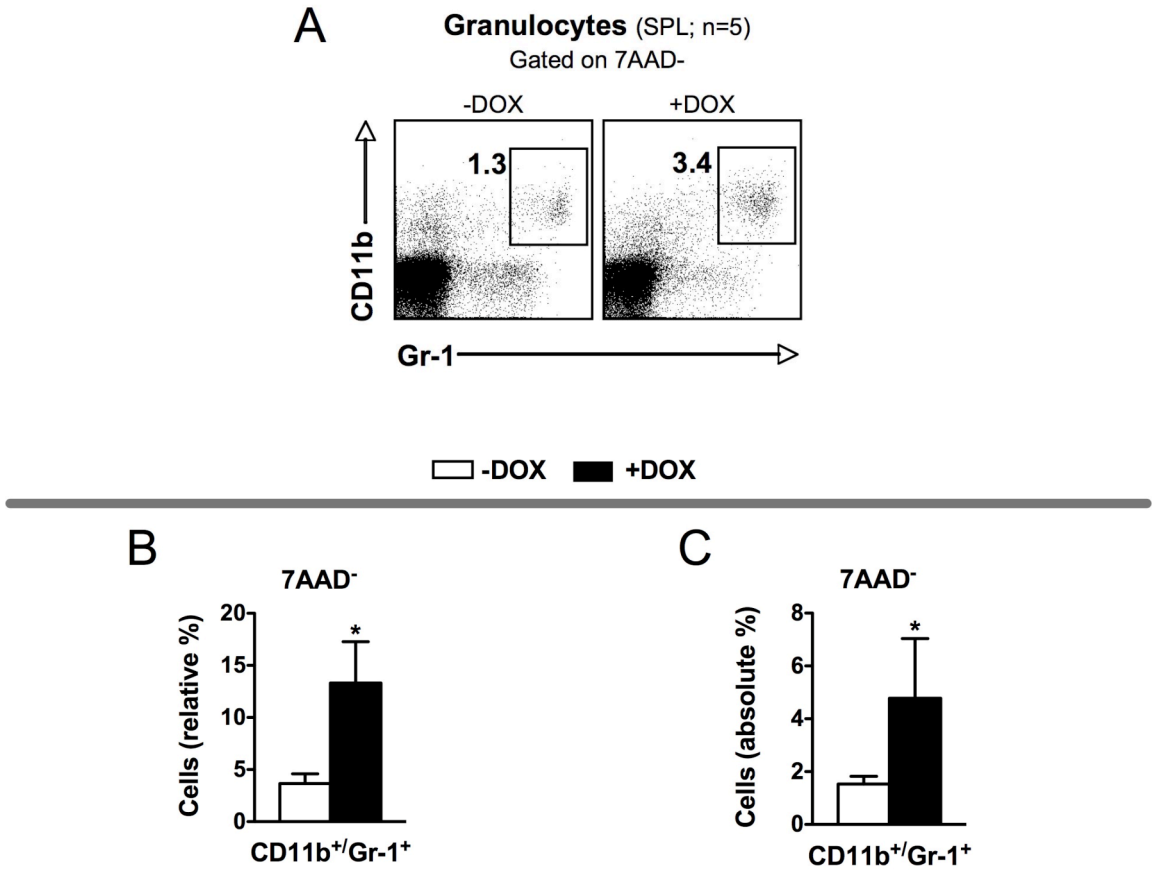

Figure 37: FACS analysis of granulocytes in the spleen
(A) Representative dot plots depicting granulocytes in the spleen from a control (left plot) and an AML1-ETO-induced mouse (right plot).
(B) Bar diagrams showing relative percentages of $CD11b^+/Gr\text{-}1^+$ cells from non-induced (-DOX, white boxes) and AML1-ETO-induced mice (+DOX, black boxes).
(C) Bar diagrams showing absolute percentages of $CD11b^+/Gr\text{-}1^+$ cells from non-induced (-DOX, white boxes) and AML1-ETO-induced mice (+DOX, black boxes).
SPL, spleen; n, number of animals; 7AAD, 7-amino-actinomycin; -DOX, without doxycycline; +DOX, with doxycycline; *p<0.05; **p<0.01. Dead cells were excluded by 7AAD staining.

3.13.6.3 Spleens of AML1-ETO-expressing animals contain more immature blasts

Since in peripheral blood samples of AML1-ETO-expressing mice an overall increase in granulocytes and a markedly expansion of LUC cells was noted (Figure 22), the percentage of immature blasts in this organ was determined. As described by Zuber and colleagues immature blasts can be defined as B220$^-$/CD3$^-$/Ter119$^-$/Sca-1$^-$/CD11b$^-$/Gr-1$^-$/F4/80^{low}/c-Kit$^+$ (Zuber et al., 2009). Figure 38A depicts a representative contour plot from a control (-DOX) and an AML1-ETO-expressing mouse (+DOX). Data analysis of these experiments indicated an increase in immature blasts in AML1-ETO-expressing mice (Figure 38B and C; +DOX) when compared to the control group (Figure 38B and C; -DOX). Taken together, in contrast to the results found in bone marrow, an increase in immature blasts was observed in the spleen of AML1-ETO-induced animals.

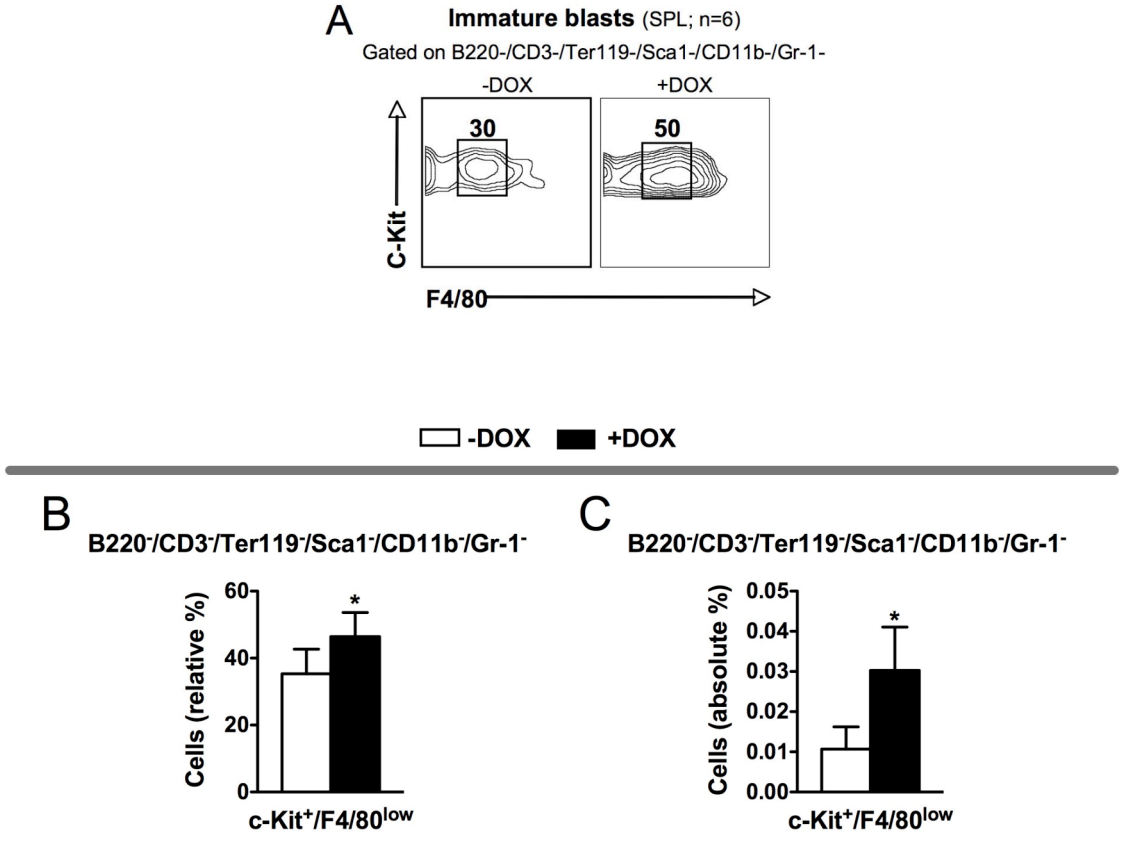

Figure 38: FACS analysis of immature blasts in the spleen
(A) Representative contour plots depicting immature blasts from a control (left plot) and an AML1-ETO-induced mouse (right plot).

(B) Bar diagrams showing relative percentages of immature blasts ($B220^-/CD3^-/Ter119^-/Sca\text{-}1^-/CD11b^-/Gr\text{-}1^-/F4/80^{low}/c\text{-}Kit^+$) from non-induced (-DOX, white boxes) and AML1-ETO-induced mice (+DOX, black boxes).
(C) Bar diagrams showing absolute percentages of immature blasts ($B220^-/CD3^-/Ter119^-/Sca\text{-}1^-/CD11b^-/Gr\text{-}1^-/F4/80^{low}/c\text{-}Kit^+$) from non-induced (-DOX, white boxes) and AML1-ETO-induced mice (+DOX, black boxes).
SPL, spleen; n, number of animals; -DOX, without doxycycline; +DOX, with doxycycline; *$p<0.05$. The bar diagrams represent the mean values of relative or absolute percentages ± standard deviations from at least five mice in each group. Used surface antigens are indicated.

3.13.6.4 LKS cells in the spleen of AML1-ETO-expressing mice are significantly increased

As reported by Weissman and colleagues, the so called LKS cells include HSCs and more committed progenitors cells (Uchida and Weissman, 1992). These cells are negative for mature blood cell markers including, CD3 (T-cells), B220 (B-cells), Gr-1 (granulocytes), CD11b (macrophages), TER119 (erythrocytes) and CD11c (dendritic cells) but positive for c-Kit and Sca-1 surface antigens. Figure 39 shows representative flow cytometric contour plots of splenic LKS cells for a control mouse (A; -DOX) and for an AML1-ETO-expressing mouse (A; +DOX). Acquired cells were negatively gated for lineage markers (data not shown) and positively gated for c-Kit and Sca-1. Statistical analyses of relative percentages showed no significant differences between control and AML1-ETO-induced mice (Figure 39B). However, absolute LKS numbers were increased in the spleen of AML1-ETO-expressing animals (Figure 39C). In aggregate, LKS cells were expanded in total numbers but not in relative percentages. This result suggests that only the pool size but not the overall maturation behavior of LKS cells was perturbed. These data, together with the increase observed in erythroid progenitors and myeloid cells, demonstrated a high extra-medullary hematopoietic activity in AML1-ETO-expressing spleens.

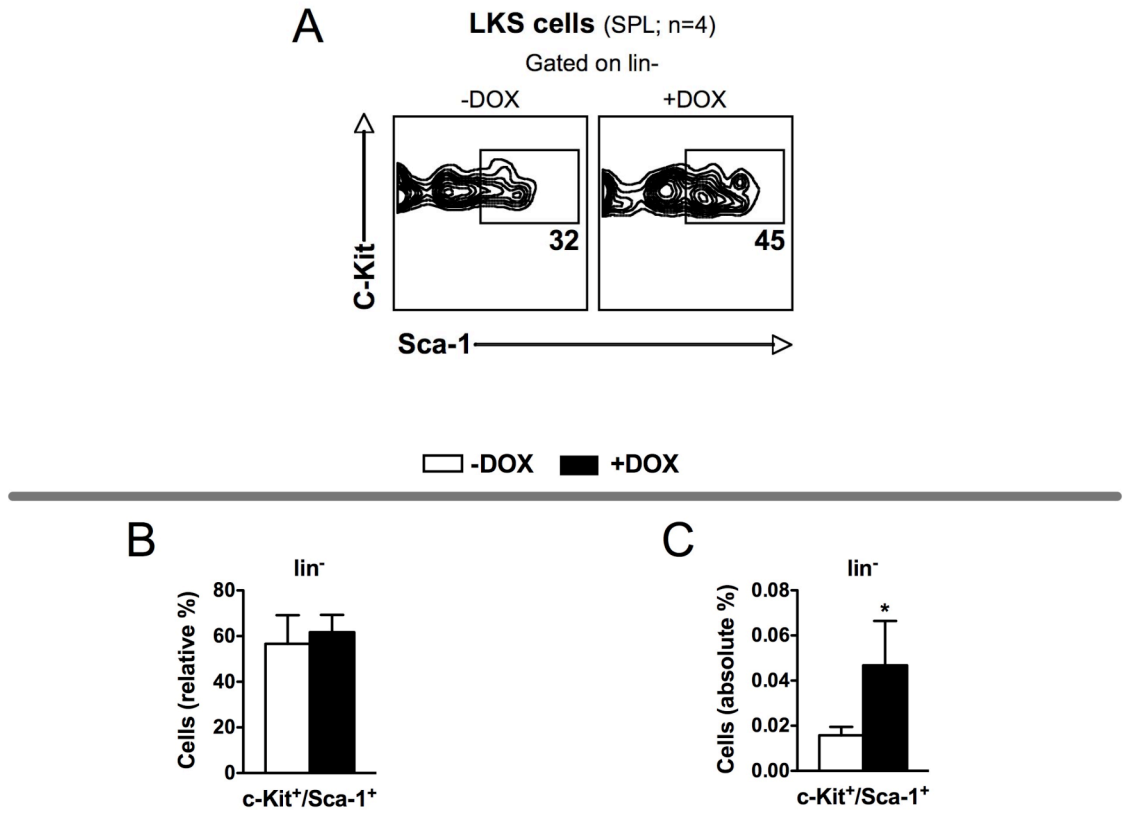

Figure 39: FACS analysis of LKS cells in the spleen
(A) Representative contour plots depicting LKS cells from a control (left plot) and an AML1-ETO-expressing mouse (right plot).
(B) Bar diagrams showing relative percentages of LKS cells from non-expressing (-DOX, white boxes) and AML1-ETO-expressing mice (+DOX, black boxes).
(C) Bar diagrams showing absolute percentages of LKS cells from non-expressing (-DOX, white boxes) and AML1-ETO-expressing mice (+DOX, black boxes).
LKS, lineage$^-$/c-Kit$^+$/Sca-1$^+$**;** SPL, spleen; n, number of animals; lin-, negative for lineage; -DOX, without doxycycline; +DOX, with doxycycline; *p<0.05. Mean values of relative or absolute percentages ± standard deviations from at least four mice in each group were depicted as bar diagrams.

3.13.7 Analysis of HSCs and committed progenitors in the bone marrow

The ability to control self-renewal, pool size and differentiation of stem cells is integral for maintaining normal homeostasis and subversion of this equilibrium is frequently associated with malignant phenotypes and cancer (Gery and Koeffler, 2007; Shivdasani and Orkin, 1996). Prior experiments reported that enforced AML1-ETO expression promoted the amplification of murine LKS or human CD34$^+$ cells in conditioned mice (de Guzman et al., 2002; Mulloy et al., 2003; Schwieger et al., 2002). However, these studies did not address whether AML1-ETO expression perturbed the

homeostatic control of HSC or if more committed progenitors were the target of AML1-ETO-mediated expansion. One of the main aims of the here presented study was to determine this issue. In order to define at which progenitor or stem cell level normal hematopoiesis was subverted by AML1-ETO expression, HSCs, common myeloid progenitors (CMP), megakaryocyte-erythroid progenitors (MEP), granulocyte-macrophage progenitors (GMP) and common lymphoid progenitors (CLP) were analyzed using flow cytometry.

3.13.7.1 Flow-cytometry reveals an amplification of LKS cells in the bone marrow of AML1-ETO-expressing mice

LKS cells, containing HSCs and immature progenitors, were analyzed as described in section 3.6.1. Firstly, acquired cells were negatively gated for lineage and positively gated for the c-Kit surface marker (data not shown). Subsequently, $lin^-/c\text{-}Kit^+$ cells were positively gated for the Sca-1 surface marker (Figure 40A). Figure 40A shows representative contour plots for LKS cells from $R26/AE/RAG2^{-/-}$ mice fed with normal drinking water (-DOX; left plot) and from DOX-exposed $R26/AE/RAG2^{-/-}$ mice (+DOX; right plot). In addition, relative and absolute numbers of LKS cells are represented as bar diagrams from at least eight animals in each group (Figure 40B and C). The statistical analysis illustrated that both absolute and relative numbers of LKS cells were substantially increased in AML1-ETO-induced animals when compared to the control group (Figure 40B and C). In summary, AML1-ETO expression led to an about two-fold increase of LKS cells in the bone marrow.

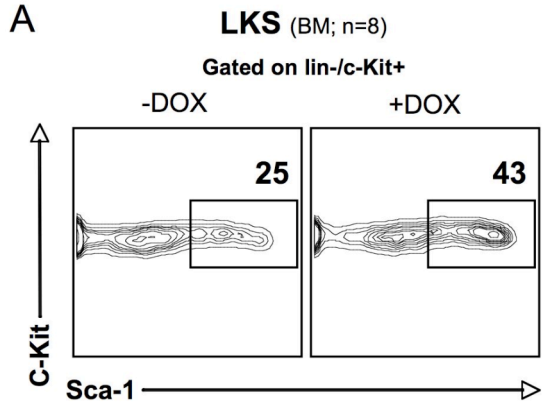

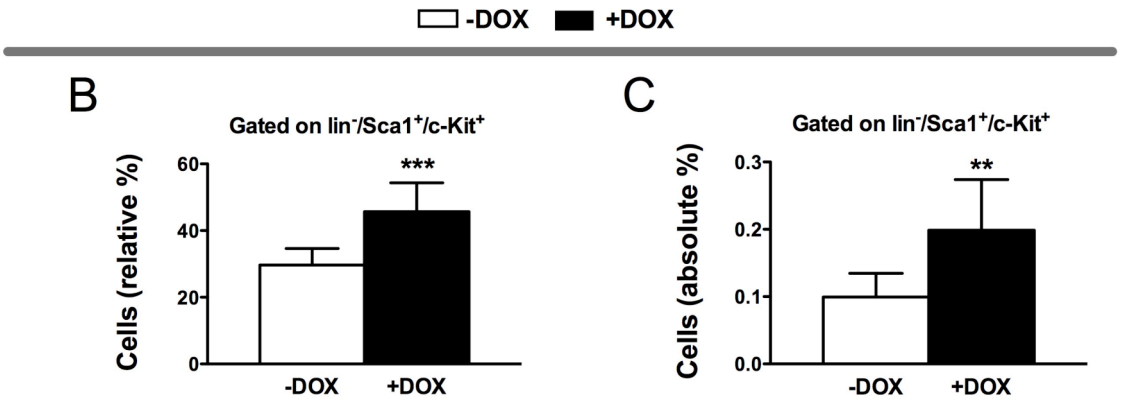

Figure 40: FACS analysis of LKS cells
(A) Representative dot plots depicting LKS cells from a control (left plot) and an AML1-ETO-induced mouse (right plot).
(B) Bar diagrams showing relative percentages of LKS cells from non-induced (-DOX, white boxes) and AML1-ETO-induced mice (+DOX, black boxes).
(C) Bar diagrams showing absolute percentages of LKS cells from non-induced (-DOX, white boxes) and AML1-ETO-induced mice (+DOX, black boxes).
LKS, lineage$^-$/c-Kit$^+$/Sca-1$^+$**;** BM, bone marrow; n, number of animals; lin-, negative for lineage; -DOX, without doxycycline; +DOX, with doxycycline; **p<0.01, ***p<0.001. Surface markers are shown for each experiment.

3.13.7.2 HSCs and MPPs from AML1-ETO-induced mice remain normal

The capacity to self-renewal and the ability to give rise to all differentiated blood cell types are the essential characteristics that define hematopoietic stem cells (HSCs) (Fleischman et al., 1982; Krause et al., 2001; Lemischka et al., 1986; Spangrude et al., 1988). By contrast, multipotent progenitors (MPPs) do not have the capacity to self-renew but have the ability to give rise to all hematopoietic lineages. The HSC/MPP population can be defined by lineage$^-$, c-Kit$^+$, Sca-1$^+$, CD48$^-$ and CD150$^+$ surface markers (Kiel et al., 2008). In addition, lineage$^-$, c-Kit$^+$, Sca-1$^+$, CD48$^+$ and CD150$^+$ cells include more differentiated immature progenitors with restricted lineage potential (Kiel et al., 2008). Since it still remained unknown if HSCs or more committed progenitors were the target of AML1-ETO expansion, it was of importance to in detail analyze the effect of aberrant AML1-ETO expression in these populations. Statistical representations of HSCs/MPPs (Figure 41A) and LKS/CD48$^+$/CD150$^+$ cells (Figure 41B) from at least six mice in each group are depicted in Figure 41. Scatter plots showing the mean values of absolute percentages ± standard deviations from control (-DOX) and AML1-ETO-

expressing mice (+DOX) are represented for each group. As shown in Figure 41A, no differences were noted between HSCs/MPPs from non-induced and AML1-ETO induced animals. However, more committed progenitors ($CD48^+$ cells) revealed a clear expansion in absolute numbers when compared to the control group (Figure 41B). These results indicated that cell-autonomous AML1-ETO expression did not promote an expansion of HSCs/MPPs. However, an increase in CD48-expressing and thus more differentiated immature progenitors was observed in the bone marrow of AML1-ETO induced mice.

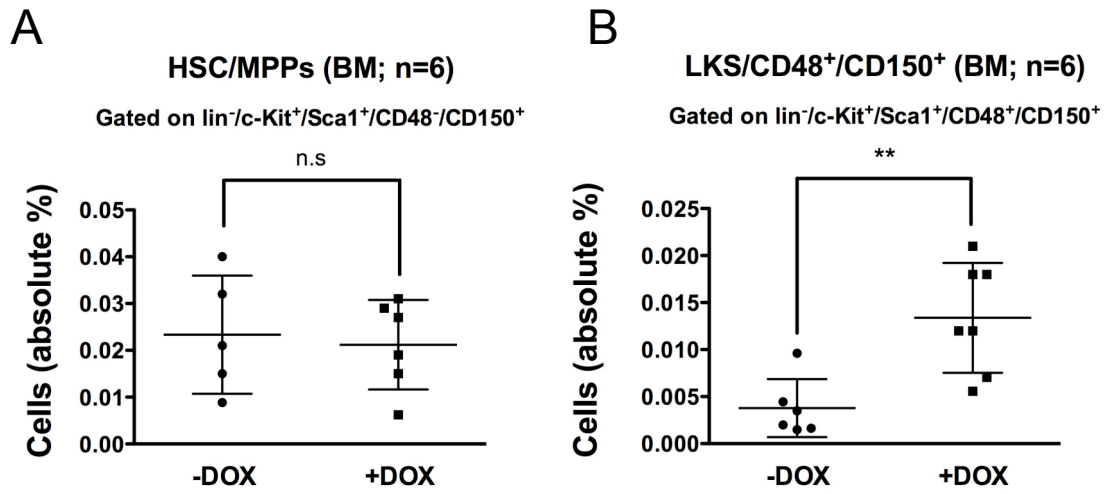

Figure 41: FACS analysis of HSCs/MPPs cells and LKS/$CD48^+$/$CD150^+$ cells
(A) Scatter plot showing the absolute percentages of HSCs/MPPs from non-induced (-DOX) and AML1-ETO-induced mice (+DOX).
(B) Scatter plot showing the absolute percentages of LKS/$CD48^+$/$CD150^+$ more differentiated progenitors from non-induced (-DOX) and AML1-ETO-induced mice (+DOX).
HSCs, hematopoietic stem cells; MPPs, multipotent progenitors; LKS, $lineage^-$, c-Kit^+, Sca-1^+; BM, bone marrow; n, number of animals; lin-, negative for lineage markers; n.s, non significant; -DOX, without doxycycline; +DOX, with doxycycline. **p<0.01. Surface markers are indicated for each experiment.

3.13.7.3 AML1-ETO expression expands GMPs but has no effect on CLPs, CMPs or MEPs

Given the increase in immature $CD48^+$ progenitors in AML1-ETO-activated chimera, it was of interest to specifically determine which progenitors where the target of AML1-ETO expansion. For this reason, common lymphoid progenitors (CLP), common myeloid progenitors (CMP), megakaryocyte-erythroid progenitors (MEP) and granulocyte-macrophage progenitors (GMP) were analyzed using flow-cytometry.

3.13.7.3.1 Analysis of CLPs

As described by Kondo and colleagues, CLPs can be defined as lin$^-$/c-Kit^{low}/ Sca-1^{low}/Thy1.1$^-$/IL-7Rα^+ (Kondo et al., 1997). As seen in Figure 42 flow-cytometry indicated no differences in absolute numbers of CLPs between control and AML1-ETO induced mice. Acquired cells were negatively gated for Thy1.1 and lineage markers, low for c-Kit and Sca-1 markers, and positive for the IL-7Rα surface marker (data not shown). These data indicated that long-term AML1-ETO expression did not affect the normal homeostasis of CLPs.

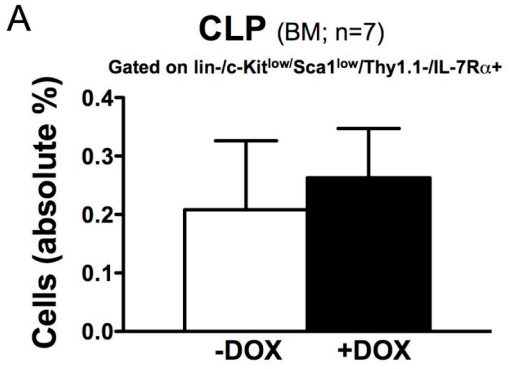

Figure 42: FACS analysis of CLPs
(A) Bar diagrams showing absolute percentages of CLPs from non-expressing (-DOX, white boxes) and AML1-ETO-expressing mice (+DOX, black boxes).
CLP, common lymphoid progenitor; BM, bone marrow; n, number of animals; lin-, negative for lineage markers; -DOX, without doxycycline; +DOX, with doxycycline. The bar diagrams represent the mean values of absolute percentages ± standard deviations from at least seven mice in each group. Used surface antigens are indicated.

3.13.7.3.2 Granulocyte-macrophage progenitors are expanded in AML1-ETO-expressing chimeras

In order to analyze CMPs, GMPs and MEPs the protocol used by Kirstetter and colleagues was followed (Kirstetter et al., 2006). This group described CMPs as LKS/ IL-7Rα^-/CD34$^+$/FcγRII/III^{low}, GMPs as LKS/IL-7Rα^-/CD34$^+$/FcγRII/III$^+$, and MEPs as LKS/IL-7Rα^-/CD34$^-$/FcγRII/III^{low}. Figure 43 shows the statistical analyses of relative and absolute percentages of CMPs, GMPs and MEPs in bar diagrams. In these experiments no differences were noted in absolute numbers of both the MEP and CMP population.

However, a slight reduction in relative percentages of MEPs was observed and CMPs from AML1-ETO-expressing animals remained invariable when compared to the control group (Figure 43B). Interestingly, GMPs showed a marked expansion both in absolute and relative numbers (Figure 43B and C). Taken together, this analysis revealed that AML1-ETO expression in R26/AE/RAG2$^{-/-}$ mice promoted a substantial expansion of GMPs in the bone marrow. These results established for the first time that AML1-ETO expression specifically expanded GMPs, but did not affect MEPs and CMPs.

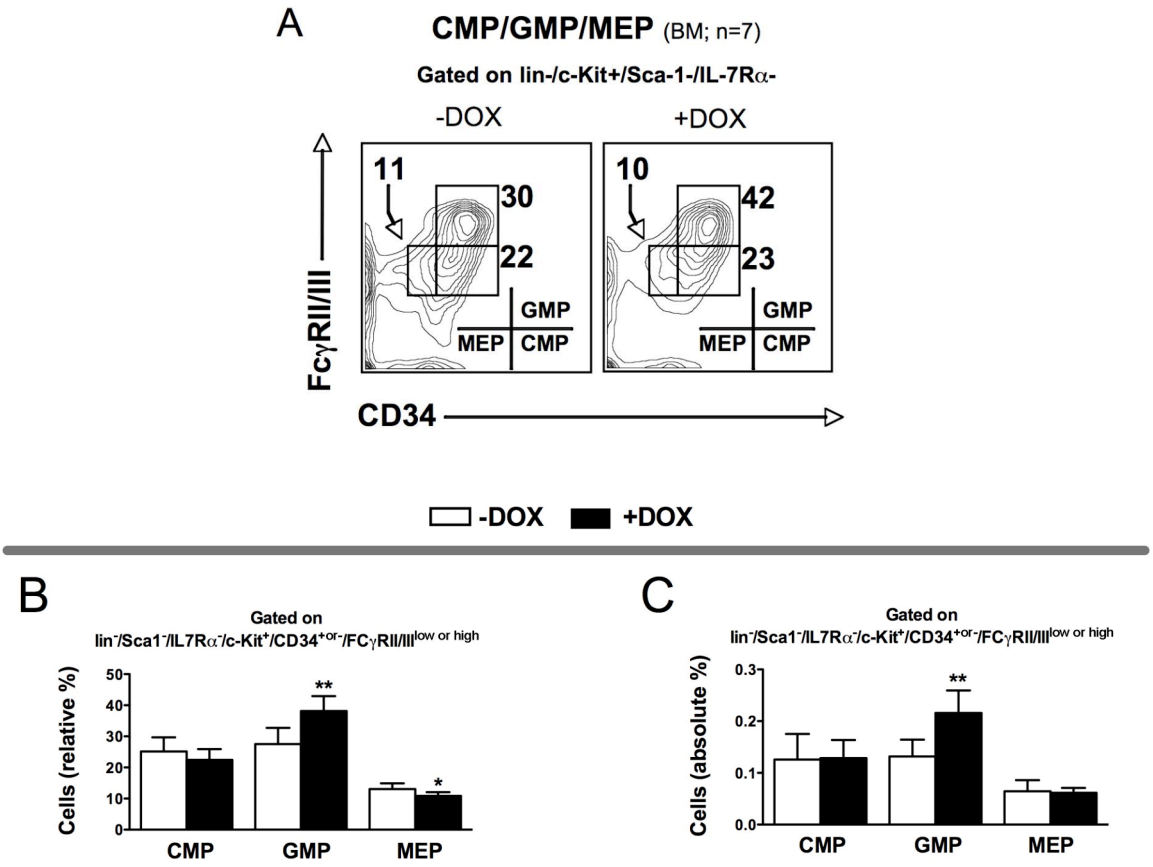

Figure 43: FACS analysis of CMPs, GMPs and MEPs
(A) Representative contour plots depicting CMPs, GMPs and MEPs from a control (left plot) and an AML1-ETO-induced mouse (right plot).
(B) Bar diagrams showing relative percentages of CMPs, GMPs and MEPs from non-induced (-DOX, white boxes) and AML1-ETO-induced mice (+DOX, black boxes).
(C) Bar diagrams showing absolute percentages of CMPs, GMPs and MEPs from non-induced (-DOX, white boxes) and AML1-ETO-induced mice (+DOX, black boxes).
CMP, common myeloid progenitor; GMP, granulocyte/macrophage progenitor; MEP, megakaryocyte/erythrocyte progenitor; BM, bone marrow; n, number of animals; lin-, negative for lineage markers; -DOX, without doxycycline; +DOX, with doxycycline; *p<0.05, **p<0.01. Mean values of absolute percentages ± standard deviations from at least seven mice in each group depicted as bar diagrams. Surface markers are indicated for each experiment.

3.13.8 AML1-ETO expression leads to an expansion of differentiated myeloid cells

Because a major clinical feature of AML-M2 t(8;21) is a block in terminal myeloid differentiation but in mouse models expressing AML1-ETO an enhanced of granulopoiesis is described (de Guzman et al., 2002; Fenske et al., 2004; Schwieger et al., 2002), it was important to test whether myelopoiesis was affected by enforced AML1-ETO expression in the R26/AE/RAG2$^{-/-}$ mice. Therefore, differentiated myeloid cell lineages were analyzed. Macrophages can be described as Gr-1^{-}/CD11b^{+}/F4/80^{+}, neutrophils as Gr-1^{+}/CD11b^{+}/F4/80^{-} and eosinophils as Gr-1^{low}/CD11b^{+}/F4/80^{lo}. Figure 44A, B and C shows representative flow cytometric dot and contour plots of macrophages, neutrophils and eosinophils from a control mouse (-DOX) and an AML1-ETO-expressing mouse (+DOX). Statistical analyses of relative and absolute percentages of myeloid cells are shown in Figures 44D, E, F, G, H and I. Interestingly, flow cytometric analysis of these populations demonstrated a higher proportion of these cells both in relative and absolute percentages in bone marrow samples of AML1-ETO expressing mice when compared to control animals. In conclusion, long-term AML1-ETO expression stimulated the amplification of macrophages, neutrophils and eosinophils in bone marrow from R26/AE/RAG2$^{-/-}$ chimeric mice. These results revealed that aberrant AML1-ETO expression did not lead to a developmental block of granulopoiesis but rather enhanced granulocytic maturation.

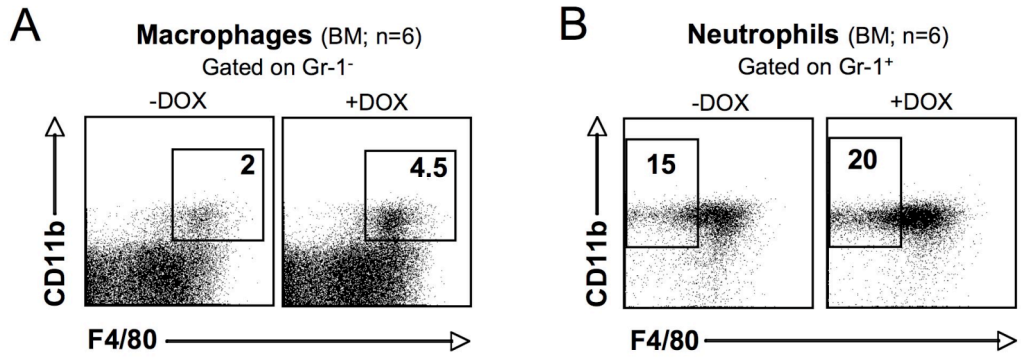

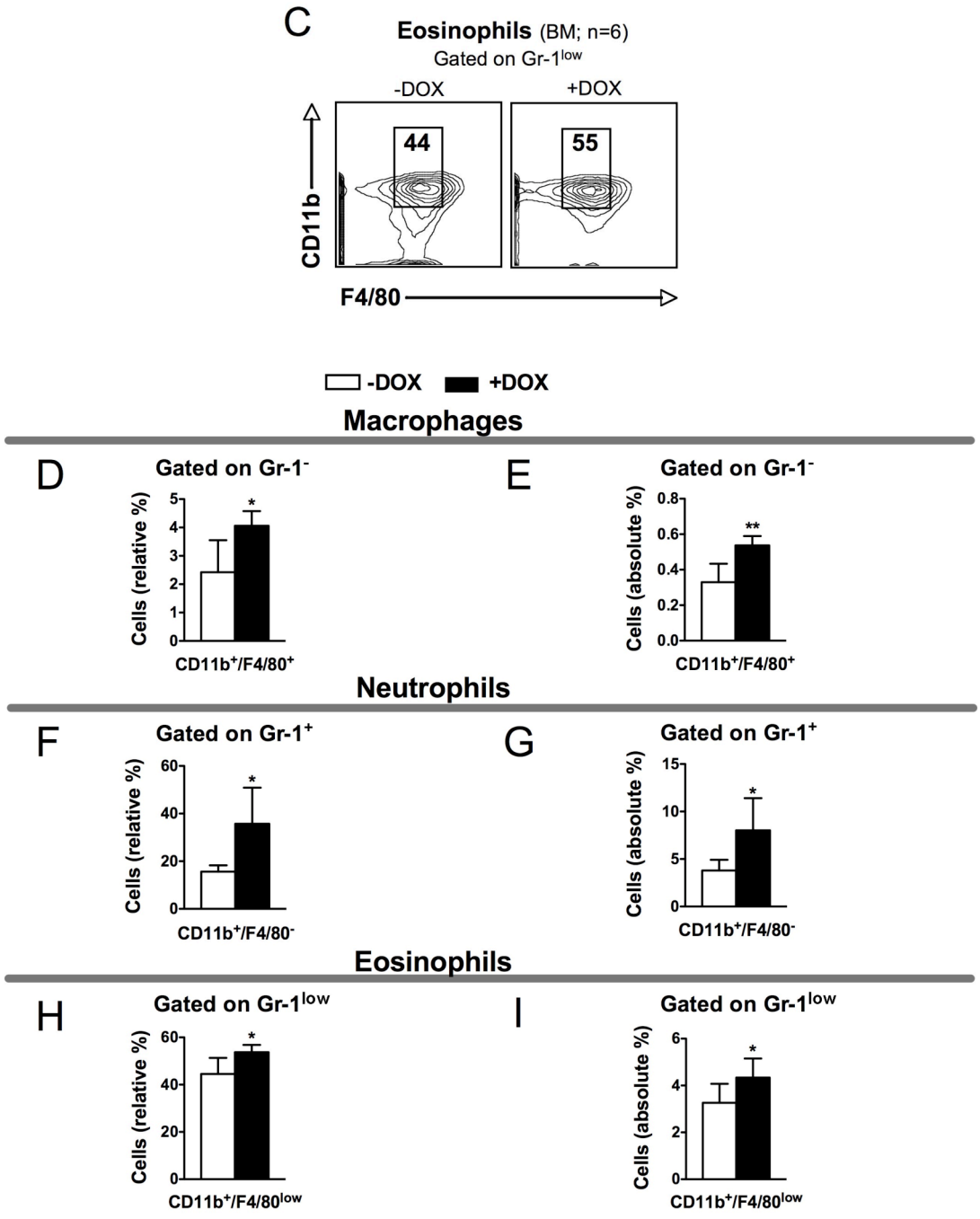

Figure 44: FACS analysis of macrophages, neutrophils and eosinophils in the bone marrow
(A) Representative dot plots depicting the macrophage population in the bone marrow from a control (left plot) and an AML1-ETO-induced mouse (right plot).
(B) Representative dot plots depicting the neutrophilic population in the bone marrow from a control (-DOX) and an AML1-ETO-activated mouse (+DOX).
(C) Representative contour plots depicting the eosinophilic population in the bone marrow from a control (left plot) and an AML1-ETO-expressing mouse (right plot).
(D) Bar diagrams showing relative percentages of the macrophage population from non-induced (-DOX, white boxes) and AML1-ETO-expressing mice (+DOX, black boxes).
(E) Bar diagrams showing absolute percentages of the macrophage population from non-induced (-DOX, white boxes) and AML1-ETO-induced mice (+DOX, black boxes).
(F) Bar diagrams showing relative percentages of the neutrophilic population from non-induced (-DOX, white boxes) and AML1-ETO-activated mice (+DOX, black boxes).

(G) Bar diagrams showing absolute percentages of the neutrophilic population from non-induced (-DOX, white boxes) and AML1-ETO-induced mice (+DOX, black boxes).
(H) Bar diagrams showing relative percentages of the eosinophilic population from non-induced (-DOX, white boxes) and AML1-ETO-expressing mice (+DOX, black boxes).
(I) Bar diagrams showing absolute percentages of the eosinophilic population from non-induced (-DOX, white boxes) and AML1-ETO-activated mice (+DOX, black boxes).
BM, bone marrow; n, number of animals; -DOX, without doxycycline; +DOX, with doxycycline; *p<0.05; **p<0.01. Bar diagrams represent the mean values of relative or absolute percentages ± standard deviations from at least six mice in each group. Used surface antigens are indicated.

3.14 Colony-forming units assays (CFUs) reveal an expansion of CFU-GM colonies

In the previously conducted flow-cytometric experiments, GMPs were expanded in AML1-ETO-induced mice. As an additional test, the *in vitro* colony-forming unit assay was performed. Using this system, it is possible to *in vitro* quantify multi-potential progenitors and lineage-restricted progenitors of the erythroid, granulocytic, monocyte-macrophage, and megakaryocyte-myelopoietic pathways. Isolated bone marrow cells from R26/AE/RAG2$^{-/-}$ mice fed with normal drinking water and cells from DOX-exposed mice were cultured in M3434 medium. M3434 is a methylcellulose semi-solid matrix supplemented with nutrients and cytokines, where individual progenitors, called colony-forming cells (CFCs), proliferate to form discrete cell clusters or colonies (www.stemcell.com). After ten days of incubation, colonies were classified and enumerated based on the morphological recognition of one or more types of hematopoietic lineage cells within each colony. To properly classify the cells light microscopy was applied and the manufacturer's instructions were followed. Colony-forming unit granulocyte/erythroid/macrophage/megakaryocyte (CFU-GEMM), colony-forming unit granulocyte/macrophage (CFU-GM) and burst-forming unit erythroid colonies (BFU-E) can thus be identified. On the right of Figure 45 the total number of colonies obtained in these experiments and on the left the counted CFU-GEMM, CFU-GM and BFU-E colonies are shown. Notably, bone marrow cells from AML1-ETO-expressing mice showed an increase in the total number of colonies when compared to the control group. Interestingly, only CFU-GM colonies were expanded upon AML1-ETO expression, whereas CFU-GEMM and BFU-E units remained normal. In conclusion, the overall number of colonies and more precisely, CFU-GM colonies, increased following blood-restricted AML1-ETO expression. These *in vitro* data directly

confirmed the *in vivo* expansion of GMPs.

The experiments conducted in this PhD thesis thus identified the cellular targets of AML1-ETO-mediated cell expansion in the HSC and hematopoietic progenitor compartment and established for the first time that AML1-ETO specifically expanded GMPs.

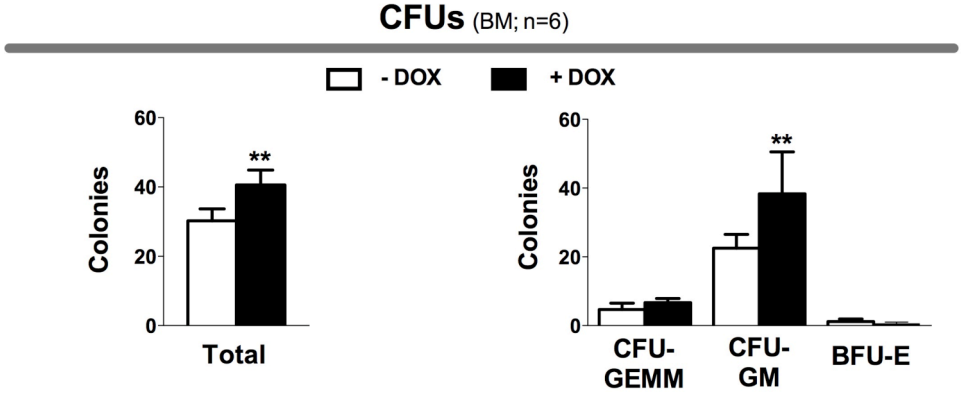

Figure 45: Colony forming assay
Bar diagrams showing total numbers of counted colonies (diagram on the left) and observed CFU-GEMM, CFU-GM and BFU-E colonies (diagram on the right) from non-induced (-DOX, white boxes) and AML1-ETO-induced mice (+DOX, black boxes).
CFUs, colony-forming units; CFU-GEMM, colony-forming unit granulocyte/erythroid/macrophage/ megakaryocyte; CFU-GM, colony-forming unit granulocyte/macrophage; BFU-E, burst-forming unit erythroid; BM, bone marrow; n, number of animals; -DOX, without doxycycline; +DOX, with doxycycline; **$p<0.01$. The bar diagrams represent the mean values of counted colonies ± standard deviations from at least six experiments in each group.

4 DISCUSSION

To date, several AML1-ETO mouse models have been generated to understand the *in vivo* role of the translocated AML1-ETO protein (reviewed in (McCormack et al., 2008; Muller et al., 2008; Peterson et al., 2007; Renneville et al., 2008)). These models provided direct proof for the concept that AML1-ETO activation itself is not sufficient for causing leukemia. However, there are still important questions to be answered and open queries that have to be clarified due to the mostly controversial results published in the past. For instance, the effect of AML1-ETO expression on hematopoietic stem cells (HSCs) or progenitors remains still elusive and in particular the ability of AML1-ETO to cause expansion of pre-malignant stem cell populations is completely unknown. This is especially surprising considering that leukemia is considered to be a stem cell disease (Huntly and Gilliland, 2005). In addition, the most striking controversy is that experiments with genetically modified mice failed to produce phenotypes seen after retroviral-mediated expression of AML1-ETO in transduced bone marrow cells followed by adoptive transfer into conditioned recipients (Buchholz et al., 2000; Bäsecke et al., 2005; Higuchi et al., 2002; Mulloy et al., 2003; Okuda et al., 1996; Rhoades et al., 2000; Schwieger et al., 2002; Yuan et al., 2001). The focus of this work was therefore to clarify these questions and to generate a novel mouse model that has the potential to closely recapitulate the pre-leukemic condition found in human patients.

Given the frequency and relevance of the t(8;21) chromosomal translocation to AML pathogenesis and recurrence, the requirement of suitable models that provide new mechanistic insights for understanding the function of AML1-ETO in hematopoiesis and during pre-leukemic stages is evident. Furthermore, a model that has the potential to recapitulate the human disease can be very useful for preclinical testing and bears the possibility to improve current therapies aimed at more effective treatment for AML patients. For this reason, was generated an appropriate murine model in which the expression of the human AML1-ETO fusion protein can be conditionally activated from the constitutively active ROSA26 (R26) locus. The here presented discussion illustrates the novelty of the developed model and highlights that the ROSA26/AML1-ETO (R26/AE) system is more suitable for understanding the pre-leukemic condition of human AML disease than previous approaches.

4.1 Generalized expression of AML1-ETO fusion protein from the R26 locus

Several studies about the *in vivo* function of AML1-ETO have been published in the past. In 2008, McCormack and colleagues and Muller and colleagues reviewed these papers (McCormack et al., 2008; Muller et al., 2008). One important lack of the previously published studies is that the level of AML1-ETO transcription was not determined. This is even more important since it has been shown that AML1-ETO expression levels play a crucial role for the prognosis of the disease (Takenokuchi et al., 2004; Yoo et al., 2005). In addition, it is known that AML patients broadly express the AML1-ETO gene in all differentiated blood cells and in HSCs (Miyamoto et al., 1996; Miyamoto et al., 2000). In order to determine quantitatively and qualitatively AML1-ETO levels in the R26/AE model, real-time PCR (QPCR) for AML1-ETO mRNA was performed in differentiated blood lineages and HSC/progenitors and the amount of AML1-ETO mRNA was also compared to the level of transcription in the human leukemic Kasumi-1 cell line. As shown in Figure 8, QPCR analysis revealed that all analyzed blood cell types and HSC/progenitors from AML1-ETO-induced mice expressed similar levels of AML1-ETO mRNA as human Kasumi-1 cells. Moreover, no sign of leakiness was found in non-induced R26/AE animals. Therefore, it is to be concluded that the R26/AE mouse is a suitable model for studying the role of AML1-ETO for hematopoiesis and most importantly, that the levels of AML1-ETO transcription are comparable to those found in AML-M2 t(8;21) patients. In addition, the absolute lack of AML1-ETO transcription detected in the absence of doxycycline (DOX) also highlights the complete conditionality of the tet on/off system used for regulating AML1-ETO expression.

In a first series of experiments the effect of ubiquitous AML1-ETO expression from the R26 locus was addressed. In these studies ten days AML1-ETO expression induced a striking phenotype that was characterized by weight loss, reduced mobility, epidermal hyperplasia and high lethality-rates (Figure 9). This obvious phenotype strongly contrasts with all previously reported alterations found in genetically modified AML1-ETO mouse models (McCormack et al., 2008; Muller et al., 2008; Peterson et al., 2007; Renneville et al., 2008). Interestingly, Fenske and colleagues also reported epidermal hyperplasia using a Sca-$1^{+/AML1\text{-}ETO}$ knock-in mouse (Fenske et al., 2004). In their study, young Sca-$1^{+/AML1\text{-}ETO}$ mice developed an apparent skin phenotype and within the first year these

lesions progressed to squamous cell carcinomas. The Sca-1 locus is known to be transcriptionally active in mammary gland epithelial progenitor cells (Welm et al., 2002), raising the possibility that in these studies, the Sca-1 promoter may also have directed expression of AML1-ETO to skin progenitors cells. In the same way, we and others found that the R26 locus was active in most tissues including the skin (Soriano, 1999; Wörtge et al., 2010; Zambrowicz et al., 1997). The here found skin hyperplasia supports the hypothesis put forward by Fenske and colleagues that AML1-ETO is directly or indirectly initiating a malignant skin condition. However, it cannot be concluded that the epidermal hyperplasia observed in AML1-ETO-induced R26/AE mice would have progressed to squamous cell carcinoma because AML1-ETO-expressing mice prematurely died after induction. In addition, the results obtained with the R26/AE mouse are not straightforwardly interpreted because of the generalized activity of the R26 locus directing AML1-ETO expression to many different cells. The generalized AML1-ETO expression therefore precluded to track down the proper identity of the cell type that promoted the skin hyperplasia.

Peripheral blood analysis from compound AML1-ETO-expressing animals indicated that normal hematopoiesis was strongly affected by expression of the AML1-ETO fusion protein (Figure 10). After a short period of time, induced animals showed increased numbers of neutrophils, basophils and large unstained myeloperoxidase-negative cells. In addition, a pronounced drop in white blood cells, lymphocytes, monocytes and platelets was noted. Based on this phenotype in peripheral blood values, it was not surprising that AML1-ETO-expressing mice died within a relatively short period of time (Figure 9B). Again the very rapid set off of the profound hematological alterations seen here contrasts with the delayed or absent phenotype reported for other genetic AML1-ETO models (McCormack et al., 2008; Muller et al., 2008; Peterson et al., 2007; Renneville et al., 2008).

The rapid and profound changes in induced R26/AE mice were not restricted to blood cells but in addition hematopoietic organs were strongly affected by the generalized expression of AML1-ETO. A remarkable thymic atrophy and an enlargement of the spleen and the lymph nodes were noted (Figure 10). Most strikingly, AML1-ETO-expressing animals showed severe splenomegaly and signs of extramedullary hematopoiesis, accompanied by an expansion of granulocytes (Figure 17B). In addition, microscopic analysis revealed a profound change in normal spleen architecture

characterized by a loss of the demarcation between red and white pulp (Figure 13), amorphous germinal centers and an increased number of apoptotic cells. These results therefore have to be interpreted in a way that generalized AML1-ETO expression is not compatible with the normal homeostasis of the spleen and that this organ possibly can not anymore sustain its normal function to control both innate and adoptive immune responses (Mebius and Kraal, 2005).

AML1-ETO-expressing mice presented a reduced thymus and microscopic analysis showed a marked atrophy of this organ (Figure 12). Moreover, T-cell maturation was disrupted at the DN3 level (double negative for CD4 and CD8 antibodies) followed by a reduction in CD4/CD8 DP (double positive for CD4 and CD8 antibodies) T-cells (Figure 19). The dysregulation of normal Runx3/AML2 and Runx2/AML3 function may explain these observations. Recent data have suggested that Runx3/AML2 is involved in immune cell differentiation and activation (Puig-Kröger and Corbí, 2006). Interestingly, ectopic expression of Runx2/AML3 in the thymus induced growth arrest in immature T-cells, but this effect was neutralized by co-expression of Myc, and the potent combination of Runx2/AML3 and Myc led also to rapid tumor formation (Blyth et al., 2001; Vaillant et al., 2002). In addition, Cheng and colleagues reported that AML1-ETO transcriptionally repressed normal Runx3/AML2 gene function (Cheng et al., 2008). Taken together, disruption of T-cell maturation and the atrophy of the thymus seen here may be explained by a repression of Runx3/AML2 and/or Runx2/AML3 gene function by aberrant expression of the AML1-ETO fusion protein.

With regard to the enlarged AML1-ETO-expressing lymph nodes, microscopic analysis showed an overall disruption of their normal structure and an increase in apoptotic cells (Figure 14). The lymph node is a secondary lymphoid organ that organizes and optimizes immune responses (Barker and Billingham, 1968). The T-cell dependent regions in the cortex are among the most important sites where antigen-specific naïve T-cells encounter their cognate antigen exposed on the surface of antigen-presenting cells (APC) (Garside et al., 1998). Based on the observations with the compound R26/AE mouse model, ubiquitous AML1-ETO expression severely interfered with the normal homeostasis of the lymph nodes. Although it is difficult to find a straightforward answer, it can be speculated that aberrant AML1-ETO expression in different cells of the lymph nodes and in immune cells dysregulated the normal function of endogenous AML1/Runx1 target genes, known to be involved in cell proliferation, differentiation and

organ homeostasis (Levanon and Groner, 2004). Aberrant AML1-ETO expression may also led to the accumulation of aggressive T-cells in the lymph nodes and thus promote an autoimmune response. Although the rapid induction of a severe and lethal phenotype might be caused by an autoimmune defect, this possibility was not further investigated.

With regard to hematopoietic lineage maturation in the bone marrow, AML1-ETO-induced mice displayed a severe perturbation in the B-cell compartment defined by less re-circulating and new produced B-cells (Figure 18). In addition, a block in erythropoiesis with reduced numbers of basophilic erythroblasts (II) and late baso- and chromatophilic erythroblasts (III) and an increase in numbers of orthochromatophilic erythroblast (IV) was observed (Figure 15). With regard to granulopoiesis, an expansion of mature and immature granulocytes was noted (Figure 17A). Finally, AML1-ETO-expressing animals presented an increased number of megakaryocytes (Figure 16). As reported by others (de Guzman et al., 2002), AML1-ETO expression induced an expansion of lineage$^-$/c-Kit$^+$/Sca1$^+$ (so called LKS) cells (Figure 20) containing HSCs and blood progenitors. All results obtained in the compound R26/AE model indicated a remarkable change in normal bone marrow homeostasis upon short-term AML1-ETO expression. Since AML1/Runx1, AML2/Runx3 and AML3/Runx2 factors act as crucial gene switches for development, cell differentiation and tissue equilibrium (Levanon and Groner, 2004), it is to be postulated that aberrant AML1-ETO expression in the compound R26/AE mouse model completely subverted normal homeostasis of the bone marrow.

Although AML1-ETO-expressing mice displayed profound changes in their hematopoietic organs, in peripheral blood values, differentiated blood lineages and progenitors/HSCs cells, a more detailed analysis was not performed. One argument to not analyze the compound AML1-ETO model was that generalized expression from the R26 locus results in an excessive complexity of different cells, moderately expressing AML1-ETO. Most importantly, the compound R26/AE model did not mirror the exclusive pan-hematopoietic activation of AML1-ETO in t(8;21)-positive patients, which was the focus of this work. Therefore, it was decided to restrict AML1-ETO expression to HSCs, blood progenitors and more mature hematopoietic cells.

4.2 Cell-autonomous AML1-ETO expression in hematopoietic cells allowed to investigate the pre-leukemic function of AML1-ETO

Modeling AML1-ETO function in mice has been challenging because depending on the techniques used to express the fusion gene, the obtained results were surprisingly different. Using different approaches for investigating the role of AML1-ETO for blood cell development several research groups reported dissimilar and confusing results for genetic mouse models and bone marrow transplantations (Buchholz et al., 2000; Bäsecke et al., 2005; Higuchi et al., 2002; Mulloy et al., 2003; Okuda et al., 1996; Rhoades et al., 2000; Schwieger et al., 2002; Yuan et al., 2001). This heterogeneity in phenotype might be the effect of variables implicit to retrovirus-mediated transduction versus genetic activation of AML1-ETO, including copy number, expression level, integration site, the presence and identity of cooperating insertional mutations, and the identity of the infected cell. Moreover, the use of retrovirally-infected cells might have specifically selected for rare clones that have high levels of proliferation and/or a low degree of death cells (Oravecz-Wilson et al., 2009). In order to investigate the role of AML1-ETO activation in HSCs, MPPs, committed progenitors and adult hematopoietic lineages, a conditionally inducible blood cell-specific system was chosen. To this end, non-induced bone marrow cells from compound R26/AE mice were adoptively transferred into RAG-$2^{-/-}$ recipients mice (Figure 21A). By using a conditionally activated system it was thus possible to express the AML1-ETO fusion protein eight weeks after bone marrow reconstitution, and therefore foreclosing any possible unwanted effects promoted by permanent high-level expression of AML1-ETO during the homing process. In this aspect it is important to note that chimeric R26/AE mice initially presented bone marrow niche colonization with "normal" HSCs lacking the aberrant expression of the AML1-ETO fusion protein.

The chimeric mice were regularly inspected for weight, general appearance and peripheral blood analysis were also carried out. During the first months of AML1-ETO expression no detectable phenotype was noticed. Nonetheless, after eight to nine months of AML1-ETO-expression, mice started to lose weight and showed less mobility when compared to the control group (data not shown). Peripheral blood analysis revealed expansion of eosinophils and large unstained myeloperoxidase-negative cells. In addition, a relevant drop in red blood cells and hemoglobin was observed (Figure 22). Interestingly, only Fenske and collaborators performed a routine peripheral blood analysis of the Sca-$1^{+/AML1\text{-}ETO}$ mice (Fenske et al., 2004). In these studies, an increase in

neutrophils was observed in the AML1-ETO-expressing mice but no changes in other parameters were detected. It is to be noticed that several reports have been published showing refractory anemia and increased peripheral blasts in AML-M2 t(8;21) patients (Czepulkowski et al., 1987; Gustafson et al., 2009; Maserati et al., 1992). In addition, the peripheral blood eosinophilia detected in AML1-ETO-induced mice may be recapitulating the frequently observed marrow eosinophilia in AML-M2 t(8;21) patients (Nucifora and Rowley, 1995; Swirsky et al., 1984). However, nothing is known about peripheral blood values presented by pre-leukemic patients. It is therefore not possible to directly extrapolate the presented results to what might be occurring in human AML. Nevertheless, analysis of peripheral blood parameters noticed to be deregulated in the R26/AE mouse model may be a possible analytical tool for the early diagnosis of t(8;21) associated leukemia following remission.

The most striking observation from the R26/AE/RAG2$^{-/-}$ mouse model was that normal red blood cell and lymphoid maturation was incompatible with AML1-ETO expression. With regard to the red blood cell phenotype found in AML1-ETO-induced animals, the presented results are in line with the impaired hematopoiesis seen in clinical cases of t(8;21)-positive AML and in previous experiments done in animal and in *ex vivo* model systems also reporting a reduction in red blood cells (Choi et al., 2006; Fenske et al., 2004; Schwieger et al., 2002). Fenske and colleagues detected increased reticulocytes in bone marrow smears from one-year-old Sca-1$^{+/AML1\text{-}ETO}$ mice (Fenske et al., 2004). In addition, Schwieger and colleagues found in their studies decreased erythrocytes using cytometry with the Ter119 marker as a single parameter (Schwieger et al., 2002). However, the here conducted analysis monitored erythroid maturation following the Lodish flow cytometric protocol (Socolovsky et al., 2001). This protocol can monitor the transition from the proerythroblast to orthochromatophilic erythroblast stage and thus will report erythroid maturation. Therefore, it was possible to for the first time establish that AML1-ETO interferes with the transition to the orthochromatophilic erythroblast stage (Figure 30). The partial block of normal bone marrow erythropoiesis thus may at least in part explain the altered morphology of peripheral red blood cells seen in induced mice (Figure 23). Moreover, the observed anemia in peripheral blood of induced animals (Figure 22) can be perfectly correlated with the disruption of normal red blood cell maturation in the bone marrow. Finally, it is also reasonable to assume that the marked

increase of erythroid progenitors in the spleen (Figure 36) may be a compensatory response to the partial impairment of normal bone marrow erythropoiesis.

In addition to the maturation block in erythropoiesis, a pronounced inhibition of B- and T-cell development was observed. The reduction of B-cells in AML1-ETO-expressing mice seen here (Figure 34) confirms preceding studies reporting the overall decrease of B-cells in the peripheral blood and the bone marrow of AML1-ETO-expressing mice (de Guzman et al., 2002; Fenske et al., 2004; Schwieger et al., 2002). However, de Guzman and colleagues analyzed B-cells exclusively in peripheral blood preparations. Additional information was provided by Fenske and colleagues who reported decreased B-cells in the peripheral blood and in the bone marrow. As a matter of fact, both groups used B220 as a single marker in that sense limiting the analysis to overall B-cell occurrence. Schwieger and colleagues showed a block at a late stage of B-cell development (Schwieger et al., 2002). In these studies, bone marrow cells were transduced with a retroviral vector carrying AML1-ETO and the infected cells later transplanted into mice. B-cell maturation was followed with IgM, CD43 and B220 antibodies and a block at a late stage of B-cell development was observed. However, using the R26/AE/RAG2$^{-/-}$ mouse model demonstrated that B-cell maturation was compromised at the pre-pro B-cell stage (Figure 34) and not at a late stage. AML1/Runx1 is expressed in B cells (Ichikawa et al., 2004) and is required for generation of B cells after bone marrow transplantation (North et al., 2004). In this respect, in the model provided by Schwieger and collaborators, AML1-ETO infected cells might have impaired bone marrow B-cell reconstitution in the transplanted mouse and therefore the human condition taking place in pre-leukemic patients may not have been appropriately mirrored in these experiments.

With regard to thymocyte maturation, studies by other groups demonstrated a critical role of AML1/Runx1 and AML2/Runx3 for T-cell development (Ichikawa et al., 2004; Woolf et al., 2003). Furthermore, Hagashi and colleagues showed that the AML1/CBFβ complex was important for the transition and maturation of DP (double positive for CD4$^+$/CD8$^+$ markers) to single positive thymocytes (CD4$^+$ or CD8$^+$) (Hayashi et al., 2001; Hayashi et al., 2000). Additional information was reported by other groups demonstrating that AML3/Runx2 is expressed in the DN subset and that its enforced expression can interfere with early T-cell development (Blyth et al., 2001; Vaillant et al., 2002). Interestingly, more recent data published by Klunker and

colleagues showed that Runx family members were important for the regulation of $Foxp3^+$ inducible regulatory T-cells (Klunker et al., 2009). Therefore, AML1-ETO most likely acts as a dominant negative factor for AML1/Runx1 gene regulation and might also transcriptionally interfere with the function of normal AML2/Runx3 gene regulation (Cheng et al., 2008). Taken together, it was somewhat not surprising that T-cell development was disturbed as found in our AML1-ETO mouse model and also by other groups (Fenske et al., 2004; Higuchi et al., 2002; Schwieger et al., 2002). Schwieger and colleagues claimed on the ground of preliminary results that AML1-ETO expression induces a block in late stages of T-cell maturation. This view was motivated by a normal presence of DP T-cells in the thymus (Schwieger et al., 2002). Additionally, Fenske and colleagues found decreased single positive ($CD4^+$ and $CD8^+$) and immature DP thymocytes but no differences in the DN (double negative for $CD4^+$ and $CD8^+$) population. However, these analyses were performed with young AML1-ETO-induced mice but not with older mice that showed myeloproliferative disease (MPD) (Fenske et al., 2004). Interestingly, enforced AML1-ETO expression in the R26/AE/$RAG2^{-/-}$ mouse model interfered with normal T-cell maturation in earlier stages of thymocyte development (Figure 35A and 35B). In the here presented model a clear reduction of DN3 and DP thymocytes was noticed. These results show that long-term AML1-ETO expression does impair T-cell maturation both in DP and likewise in DN3 thymocytes. The partial block seen in the transition from the DN2 to the DN3 stage together with the apparent decrease in DP T-cells is compatible with the interpretation that double positive T-cells are reduced in numbers due to the preceding reduction of DN3 thymocytes. Moreover, these results correlate with a report demonstrating that AML3/Runx2 is expressed in DN subsets and that enforced expression can interfere with early T-cell development (Blyth et al., 2001; Vaillant et al., 2002). Together this suggests the interference of AML1-ETO with normal AML3/Runx2 function in T-cells (Cheng et al., 2008). In addition, the AML1/CBFβ complex is likely to be important for the transition and maturation of DP to single positive thymocytes (Hayashi et al., 2001; Hayashi et al., 2000). Alternatively, it also may be possible that a reduced crosstalk between double negative thymocytes and medullary epithelial cells, needed for the establishment of an appropriate thymic microenvironment, does not allow further progression to TCRαβ double positive T-cells. In analogy to the pronounced atrophy of lymphoid organs in mice that lack B- and T-cells (Naquet et al., 1999), the apparent size reduction of thymus and

lymph nodes seen here (Figure 24) is probably a direct consequence of the decreased lymphopoiesis in the R26/AE/RAG2$^{-/-}$ mice. Also of note is that the compromised erythro- and lymphopoiesis seen in chimeric mice is highly reminiscent to the clinical appearance of refractory anemia (Czepulkowski et al., 1987; Gustafson et al., 2009; Maserati et al., 1992) and the very low proportion or complete absence of AML1-ETO expressing T- and B-cells in t(8;21) AML patients (Miyamoto et al., 2000).

A general pathological characteristic of AML-M2 t(8;21) is the marked increase in leukemic blasts accumulating in the bone marrow and the infiltration of extramedullary organs (Estey and Dohner, 2006). Experimental mouse models demonstrated that AML1-ETO expression promoted a specific expansion of medullary granulopoiesis (de Guzman et al., 2002; Fenske et al., 2004; Schwieger et al., 2002). However, several controversial results were reported. Fenske and colleagues found an expansion that was restricted to mature myeloid cells (CD11b^{+}/Gr-1^{+}) in peripheral blood, bone marrow and spleen without evidence of any maturation block (Fenske et al., 2004). By contrast, de Guzman and collaborators reported increased immature and mature granulocytes (CD11b^{high}/Gr-1^{med} and CD11b^{high}/Gr-1^{high}) in the bone marrow of AML1-ETO-expressing animals (de Guzman et al., 2002). To make matters even more unclear, Schwieger and colleagues reported a shift to immature granulopoiesis (CD11b^{high}/Gr-1^{med}) and observed an increased proportion of blast forms in bone marrow cytospins (Schwieger et al., 2002). These controversies can be explained by the different approaches used for the *in vivo* expression of AML1-ETO fusion protein. Therefore it was of interest to determine the consequences of AML1-ETO expression for granulopoiesis in a more physiological setting that also better reflects the condition found in human patients. Interestingly, flow cytometry analysis showed an increase of both immature and mature granulocytes in the bone marrow of AML1-ETO-expressing animals (Figure 32A, 32B and 32C). These findings were confirmed by histopathological analysis of bone marrow cytospins where increased granulopoiesis was observed (Figure 23D). Furthermore, multi-parameter flow cytometry revealed no accumulation of immature and mature blasts in the bone marrow of AML1-ETO-induced mice (Figure 33A and 33B). These results were further corroborated by a bone marrow cytospin analysis where no sign of malignant amplification of bone marrow blasts was detected. With regard to other differentiated myeloid lineages, it is worth noting that macrophages, neutrophils and eosinophils were also characterized in the R26/AE mouse model and in agreement with the enhanced

granulopoiesis found in AML1-ETO-expressing animals, these differentiated myeloid cells were found to be expanded (Figure 44). Therefore, these results provide direct experimental evidence that AML1-ETO expression can enhance granulopoiesis without promoting the accumulation of blast in the bone marrow.

Patients with t(8;21)-associated leukemia often present splenomegaly (Abdel Rahman et al., 2007). In correlation with this situation, enlarged spleens were found in AML1-ETO-expressing mice (Figure 24). These data also confirm the findings by Fenske and collaborators reporting splenomegaly in the Sca-$1^{+/AML1\text{-}ETO}$ mice (Fenske et al., 2004). In addition, histopathological analysis revealed changes in the morpho-pathology of the spleen without obvious alterations in the overall structure of this organ (Figure 25). Surprisingly, none of the before published studies reported any abnormalities in differentiated blood cell populations or progenitors using flow cytometry of splenic cells. With regard to B-cells, $IgM^+/B220^+$ cells were underrepresented in AML1-ETO-induced spleens (Figure 34B). These data are in line with the B-cell maturation block found in the AML1-ETO-induced bone marrows (Figure 34) and directly suggest an impaired migration of B-cells from the bone marrow to the spleen (Mebius and Kraal, 2005). In addition, red blood cell progenitors were expanded in AML1-ETO-induced spleens. These results perfectly agree with the increased numbers of proerythroblasts (I, red blood cell progenitors) seen in AML1-ETO-expressing bone marrow (Figure 30). Additionally, splenic granulopoiesis ($CD11b^+/Gr\text{-}1^+$) was also expanded in AML1-ETO induced animals (Figure 37). These findings correlate with the expansion of immature and mature granulocytes ($CD11b^{high}/Gr\text{-}1^{med}$ and $CD11b^{high}/Gr\text{-}1^{high}$) seen in the bone marrow of R26/AE/$RAG2^{-/-}$ mice (Figure 32). Interestingly, immature blasts were also expanded in AML1-ETO-expressing spleens (Figure 38). Thus the here presented data supports previous findings by Fenske and colleagues who reported an increase of *in vitro* splenic granulocyte-macrophages colony forming units (CFU-GM) (Fenske et al., 2004). Moreover, the marked increase of blasts (LUC cells) in the periphery seen in the AML1-ETO-expressing R26/AE/$RAG2^{-/-}$ mice (Figure 22), raises the possibility that cell-autonomous AML1-ETO expression leads to the mobilization of hematopoietic stem cells (HSCs) and/or more mature progenitors to the blood and subsequently to the spleen. The presented results showing that relative and absolute numbers of splenic LKS ($lineage^-$/ $c\text{-}Kit^+/Sca\text{-}1^+$) cells were increased (Figure 39), directly support this notion and suggest that following AML1-ETO activation HSCs and/or early progenitors may leave the bone

marrow and colonize the spleen. Alternatively, AML1-ETO may directly enhance extramedullary hematopoiesis in the spleen. However, the here conducted experiments cannot distinguish between these possibilities. In addition, our data does not demonstrate if the elevated numbers of immature erythrocytes, blasts and mature granulocytes seen in the spleen are produced by extramedullary hematopoiesis or if these cells originate from the bone marrow and subsequently colonize the spleen. The presented experimental data demonstrate for the first time that enforced AML1-ETO expression in mice does not primarily lead to the accumulation of blasts in the bone marrow but rather induces an increase of these cells in the spleen. However, if this also applies to the situation found in human patients is not known.

Although all AML cells are thought to harbor cell-autonomous mutations that are causally implicated in the pathogenesis of the disease, there is also emerging evidence for a functional diversity among AML cells. For instance, it is thought that there is a subpopulation of AML cells referred to as “leukemic stem cells” (LSC) that when transplanted into immunodeficient NOD/SCID mice will have long-term repopulating potential and the ability to propagate and maintain the AML phenotype. The existence of LSCs, and the role of this type of stem cells in other solid tumors has also been postulated (Huntly and Gilliland, 2005). Therefore, in recent years leukemia is increasingly viewed as a stem cell disorder in which the continued growth and propagation of the cancer originates from and depends on a small subpopulation of self-renewing LSCs. LSCs can also have an immunophenotype that is more mature than seen in normal HSCs (Krivtsov et al., 2006; Somervaille and Cleary, 2006) and in this case LCS cells are assumed to have acquired unrestricted self-renewal capacity through additional oncogenic transformations at later stages of development leading to the activation of a stem cell like gene expression program (Krivtsov et al., 2006). These observations create new questions about the origin of LSCs. As for today, cumulative data suggests that LSCs might raise from mutations occurring in either the HSC or alternatively in the committed progenitor compartment, at least in murine models (Cozzio et al., 2003; Huntly et al., 2004; Krivtsov et al., 2006). Clinical evidence clearly demonstrates that the t(8;21) cytogenetic abnormality is consistently associated with AML (Erickson et al., 1992; Erickson et al., 1994; Gao et al., 1991; Miyoshi et al., 1991; Nisson et al., 1992; Shimizu et al., 1992). However, it is not known if aberrant AML1-ETO expression can disrupt the normal homeostasis of HSCs, multipotent progenitors (MPPs) or lineage committed progenitors.

To date, several groups reported (by using *in vitro* colony forming units (CFU) assays) that myeloid progenitors were expanded in AML1-ETO-induced animals (de Guzman et al., 2002; Schwieger et al., 2002). However, and due to other controversial results, it was of interest to answer the same question using the R26/AE/RAG2$^{-/-}$ mice. Interestingly, the here performed *in vitro* CFU assay corroborated the already published results, indicating an expansion of CFU-GM and an increase in the total number of colonies in AML1-ETO-expressing mice (Figure 45). While these findings suggested an alteration in myeloid progenitors, it was still unclear which stem cell population was targeted for expansion by the AML1-ETO fusion protein. In this regard, flow cytometry was chosen as a suitable tool for determining if AML1-ETO disrupts HSC, MPPs or lineage committed progenitors. The here presented experiments demonstrate for the first time that both relative percentages and absolute numbers of HSCs/MPPs remained unchanged in long-term AML1-ETO-induced animals (Figure 41). In addition, no differences were found in common lymphoid progenitors (CLPs) (Figure 42), common myeloid progenitors (CMPs) and megakaryocytes-erythroid progenitors (MEPs) when compared to control animals (Figure 43). By contrast, the granulocyte-macrophage progenitor (GMP) population in induced R26/AE/RAG2$^{-/-}$ mice was significantly increased upon AML1-ETO activation (Figure 43). These findings clearly demonstrate that AML1-ETO does not alter the normal homeostasis of HSCs/MPPs and lineage-committed progenitors with the exception of GMPs.

In summary, conditional expression of the AML1-ETO fusion protein from the R26 locus induced profound changes in normal hematopoiesis. Peripheral blood analysis from AML1-ETO-expressing mice showed increased numbers of eosinophils and large unstained myeloperoxidase-negative cells together with decreased red blood cells and hemoglobin. In addition, AML1-ETO-expressing mice displayed splenomegaly, an expansion of immature blasts, red blood cell progenitors and granulocytes and a decreasing B-cells. With regard to bone marrow hematopoiesis, a clear block of red blood cell development, an inhibition of B-cell maturation and an enhanced granulopoiesis were measured. AML1-ETO-expressing mice presented a reduction in thymus size and analysis of T-cell development revealed a clear disruption of T-cell maturation at early stages. Furthermore, AML1-ETO-induced mice did not have increased HSCs, MPPs, CLPs, CMPs and MEPs but AML1-ETO expression promoted the selective amplification of GMPs. Figure 46 summarizes the *in vivo* consequences of AML1-ETO fusion protein

expression for hematopoiesis.

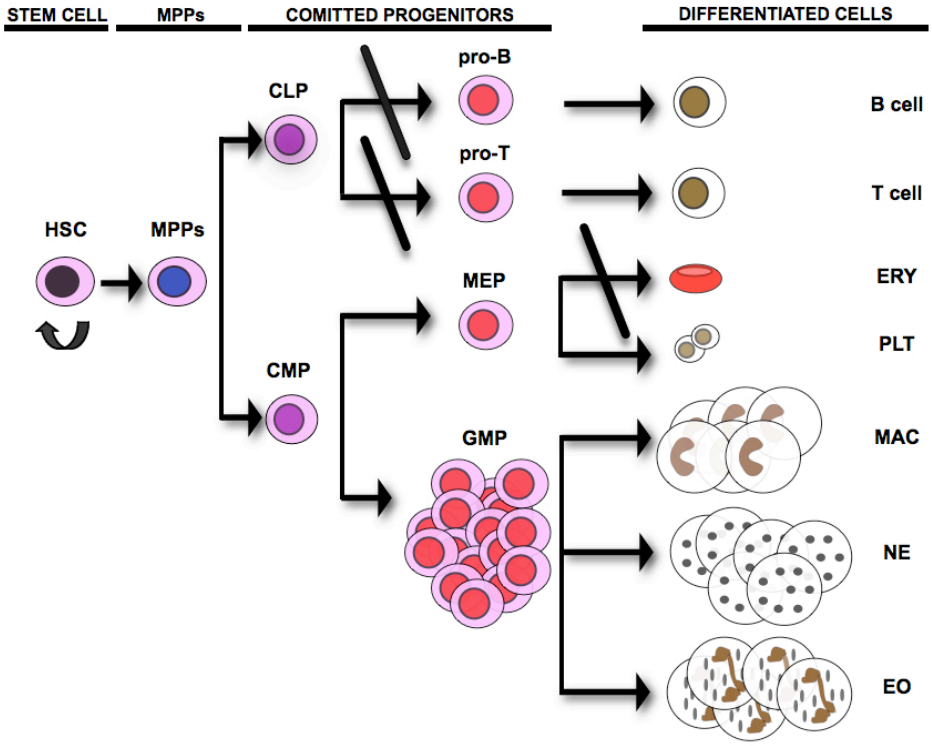

Figure 46: **Schematic representation of the *in vivo* consequences of AML1-ETO expression for hematopoiesis**

HSC, hematopoietic stem cell; MPPs, multi potent progenitors; CLP, common lymphoid progenitor; pro-B, pro-B cell; pro-T, pro-T cell; CMP, common myeloid progenitor; MEP, megakaryocyte-erythroid progenitor; ERY, erythrocyte; PLT, platelet; GMP, granulocyte-macrophage progenitor; MAC, macrophage; NE, neutrophils; EO, eosinophils. Black crossed lines indicate a block in maturation.

Interestingly, the R26/AE/RAG2$^{-/-}$ mouse model as other models already published, did not spontaneously develop AML and it is reasonable to suggest that for AML induction, additional secondary genetic alterations must be introduced in combination with AML1-ETO (Buchholz et al., 2000; Bäsecke et al., 2005; Higuchi et al., 2002; Mulloy et al., 2003; Okuda et al., 1996; Rhoades et al., 2000; Schwieger et al., 2002; Yuan et al., 2001). Experimental and clinical data indicate that AML arises through the stepwise acquisition of genetic and epigenetic changes. In particular, AML seems to be promoted by the collaboration between balanced translocations, that are considered to be initiating lesions, and secondary mutations affecting signaling modulators including

RAS, c-Kit and Flt-3 or transcriptional factors as for example WT-1 (Kelly and Gilliland, 2002; Moore, 2005). In agreement with this fact, clinical data from AML-M2 t(8;21) patients revealed that c-Kit, Flt-3, RAS or WT-1 appear to be highly mutated in t(8;21)-AML patients (Kottaridis et al., 2002; Kottaridis et al., 2003; Shih et al., 2006; Wang et al., 2005). In this regard, previous *in vivo* studies have demonstrated that mouse models that express Flt-3 or WT-1 proteins together with the AML1-ETO fusion protein develop AML disease (Nishida et al., 2006; Schessl et al., 2005). These mouse models are important tools for studying overt AML. However, the aim of this PhD thesis was to clarify the role of aberrant AML1-ETO expression for hematopoiesis and to generate a model for studying the pre-leukemic stages of the disease.

4.3 Future applications

Although the diagnosis and therapy of leukemia improved over the last decades, high number of diagnosed leukemic patients die every year (Ten Cate et al., 2010). Therefore and in addition to elucidating the contextual consequences of AML1-ETO function in the stem cell compartment, our mouse model carries implications for understanding t(8;21)-associated disease etiology and possibly also for developing future therapeutic strategies. For example, since AML1-ETO expression does not expand HSC and MPP pools, curative therapies targeting proliferating cells will only eliminate rapidly dividing blasts but might not remove t(8;21)-positive clones from the stem cell compartment. In actual fact, current clinical protocols targeting proliferating cells show a good primary response but often fatally relapse (Estey and Dohner, 2006). By contrast, therapeutic strategies that could be aimed at AML1-ETO-expressing cells might have the potential to cure the disease, because self-renewing HSCs, that continuously pass on the t(8;21) mutation to the downstream progeny, would be specifically eliminated and thus the risk to relapse markedly reduced. Based on the expansion of GMPs seen in our model and on the ground of statistical considerations (Haeno et al., 2009), it is tempting to speculate that complementary mutations required for initiating aggressive AML are very likely to take place in the expanded compartment of committed GMPs and not in AML1-ETO-expressing HSC. Following this interpretation, the etiology of t(8;21)-associated AML would involve two independent genetic lesions in different blood cell types. Namely self-renewing HSCs that acquire and perpetuate the initial t(8;21) translocation

followed by secondary lesions conferring increased self-renewal, proliferation and uncontrolled growth occurring in the amplified GMP compartment.

This new hypothesis can now be tested with the here established mouse model and will show if AML1-ETO expressing progenitors are indeed leukemia initiator cells or if both genetic hits required to induce overt leukemia have to take place in HSCs.

5 REFERENCES

Abdel Rahman, H., Farrag, S. and El-Attar, I. (2007). AML1/ETO Fusion Gene in de novo Pediatric Acute Myeloid Leukemia: Clinical Significance and Prognostic Implications. *J Egypt Natl Canc Inst* **19**, 39-47.

Abdou, N. and Abdou, N. (1973). Immunoglobulin receptors on human leucocytes. 3. Comparative study of human bone marrow and blood B cells: role of IgM receptors. *Clin Exp Immunol* **13**, 45-54.

Abdou, N. and Richter, M. (1970). The role of bone marrow in the immune response. *Adv Immunol* **12**, 201-70.

Akashi, K., Reya, T., Dalma-Weiszhausz, D. and Weissman, I. (2000a). Lymphoid precursors. *Curr Opin Immunol* **12**, 144-50.

Akashi, K., Traver, D., Miyamoto, T. and Weissman, I. (2000b). A clonogenic common myeloid progenitor that gives rise to all myeloid lineages. *Nature* **404**, 193-7.

Asou, H., Tashiro, S., Hamamoto, K., Otsuji, A., Kita, K. and Kamada, N. (1991). Establishment of a human acute myeloid leukemia cell line (Kasumi-1) with 8;21 chromosome translocation. *Blood* **77**, 2031-6.

Banker, D., Radich, J., Becker, A., Kerkof, K., Norwood, T., Willman, C. and Appelbaum, F. (1998). The t(8;21) translocation is not consistently associated with high Bcl-2 expression in de novo acute myeloid leukemias of adults. *Clin Cancer Res* **4**, 3051-62.

Barker, C. and Billingham, R. (1968). The role of afferent lymphatics in the rejection of skin homografts. *J Exp Med* **128**, 197-221.

Basu, S., Zhang, H., Quilici, C. and Dunn, A. (2004). Candida albicans can stimulate stromal cells resulting in enhanced granulopoiesis. *Stem Cells Dev* **13**, 39-50.

Blair, A., Hogge, D., Ailles, L., Lansdorp, P. and Sutherland, H. (1997). Lack of expression of Thy-1 (CD90) on acute myeloid leukemia cells with long-term proliferative ability in vitro and in vivo. *Blood* **89**, 3104-12.

Blyth, K., Terry, A., Mackay, N., Vaillant, F., Bell, M., Cameron, E., Neil, J. and Stewart, M. (2001). Runx2: a novel oncogenic effector revealed by in vivo complementation and retroviral tagging. *Oncogene* **20**, 295-302.

Bockamp, E., Maringer, M., Spangenberg, C., Fees, S., Fraser, S., Eshkind, L., Oesch, F. and Zabel, B. (2002). Of mice and models: improved animal models for biomedical research. *Physiol Genomics* **11**, 115-32.

Bockamp, E., Sprengel, R., Eshkind, L., Lehmann, T., Braun, J., Emmrich, F. and Hengstler, J. (2008). Conditional transgenic mouse models: from the basics to genome-wide sets of knockouts and current studies of tissue regeneration. *Regen Med* **3**, 217-35.

Boehm, T., Folkman, J., Browder, T. and O'Reilly, M. (1997). Antiangiogenic therapy of experimental cancer does not induce acquired drug resistance. *Nature* **390**, 404-7.

Bonnet, D. and Dick, J. (1997). Human acute myeloid leukemia is organized as a hierarchy that originates from a primitive hematopoietic cell. *Nat Med* **3**, 730-7.

Bornkamm, G. W., Berens, C., Kuklik-Roos, C., Bechet, J. M., Laux, G., Bachl, J., Korndoerfer, M., Schlee, M., Holzel, M., Malamoussi, A. et al. (2005). Stringent doxycycline-dependent control of gene activities using an episomal one-vector system. *Nucleic Acids Res* **33**, e137.

Brendel, C. and Neubauer, A. (2000). Characteristics and analysis of normal and leukemic stem cells: current concepts and future directions. *Leukemia* **14**, 1711-7.

Bronson, S., Plaehn, E., Kluckman, K., Hagaman, J., Maeda, N. and Smithies, O. (1996). Single-copy transgenic mice with chosen-site integration. *Proc Natl Acad Sci U S A* **93**, 9067-72.

Buchholz, F., Refaeli, Y., Trumpp, A. and Bishop, J. M. (2000). Inducible chromosomal translocation of AML1 and ETO genes through Cre/loxP-mediated recombination in the mouse. *EMBO Rep* **1**, 133-9.

Bäsecke, J., Schwieger, M., Griesinger, F., Schiedlmeier, B., Wulf, G., Trümper, L. and Stocking, C. (2005). AML1/ETO promotes the maintenance of early hematopoietic progenitors in NOD/SCID mice but does not abrogate their lineage specific differentiation. *Leuk Lymphoma* **46**, 265-72.

Calabi, F., Pannell, R. and Pavloska, G. (2001). Gene targeting reveals a crucial role for MTG8 in the gut. *Mol Cell Biol* **21**, 5658-66.

Chao, M., Seita, J. and Weissman, I. (2008). Establishment of a normal hematopoietic and leukemia stem cell hierarchy. *Cold Spring Harb Symp Quant Biol* **73**, 439-49.

Cheng, C., Li, L., Cheng, S., Lau, K., Chan, N., Wong, R., Shing, M., Li, C. and Ng, M. (2008). Transcriptional repression of the RUNX3/AML2 gene by the t(8;21) and inv(16) fusion proteins in acute myeloid leukemia. *Blood* **112**, 3391-402.

Choi, Y., Elagib, K., Delehanty, L. and Goldfarb, A. (2006). Erythroid inhibition by the leukemic fusion AML1-ETO is associated with impaired acetylation of the major erythroid transcription factor GATA-1. *Cancer Res* **66**, 2990-6.

Corsetti, M. and Calabi, F. (1997). Lineage- and stage-specific expression of runt box polypeptides in primitive and definitive hematopoiesis. *Blood* **89**, 2359-68.

Cozzio, A., Passegué, E., Ayton, P., Karsunky, H., Cleary, M. and Weissman, I. (2003). Similar MLL-associated leukemias arising from self-renewing stem cells and short-lived myeloid progenitors. *Genes Dev* **17**, 3029-35.

Cvetkovic, B., Yang, B., Williamson, R. and Sigmund, C. (2000). Appropriate tissue- and cell-specific expression of a single copy human angiotensinogen transgene specifically targeted upstream of the HPRT locus by homologous recombination. *J Biol Chem* **275**, 1073-8.

Czepulkowski, B., Gibbons, B., Tucker, J., Amess, J. and Lister, T. (1987). Duplication of one of the products of the t(8;21) translocation in a patient with refractory anemia with excess blasts in transformation. *Cancer Genet Cytogenet* **25**, 175-7.

De Braekeleer, E., Férec, C. and De Braekeleer, M. (2009). RUNX1 translocations in malignant hemopathies. *Anticancer Res* **29**, 1031-7.

de Guzman, C., Warren, A., Zhang, Z., Gartland, L., Erickson, P., Drabkin, H., Hiebert, S. and Klug, C. (2002). Hematopoietic stem cell expansion and distinct myeloid developmental abnormalities in a murine model of the AML1-ETO translocation. *Mol Cell Biol* **22**, 5506-17.

de Visser, K., Eichten, A. and Coussens, L. (2006). Paradoxical roles of the immune system during cancer development. *Nat Rev Cancer* **6**, 24-37.

Doetschman, T., Gregg, R., Maeda, N., Hooper, M., Melton, D., Thompson, S. and Smithies, O. Targetted correction of a mutant HPRT gene in mouse embryonic stem cells. *Nature* **330**, 576-8.

Domen, J. and Weissman, I. (1999). Self-renewal, differentiation or death: regulation and manipulation of hematopoietic stem cell fate. *Mol Med Today* **5**, 201-8.

Dunn, G., Old, L. and Schreiber, R. (2004). The three Es of cancer immunoediting. *Annu Rev Immunol* **22**, 329-60.

Elagib, K. and Goldfarb, A. (2007). Oncogenic pathways of AML1-ETO in acute myeloid leukemia: multifaceted manipulation of marrow maturation. *Cancer Lett* **251**, 179-86.

Erickson, P., Gao, J., Chang, K., Look, T., Whisenant, E., Raimondi, S., Lasher, R., Trujillo, J., Rowley, J. and Drabkin, H. (1992). Identification of breakpoints in t(8;21) acute myelogenous leukemia and isolation of a fusion transcript, AML1/ETO, with similarity to Drosophila segmentation gene, runt. *Blood* **80**, 1825-31.

Erickson, P., Robinson, M., Owens, G. and Drabkin, H. (1994). The ETO portion of acute myeloid leukemia t(8;21) fusion transcript encodes a highly evolutionarily conserved, putative transcription factor. *Cancer Res* **54**, 1782-6.

Estey, E. and Dohner, H. (2006). Acute myeloid leukaemia. *Lancet* **368**, 1894-907.

Evans, M. and Kaufman, M. (1981). Establishment in culture of pluripotential cells from mouse embryos. *Nature* **292**, 154-6.

Evans, V., Hatzopoulos, A., Aird, W., Rayburn, H., Rosenberg, R. and Kuivenhoven, J. (2000). Targeting the Hprt locus in mice reveals differential regulation of Tie2 gene expression in the endothelium. *Physiol Genomics* **2**, 67-75.

Feinstein, P., Kornfeld, K., Hogness, D. and Mann, R. (1995). Identification of homeotic target genes in Drosophila melanogaster including nervy, a proto-oncogene homologue. *Genetics* **140**, 573-86.

Fenske, T., Pengue, G., Mathews, V., Hanson, P., Hamm, S., Riaz, N. and Graubert, T. (2004). Stem cell expression of the AML1/ETO fusion protein induces a myeloproliferative disorder in mice. *Proc Natl Acad Sci U S A* **101**, 15184-9.

Fleischman, R., Custer, R. and Mintz, B. (1982). Totipotent hematopoietic stem cells: normal self-renewal and differentiation after transplantation between mouse fetuses. *Cell* **30**, 351-9.

Frese, K. and Tuveson, D. (2007). Maximizing mouse cancer models. *Nat Rev Cancer* **7**, 645-58.

Fugmann, S., Lee, A., Shockett, P., Villey, I. and Schatz, D. (2000). The RAG proteins and V(D)J recombination: complexes, ends, and transposition. *Annu Rev Immunol* **18**, 495-527.

Fukumura, D., Xavier, R., Sugiura, T., Chen, Y., Park, E., Lu, N., Selig, M., Nielsen, G., Taksir, T., Jain, R. et al. (1998). Tumor induction of VEGF promoter activity in stromal cells. *Cell* **94**, 715-25.

Gao, J., Erickson, P., Gardiner, K., Le Beau, M., Diaz, M., Patterson, D., Rowley, J. and Drabkin, H. (1991). Isolation of a yeast artificial chromosome spanning the 8;21 translocation breakpoint t(8;21)(q22;q22.3) in acute myelogenous leukemia. *Proc Natl Acad Sci U S A* **88**, 4882-6.

Garside, P., Ingulli, E., Merica, R., Johnson, J., Noelle, R. and Jenkins, M. (1998). Visualization of specific B and T lymphocyte interactions in the lymph node. *Science* **281**, 96-9.

Gelmetti, V., Zhang, J., Fanelli, M., Minucci, S., Pelicci, P. and Lazar, M. (1998). Aberrant recruitment of the nuclear receptor corepressor-histone deacetylase complex by the acute myeloid leukemia fusion partner ETO. *Mol Cell Biol* **18**, 7185-91.

Gery, S. and Koeffler, H. (2007). Transcription factors in hematopoietic malignancies. *Curr Opin Genet Dev* **17**, 78-83.

Gopinathan, A. and Tuveson, D. The use of GEM models for experimental cancer therapeutics. *Dis Model Mech* **1**, 83-6.

Gordon, J., Scangos, G., Plotkin, D., Barbosa, J. and Ruddle, F. (1980). Genetic transformation of mouse embryos by microinjection of purified DNA. *Proc Natl Acad Sci U S A* **77**, 7380-4.

Gossen, M. and Bujard, H. (2002). Studying gene function in eukaryotes by conditional gene inactivation. *Annu Rev Genet* **36**, 153-73.

Grisolano, J., O'Neal, J., Cain, J. and Tomasson, M. (2003). An activated receptor tyrosine kinase, TEL/PDGFbetaR, cooperates with AML1/ETO to induce acute myeloid leukemia in mice. *Proc Natl Acad Sci U S A* **100**, 9506-11.

Gustafson, S., Lin, P., Chen, S., Chen, L., Abruzzo, L., Luthra, R., Medeiros, L. and Wang, S. (2009). Therapy-related acute myeloid leukemia with t(8;21) (q22;q22) shares many features with de novo acute myeloid leukemia with t(8;21)(q22;q22) but does not have a favorable outcome. *Am J Clin Pathol* **131**, 647-55.

Haeno, H., Levine, R., Gilliland, D. and Michor, F. (2009). A progenitor cell origin of myeloid malignancies. *Proc Natl Acad Sci U S A* **106**, 16616-21.

Hamilton, D. and Abremski, K. (1984). Site-specific recombination by the bacteriophage P1 lox-Cre system. Cre-mediated synapsis of two lox sites. *J Mol Biol* **178**, 481-6.

Harada, Y. and Harada, H. (2009). Molecular pathways mediating MDS/AML with focus on AML1/RUNX1 point mutations. *J Cell Physiol* **220**, 16-20.

Hayashi, K., Abe, N., Watanabe, T., Obinata, M., Ito, M., Sato, T., Habu, S. and Satake, M. (2001). Overexpression of AML1 transcription factor drives thymocytes into the CD8 single-positive lineage. *J Immunol* **167**, 4957-65.

Hayashi, K., Natsume, W., Watanabe, T., Abe, N., Iwai, N., Okada, H., Ito, Y., Asano, M., Iwakura, Y., Habu, S. et al. (2000). Diminution of the AML1 transcription factor function causes differential effects on the fates of CD4 and CD8 single-positive T cells. *J Immunol* **165**, 6816-24.

Higuchi, M., O'Brien, D., Kumaravelu, P., Lenny, N., Yeoh, E. J. and Downing, J. R. (2002). Expression of a conditional AML1-ETO oncogene bypasses embryonic lethality and establishes a murine model of human t(8;21) acute myeloid leukemia. *Cancer Cell* **1**, 63-74.

Hoess, R., Ziese, M. and Sternberg, N. (1982). P1 site-specific recombination: nucleotide sequence of the recombining sites. *Proc Natl Acad Sci U S A* **79**, 3398-402.

Hoffman, E., Passoni, L., Crompton, T., Leu, T., Schatz, D., Koff, A., Owen, M. and Hayday, A. (1996). Productive T-cell receptor beta-chain gene rearrangement: coincident regulation of cell cycle and clonality during development in vivo. *Genes Dev* **10**, 948-62.

Hug, B. and Lazar, M. (2004). ETO interacting proteins. *Oncogene* **23**, 4270-4.

Huntly, B., Shigematsu, H., Deguchi, K., Lee, B., Mizuno, S., Duclos, N., Rowan, R., Amaral, S., Curley, D., Williams, I. et al. (2004). MOZ-TIF2, but not BCR-ABL, confers properties of leukemic stem cells to committed murine hematopoietic progenitors. *Cancer Cell* **6**, 587-96.

Huntly, B. J. and Gilliland, D. G. (2005). Leukaemia stem cells and the evolution of cancer-stem-cell research. *Nat Rev Cancer* **5**, 311-21.

Ichikawa, M., Asai, T., Saito, T., Seo, S., Yamazaki, I., Yamagata, T., Mitani, K., Chiba, S., Ogawa, S., Kurokawa, M. et al. (2004). AML-1 is required for megakaryocytic maturation and lymphocytic differentiation, but not for maintenance of hematopoietic stem cells in adult hematopoiesis. *Nat Med* **10**, 299-304.

Ito, Y. (2004). Oncogenic potential of the RUNX gene family: 'overview'. *Oncogene* **23**, 4198-208.

Katsantoni, E. Z., Anghelescu, N. E., Rottier, R., Moerland, M., Antoniou, M., de Crom, R., Grosveld, F. and Strouboulis, J. (2007). Ubiquitous expression of the rtTA2S-M2 inducible system in transgenic mice driven by the human hnRNPA2B1/CBX3 CpG island. *BMC Dev Biol* **7**, 108.

Kelly, L. and Gilliland, D. (2002). Genetics of myeloid leukemias. *Annu Rev Genomics Hum Genet* **3**, 179-98.

Kiel, M., Yilmaz, O. and Morrison, S. (2008). CD150- cells are transiently reconstituting multipotent progenitors with little or no stem cell activity. *Blood* **111**, 4413-4; author reply 4414-5.

Kilby, N., Snaith, M. and Murray, J. (1993). Site-specific recombinases: tools for genome engineering. *Trends Genet* **9**, 413-21.

Kirstetter, P., Anderson, K., Porse, B., Jacobsen, S. and Nerlov, C. (2006). Activation of the canonical Wnt pathway leads to loss of hematopoietic stem cell repopulation and multilineage differentiation block. *Nat Immunol* **7**, 1048-56.

Klampfer, L., Zhang, J., Zelenetz, A., Uchida, H. and Nimer, S. (1996). The AML1/ETO fusion protein activates transcription of BCL-2. *Proc Natl Acad Sci U S A* **93**, 14059-64.

Klunker, S., Chong, M., Mantel, P., Palomares, O., Bassin, C., Ziegler, M., Rückert, B., Meiler, F., Akdis, M., Littman, D. et al. (2009). Transcription factors RUNX1 and RUNX3 in the induction and suppressive function of Foxp3+ inducible regulatory T cells. *J Exp Med* **206**, 2701-15.

Koentgen, F., Suess, G. and Naf, D. (2010). Engineering the mouse genome to model human disease for drug discovery. *Methods Mol Biol* **602**, 55-77.

Kondo, M., Weissman, I. and Akashi, K. (1997). Identification of clonogenic common lymphoid progenitors in mouse bone marrow. *Cell* **91**, 661-72.

Kopp, H., Hooper, A., Avecilla, S. and Rafii, S. (2009). Functional heterogeneity of the bone marrow vascular niche. *Ann N Y Acad Sci* **1176**, 47-54.

Kottaridis, P., Gale, R., Langabeer, S., Frew, M., Bowen, D. and Linch, D. (2002). Studies of FLT3 mutations in paired presentation and relapse samples from patients with acute myeloid leukemia: implications for the role of FLT3 mutations in leukemogenesis, minimal residual disease detection, and possible therapy with FLT3 inhibitors. *Blood* **100**, 2393-8.

Kottaridis, P., Gale, R. and Linch, D. (2003). Flt3 mutations and leukaemia. *Br J Haematol* **122**, 523-38.

Krause, D., Theise, N., Collector, M., Henegariu, O., Hwang, S., Gardner, R., Neutzel, S. and Sharkis, S. (2001). Multi-organ, multi-lineage engraftment by a single bone marrow-derived stem cell. *Cell* **105**, 369-77.

Krause, D. and Van Etten, R. (2007). Right on target: eradicating leukemic stem cells. *Trends Mol Med* **13**, 470-81.

Krivtsov, A., Twomey, D., Feng, Z., Stubbs, M., Wang, Y., Faber, J., Levine, J., Wang, J., Hahn, W., Gilliland, D. et al. (2006). Transformation from committed progenitor to leukaemia stem cell initiated by MLL-AF9. *Nature* **442**, 818-22.

Kulke, M., Demetri, G., Sharpless, N., Ryan, D., Shivdasani, R., Clark, J., Spiegelman, B., Kim, H., Mayer, R. and Fuchs, C. A phase II study of troglitazone, an activator of the PPARgamma receptor, in patients with chemotherapy-resistant metastatic colorectal cancer. *Cancer J* **8**, 395-9.

Lakso, M., Sauer, B., Mosinger, B. J., Lee, E., Manning, R., Yu, S., Mulder, K. and Westphal, H. (1992). Targeted oncogene activation by site-specific recombination in transgenic mice. *Proc Natl Acad Sci U S A* **89**, 6232-6.

Langabeer, S., Walker, H., Rogers, J., Burnett, A., Wheatley, K., Swirsky, D., Goldstone, A. and Linch, D. (1997). Incidence of AML1/ETO fusion transcripts in patients entered into the MRC AML trials. MRC Adult Leukaemia Working Party. *Br J Haematol* **99**, 925-8.

Lemischka, I., Raulet, D. and Mulligan, R. (1986). Developmental potential and dynamic behavior of hematopoietic stem cells. *Cell* **45**, 917-27.

Levanon, D. and Groner, Y. (2004). Structure and regulated expression of mammalian RUNX genes. *Oncogene* **23**, 4211-9.

Link, K., Chou, F. and Mulloy, J. (2010). Core binding factor at the crossroads: determining the fate of the HSC. *J Cell Physiol* **222**, 50-6.

Lutterbach, B., Westendorf, J., Linggi, B., Patten, A., Moniwa, M., Davie, J., Huynh, K., Bardwell, V., Lavinsky, R., Rosenfeld, M. et al. (1998). ETO, a target of t(8;21) in acute leukemia, interacts with the N-CoR and mSin3 corepressors. *Mol Cell Biol* **18**, 7176-84.

Martin, G. (1981). Isolation of a pluripotent cell line from early mouse embryos cultured in medium conditioned by teratocarcinoma stem cells. *Proc Natl Acad Sci U S A* **78**, 7634-8.

Maserati, E., Casali, M., Pasquali, F., Locatelli, F., Giani, S., Prete, L., Zecca, M., Invernizzi, R. and Bassan, R. (1992). Translocation (8;21) in two cases of refractory anemia with excess of blasts in transformation. *Cancer Genet Cytogenet* **58**, 76-8.

McCormack, E., Bruserud, O. and Gjertsen, B. T. (2008). Review: genetic models of acute myeloid leukaemia. *Oncogene* **27**, 3765-79.

Mebius, R. and Kraal, G. (2005). Structure and function of the spleen. *Nat Rev Immunol* **5**, 606-16.

Metcalf, D. (2007). On hematopoietic stem cell fate. *Immunity* **26**, 669-73.

Meyers, S., Downing, J. and Hiebert, S. (1993). Identification of AML-1 and the (8;21) translocation protein (AML-1/ETO) as sequence-specific DNA-binding proteins: the runt homology domain is required for DNA binding and protein-protein interactions. *Mol Cell Biol* **13**, 6336-45.

Misaghian, N., Ligresti, G., Steelman, L., Bertrand, F., Bäsecke, J., Libra, M., Nicoletti, F., Stivala, F., Milella, M., Tafuri, A. et al. (2009). Targeting the leukemic stem cell: the Holy Grail of leukemia therapy. *Leukemia* **23**, 25-42.

Misra, R., Bronson, S., Xiao, Q., Garrison, W., Li, J., Zhao, R. and Duncan, S. (2001). Generation of single-copy transgenic mouse embryos directly from ES cells by tetraploid embryo complementation. *BMC Biotechnol* **1**, 12.

Miyamoto, T., Nagafuji, K., Akashi, K., Harada, M., Kyo, T., Akashi, T., Takenaka, K., Mizuno, S., Gondo, H., Okamura, T. et al. (1996). Persistence of multipotent progenitors expressing AML1/ETO transcripts in long-term remission patients with t(8;21) acute myelogenous leukemia. *Blood* **87**, 4789-96.

Miyamoto, T., Weissman, I. L. and Akashi, K. (2000). AML1/ETO-expressing nonleukemic stem cells in acute myelogenous leukemia with 8;21 chromosomal translocation. *Proc Natl Acad Sci U S A* **97**, 7521-6.

Miyoshi, H., Shimizu, K., Kozu, T., Maseki, N., Kaneko, Y. and Ohki, M. (1991). t(8;21) breakpoints on chromosome 21 in acute myeloid leukemia are clustered within a limited region of a single gene, AML1. *Proc Natl Acad Sci U S A* **88**, 10431-4.

Moore, M. (2005). Converging pathways in leukemogenesis and stem cell self-renewal. *Exp Hematol* **33**, 719-37.

Morrison, S., Uchida, N. and Weissman, I. (1995). The biology of hematopoietic stem cells. *Annu Rev Cell Dev Biol* **11**, 35-71.

Morrison, S., Wandycz, A., Hemmati, H., Wright, D. and Weissman, I. (1997). Identification of a lineage of multipotent hematopoietic progenitors. *Development* **124**, 1929-39.

Muller, A. M., Duque, J., Shizuru, J. A. and Lubbert, M. (2008). Complementing mutations in core binding factor leukemias: from mouse models to clinical applications. *Oncogene* **27**, 5759-73.

Mulloy, J., Cammenga, J., Berguido, F., Wu, K., Zhou, P., Comenzo, R., Jhanwar, S., Moore, M. and Nimer, S. (2003). Maintaining the self-renewal and differentiation potential of human CD34+ hematopoietic cells using a single genetic element. *Blood* **102**, 4369-76.

Na Nakorn, T., Traver, D., Weissman, I. and Akashi, K. (2002). Myeloerythroid-restricted progenitors are sufficient to confer radioprotection and provide the majority of day 8 CFU-S. *J Clin Invest* **109**, 1579-85.

Naquet, P., Naspetti, M. and Boyd, R. (1999). Development, organization and function of the thymic medulla in normal, immunodeficient or autoimmune mice. *Semin Immunol* **11**, 47-55.

Nishida, S., Hosen, N., Shirakata, T., Kanato, K., Yanagihara, M., Nakatsuka, S., Hoshida, Y., Nakazawa, T., Harada, Y., Tatsumi, N. et al. (2006). AML1-ETO rapidly induces acute myeloblastic leukemia in cooperation with the Wilms tumor gene, WT1. *Blood* **107**, 3303-12.

Nisson, P., Watkins, P. and Sacchi, N. (1992). Transcriptionally active chimeric gene derived from the fusion of the AML1 gene and a novel gene on chromosome 8 in t(8;21) leukemic cells. *Cancer Genet Cytogenet* **63**, 81-8.

North, T., Stacy, T., Matheny, C., Speck, N. and de Bruijn, M. (2004). Runx1 is expressed in adult mouse hematopoietic stem cells and differentiating myeloid and lymphoid cells, but not in maturing erythroid cells. *Stem Cells* **22**, 158-68.

Nucifora, G., Larson, R. A. and Rowley, J. D. (1993). Persistence of the 8;21 translocation in patients with acute myeloid leukemia type M2 in long-term remission. *Blood* **82**, 712-5.

Nucifora, G. and Rowley, J. (1995). AML1 and the 8;21 and 3;21 translocations in acute and chronic myeloid leukemia. *Blood* **86**, 1-14.

Okuda, T., Cai, Z., Yang, S., Lenny, N., Lyu, C. J., van Deursen, J. M., Harada, H. and Downing, J. R. (1998). Expression of a knocked-in AML1-ETO leukemia gene inhibits the establishment of normal definitive hematopoiesis and directly generates dysplastic hematopoietic progenitors. *Blood* **91**, 3134-43.

Okuda, T., van Deursen, J., Hiebert, S., Grosveld, G. and Downing, J. (1996a). AML1, the target of multiple chromosomal translocations in human leukemia, is essential for normal fetal liver hematopoiesis. *Cell* **84**, 321-30.

Oravecz-Wilson, K., Philips, S., Yilmaz, O., Ames, H., Li, L., Crawford, B., Gauvin, A., Lucas, P., Sitwala, K., Downing, J. et al. (2009). Persistence of leukemia-initiating cells in a conditional knockin model of an imatinib-responsive myeloproliferative disorder. *Cancer Cell* **16**, 137-48.

Orban, P., Chui, D. and Marth, J. (1992). Tissue- and site-specific DNA recombination in transgenic mice. *Proc Natl Acad Sci U S A* **89**, 6861-5.

Owen, J. and Jenkinson, E. (1992). Apoptosis and T-cell repertoire selection in the thymus. *Ann N Y Acad Sci* **663**, 305-10.

Pardal, R., Clarke, M. and Morrison, S. (2003). Applying the principles of stem-cell biology to cancer. *Nat Rev Cancer* **3**, 895-902.

Park, C., Bergsagel, D. and McCulloch, E. (1971). Mouse myeloma tumor stem cells: a primary cell culture assay. *J Natl Cancer Inst* **46**, 411-22.

Passegué, E., Jamieson, C., Ailles, L. and Weissman, I. (2003). Normal and leukemic hematopoiesis: are leukemias a stem cell disorder or a reacquisition of stem cell characteristics? *Proc Natl Acad Sci U S A* **100 Suppl 1**, 11842-9.

Peterson, L. and Zhang, D. (2004). The 8;21 translocation in leukemogenesis. *Oncogene* **23**, 4255-62.

Peterson, L. F., Boyapati, A., Ahn, E. Y., Biggs, J. R., Okumura, A. J., Lo, M. C., Yan, M. and Zhang, D. E. (2007). Acute myeloid leukemia with the 8q22;21q22 translocation: secondary mutational events and alternative t(8;21) transcripts. *Blood* **110**, 799-805.

Puig-Kröger, A. and Corbí, A. (2006). RUNX3: a new player in myeloid gene expression and immune response. *J Cell Biochem* **98**, 744-56.

Ravandi, F. and Estrov, Z. (2006). Eradication of leukemia stem cells as a new goal of therapy in leukemia. *Clin Cancer Res* **12**, 340-4.

Rege, K., Swansbury, G., Atra, A., Horton, C., Min, T., Dainton, M., Matutes, E., Durosinmi, M., Treleaven, J., Powles, R. et al. (2000). Disease features in acute myeloid leukemia with t(8;21)(q22;q22). Influence of age, secondary karyotype abnormalities, CD19 status, and extramedullary leukemia on survival. *Leuk Lymphoma* **40**, 67-77.

Renneville, A., Roumier, C., Biggio, V., Nibourel, O., Boissel, N., Fenaux, P. and Preudhomme, C. (2008). Cooperating gene mutations in acute myeloid leukemia: a review of the literature. *Leukemia* **22**, 915-31.

Reya, T., Morrison, S., Clarke, M. and Weissman, I. (2001). Stem cells, cancer, and cancer stem cells. *Nature* **414**, 105-11.

Rhoades, K., Hetherington, C., Rowley, J., Hiebert, S., Nucifora, G., Tenen, D. and Zhang, D. (1996). Synergistic up-regulation of the myeloid-specific promoter for the macrophage colony-stimulating factor receptor by AML1 and the t(8;21) fusion protein may contribute to leukemogenesis. *Proc Natl Acad Sci U S A* **93**, 11895-900.

Rhoades, K. L., Hetherington, C. J., Harakawa, N., Yergeau, D. A., Zhou, L., Liu, L. Q., Little, M. T., Tenen, D. G. and Zhang, D. E. (2000). Analysis of the role of AML1-ETO in leukemogenesis, using an inducible transgenic mouse model. *Blood* **96**, 2108-15.

Rijkers, T., Peetz, A. and Rüther, U. (1994). Insertional mutagenesis in transgenic mice. *Transgenic Res* **3**, 203-15.

Rodríguez, C., Buchholz, F., Galloway, J., Sequerra, R., Kasper, J., Ayala, R., Stewart, A. and Dymecki, S. (2000). High-efficiency deleter mice show that FLPe is an alternative to Cre-loxP. *Nat Genet* **25**, 139-40.

Roth, S., Franken, P., van Veelen, W., Blonden, L., Raghoebir, L., Beverloo, B., van Drunen, E., Kuipers, E. J., Rottier, R., Fodde, R. et al. (2009). Generation of a tightly regulated doxycycline-inducible model for studying mouse intestinal biology. *Genesis* **47**, 7-13.

Rowe, D., Cotterill, S., Ross, F., Bunyan, D., Vickers, S., Bryon, J., McMullan, D., Griffiths, M., Reilly, J., Vandenberghe, E. et al. (2000). Cytogenetically cryptic AML1-ETO and CBF beta-MYH11 gene rearrangements: incidence in 412 cases of acute myeloid leukaemia. *Br J Haematol* **111**, 1051-6.

Rowley, J. (1973). Identificaton of a translocation with quinacrine fluorescence in a patient with acute leukemia. *Ann Genet* **16**, 109-12.

Rubio-Viqueira, B., Jimeno, A., Cusatis, G., Zhang, X., Iacobuzio-Donahue, C., Karikari, C., Shi, C., Danenberg, K., Danenberg, P., Kuramochi, H. et al. (2006). An in vivo platform for translational drug development in pancreatic cancer. *Clin Cancer Res* **12**, 4652-61.

Sakano, H. (1996). [Developmental regulation of V(D)J type recombination in the antigen receptor genes in lymphocytes]. *Seikagaku* **68**, 1470-4.

Salek-Ardakani, S., Smooha, G., de Boer, J., Sebire, N., Morrow, M., Rainis, L., Lee, S., Williams, O., Izraeli, S. and Brady, H. (2009). ERG is a megakaryocytic oncogene. *Cancer Res* **69**, 4665-73.

Sarraf, P., Mueller, E., Jones, D., King, F., DeAngelo, D., Partridge, J., Holden, S., Chen, L., Singer, S., Fletcher, C. et al. (1998). Differentiation and reversal of malignant changes in colon cancer through PPARgamma. *Nat Med* **4**, 1046-52.

Schessl, C., Rawat, V., Cusan, M., Deshpande, A., Kohl, T., Rosten, P., Spiekermann, K., Humphries, R., Schnittger, S., Kern, W. et al. (2005). The AML1-ETO fusion gene and the FLT3 length mutation collaborate in inducing acute leukemia in mice. *J Clin Invest* **115**, 2159-68.

Schmittgen, T. (2001). Real-time quantitative PCR. *Methods* **25**, 383-5.

Schwarz, B. and Bhandoola, A. (2006). Trafficking from the bone marrow to the thymus: a prerequisite for thymopoiesis. *Immunol Rev* **209**, 47-57.

Schwieger, M., Lohler, J., Friel, J., Scheller, M., Horak, I. and Stocking, C. (2002). AML1-ETO inhibits maturation of multiple lymphohematopoietic lineages and induces myeloblast transformation in synergy with ICSBP deficiency. *J Exp Med* **196**, 1227-40.

Shih, L., Liang, D., Huang, C., Wu, J., Lin, T., Wang, P., Dunn, P., Kuo, M. and Tang, T. (2006). AML patients with CEBPalpha mutations mostly retain identical mutant patterns but frequently change in allelic distribution at relapse: a comparative analysis on paired diagnosis and relapse samples. *Leukemia* **20**, 604-9.

Shimizu, K., Miyoshi, H., Kozu, T., Nagata, J., Enomoto, K., Maseki, N., Kaneko, Y. and Ohki, M. (1992). Consistent disruption of the AML1 gene occurs within a single intron in the t(8;21) chromosomal translocation. *Cancer Res* **52**, 6945-8.

Shinkai, Y., Rathbun, G., Lam, K., Oltz, E., Stewart, V., Mendelsohn, M., Charron, J., Datta, M., Young, F. and Stall, A. (1992). RAG-2-deficient mice lack mature lymphocytes owing to inability to initiate V(D)J rearrangement. *Cell* **68**, 855-67.

Shivdasani, R. and Orkin, S. (1996). The transcriptional control of hematopoiesis. *Blood* **87**, 4025-39.

Shu, Q., Wong, K., Su, J., Adesina, A., Yu, L., Tsang, Y., Antalffy, B., Baxter, P., Perlaky, L., Yang, J. et al. (2008). Direct orthotopic transplantation of fresh surgical specimen preserves CD133+ tumor cells in clinically relevant mouse models of medulloblastoma and glioma. *Stem Cells* **26**, 1414-24.

Smithies, O., Gregg, R., Boggs, S., Koralewski, M. and Kucherlapati, R. Insertion of DNA sequences into the human chromosomal beta-globin locus by homologous recombination. *Nature* **317**, 230-4.

Society, A. C. (2009). Cancer Facts &
Figures 2009.

Socolovsky, M., Nam, H., Fleming, M., Haase, V., Brugnara, C. and Lodish, H. (2001). Ineffective erythropoiesis in Stat5a(-/-)5b(-/-) mice due to decreased survival of early erythroblasts. *Blood* **98**, 3261-73.

Somervaille, T. and Cleary, M. (2006). Identification and characterization of leukemia stem cells in murine MLL-AF9 acute myeloid leukemia. *Cancer Cell* **10**, 257-68.

Soriano, P. (1999). Generalized lacZ expression with the ROSA26 Cre reporter strain. *Nat Genet* **21**, 70-1.

Spangrude, G., Heimfeld, S. and Weissman, I. (1988). Purification and characterization of mouse hematopoietic stem cells. *Science* **241**, 58-62.

Sprengel, R. and Hasan, M. T. (2007). Tetracycline-controlled genetic switches. *Handb Exp Pharmacol*, 49-72.

Strauss-Ayali, D., Conrad, S. and Mosser, D. (2007). Monocyte subpopulations and their differentiation patterns during infection. *J Leukoc Biol* **82**, 244-52.

Swirsky, D., Li, Y., Matthews, J., Flemans, R., Rees, J. and Hayhoe, F. (1984). 8;21 translocation in acute granulocytic leukaemia: cytological, cytochemical and clinical features. *Br J Haematol* **56**, 199-213.

Takahama, Y., Shores, E. and Singer, A. (1992). Negative selection of precursor thymocytes before their differentiation into CD4+CD8+ cells. *Science* **258**, 653-6.

Takenokuchi, M., Yasuda, C., Takeuchi, K., Nakamachi, Y., Mukai, M., Kondo, S., Kumagai, S., Saigo, K., Murayama, T., Koizumi, T. et al. (2004). Quantitative nested reverse transcriptase PCR vs. real-time PCR for measuring AML1/ETO (MTG8) transcripts. *Clin Lab Haematol* **26**, 107-14.

Ten Cate, B., de Bruyn, M., Wei, Y., Bremer, E. and Helfrich, W. (2010). Targeted elimination of leukemia stem cells; a new therapeutic approach in hemato-oncology. *Curr Drug Targets* **11**, 95-110.

Thomas, K. and Capecchi, M. (1987). Site-directed mutagenesis by gene targeting in mouse embryo-derived stem cells. *Cell* **51**, 503-12.

Till, J. and McCulloch, E. (1961). A direct measurement of the radiation sensitivity of normal mouse bone marrow cells. *Radiat Res* **14**, 213-22.

Twombly, R. (2002). First clinical trials of endostatin yield lukewarm results. *J Natl Cancer Inst* **94**, 1520-1.

Uchida, N. and Weissman, I. (1992). Searching for hematopoietic stem cells: evidence that Thy-1.1lo Lin- Sca-1+ cells are the only stem cells in C57BL/Ka-Thy-1.1 bone marrow. *J Exp Med* **175**, 175-84.

Vaillant, F., Blyth, K., Andrew, L., Neil, J. and Cameron, E. (2002). Enforced expression of Runx2 perturbs T cell development at a stage coincident with beta-selection. *J Immunol* **169**, 2866-74.

Vardiman, J. (2009). The World Health Organization (WHO) classification of tumors of the hematopoietic and lymphoid tissues: An overview with emphasis on the myeloid neoplasms. *Chem Biol Interact*.

Vardiman, J., Thiele, J., Arber, D., Brunning, R., Borowitz, M., Porwit, A., Harris, N., Le Beau, M., Hellström-Lindberg, E., Tefferi, A. et al. (2009). The 2008 revision of the World Health Organization (WHO) classification of myeloid neoplasms and acute leukemia: rationale and important changes. *Blood* **114**, 937-51.

Wang, J., Hoshino, T., Redner, R., Kajigaya, S. and Liu, J. (1998). ETO, fusion partner in t(8;21) acute myeloid leukemia, represses transcription by interaction with the human N-CoR/mSin3/HDAC1 complex. *Proc Natl Acad Sci U S A* **95**, 10860-5.

Wang, Q., Stacy, T., Binder, M., Marin-Padilla, M., Sharpe, A. and Speck, N. (1996). Disruption of the Cbfa2 gene causes necrosis and hemorrhaging in the central nervous system and blocks definitive hematopoiesis. *Proc Natl Acad Sci U S A* **93**, 3444-9.

Wang, Y., Zhou, G., Yin, T., Chen, B., Shi, J., Liang, W., Jin, X., You, J., Yang, G., Shen, Z. et al. (2005). AML1-ETO and C-KIT mutation/overexpression in t(8;21) leukemia: implication in stepwise leukemogenesis and response to Gleevec. *Proc Natl Acad Sci U S A* **102**, 1104-9.

Welm, B., Tepera, S., Venezia, T., Graubert, T., Rosen, J. and Goodell, M. (2002). Sca-1(pos) cells in the mouse mammary gland represent an enriched progenitor cell population. *Dev Biol* **245**, 42-56.

Wiemels, J. L., Xiao, Z., Buffler, P. A., Maia, A. T., Ma, X., Dicks, B. M., Smith, M. T., Zhang, L., Feusner, J., Wiencke, J. et al. (2002). In utero origin of t(8;21) AML1-ETO translocations in childhood acute myeloid leukemia. *Blood* **99**, 3801-5.

Willerford, D., Swat, W. and Alt, F. (1996). Developmental regulation of V(D)J recombination and lymphocyte differentiation. *Curr Opin Genet Dev* **6**, 603-9.

Wilson, A. and Trumpp, A. (2006). Bone-marrow haematopoietic-stem-cell niches. *Nat Rev Immunol* **6**, 93-106.

Wilson, C., Bellen, H. and Gehring, W. (1990). Position effects on eukaryotic gene expression. *Annu Rev Cell Biol* **6**, 679-714.

Wodinsky, I., Swiniarski, J. and Kensler, C. (1968). Spleen colony studies of leukemia L1210. IV. Sensitivities of L1210 and L1210/6-MP to triazenoimidazolecarboxamides--a preliminary report. *Cancer Chemother Rep* **52**, 393-8.

Woolf, E., Xiao, C., Fainaru, O., Lotem, J., Rosen, D., Negreanu, V., Bernstein, Y., Goldenberg, D., Brenner, O., Berke, G. et al. (2003). Runx3 and Runx1 are required for CD8 T cell development during thymopoiesis. *Proc Natl Acad Sci U S A* **100**, 7731-6.

Wörtge, S., Eshkind, L., Cabezas-Wallscheid, N., Lakaye, B., Kim, J., Heck, R., Abassi, Y., Diken, M., Sprengel, R. and Bockamp, E. (2010). Tetracycline-controlled transgene activation with the GFP-equipped ROSA26-iM2
mouse allows conditional mosaic expression in mice. *submitted*.

Yergeau, D. A., Hetherington, C. J., Wang, Q., Zhang, P., Sharpe, A. H., Binder, M., Marin-Padilla, M., Tenen, D. G., Speck, N. A. and Zhang, D. E. (1997). Embryonic lethality and impairment of haematopoiesis in mice heterozygous for an AML1-ETO fusion gene. *Nat Genet* **15**, 303-6.

Yoo, S., Chi, H., Jang, S., Seo, E., Seo, J., Lee, J., Park, H. and Park, C. (2005). Quantification of AML1-ETO fusion transcript as a prognostic indicator in acute myeloid leukemia. *Haematologica* **90**, 1493-501.

Yoshida, H. and Kitabayashi, I. (2008). Chromatin regulation by AML1 complex. *Int J Hematol* **87**, 19-24.

Yuan, Y., Zhou, L., Miyamoto, T., Iwasaki, H., Harakawa, N., Hetherington, C. J., Burel, S. A., Lagasse, E., Weissman, I. L., Akashi, K. et al. (2001). AML1-ETO expression is directly

involved in the development of acute myeloid leukemia in the presence of additional mutations. *Proc Natl Acad Sci U S A* **98**, 10398-403.

Zambrowicz, B., Imamoto, A., Fiering, S., Herzenberg, L., Kerr, W. and Soriano, P. (1997). Disruption of overlapping transcripts in the ROSA beta geo 26 gene trap strain leads to widespread expression of beta-galactosidase in mouse embryos and hematopoietic cells. *Proc Natl Acad Sci U S A* **94**, 3789-94.

Zhang, J., Niu, C., Ye, L., Huang, H., He, X., Tong, W., Ross, J., Haug, J., Johnson, T., Feng, J. et al. (2003). Identification of the haematopoietic stem cell niche and control of the niche size. *Nature* **425**, 836-41.

Zuber, J., Radtke, I., Pardee, T., Zhao, Z., Rappaport, A., Luo, W., McCurrach, M., Yang, M., Dolan, M., Kogan, S. et al. (2009). Mouse models of human AML accurately predict chemotherapy response. *Genes Dev* **23**, 877-89.